

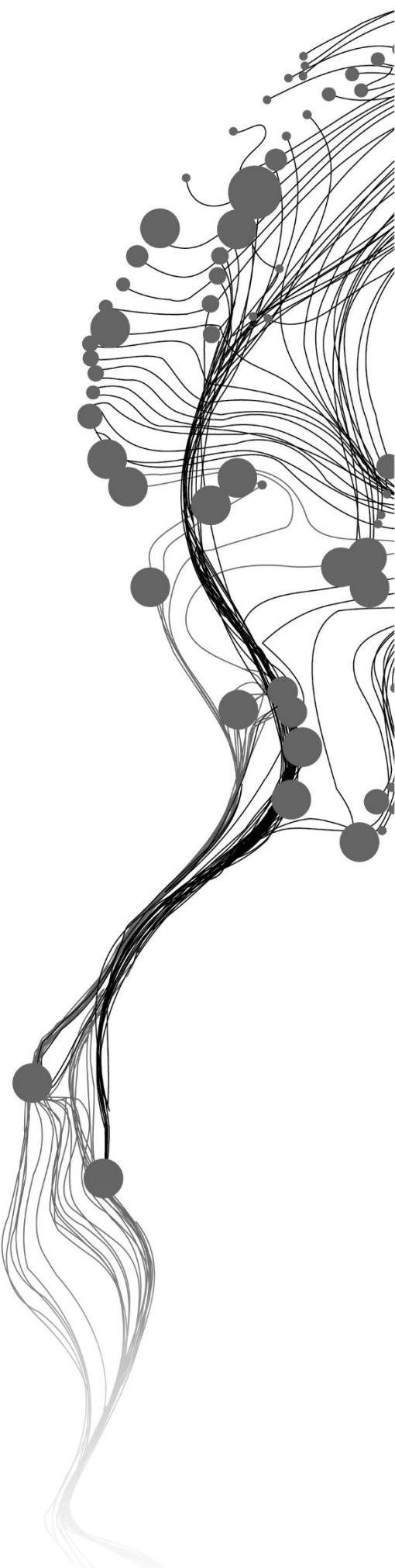
GROUNDWATER RESOURCES EVALUATION IN KALAHARI KAROO BASIN

KISENDI, EMMANUEL EZEKIEL
February, 2016

SUPERVISORS:
Dr. M. W. Lubczynski, (Maciek)
[Drs. Robert Becht

ADVISOR:

Moiteela Lekula - (PhD Candidate)



GROUNDWATER RESOURCES EVALUATION IN KALAHARI - KAROO BASIN

KISENDI, EMMANUEL EZEKIEL

Enschede. The Netherlands. Februarv. 2016

Thesis submitted to the Faculty of Geo-Information Science and Earth Observation of the University of Twente in partial fulfilment of the requirements for the degree of Master of Science in Geo-information Science and Earth Observation.

Specialization: [Name course (e.g. Applied Earth Sciences)]

SUPERVISORS:

Dr. M. W. Lubczynski, (Maciek)

Drs. Robert Becht

THESIS ASSESSMENT BOARD:

Prof.dr.Z.Su (Bob), (Chair)

Dr. A. P. Frances (Alain), (External Examiner, National Laboratory for Energy and Geology)

DISCLAIMER

This document describes work undertaken as part of a programme of study at the Faculty of Geo-Information Science and Earth Observation of the University of Twente. All views and opinions expressed therein remain the sole responsibility of the author, and do not necessarily represent those of the Faculty.

Dedicated to Precious, Prince-bright, Ezekiel and Salma Kisendi.

ABSTRACT

Groundwater resources evaluation is an important aspect of water resources' management. It is most important in dry areas where there is no surface water, and hence groundwater becomes the only source of portable water. Groundwater resources are optimally evaluated by distributed numerical models which however require accurate definition of external driving forces and good understanding of aquifer geometry and vertical and horizontal heterogeneity of the aquifer systems.

The main objective of this study was to evaluate groundwater recharge and groundwater resources in the Lokalane - Ncojane Karoo Basin (LNKB). At first, cross-sections over much larger, regional Kalahari Karoo Basin (KKB) were developed to assess the vertical extension of each layer unit. Then, using the RockWorks software, a 3D litho-stratigraphic model of the Kalahari Karoo Basin (KKB) was developed. The cross-sections of that model were first developed for all formations following Smith (1984), and further narrowed down to include only five hydrostratigraphic layers on top of the impermeable rock basement.

The five hydrostratigraphic layers included; 0-189 m Kalahari Sand saturated/unsaturated zone layer, 0-329 m Stormberg Basalt aquitard, 0-230 m Ntane Sandstone aquifer, 0-282 m Mosolotsane-Kwetla Mudstone aquitard and 0-275 m for Ecca Sandstone aquifer. The Kalahari Sand and Ecca Sandstone have spatially continuous extent, while Stormberg Basalt, Ntane Sandstone and Mosolotsane-Kwetla Mudstone are spatially limited. The calculated thicknesses of the five hydro-stratigraphic layers were compared with the known regional geology of Botswana.

Once understanding the spatial extent of the KKB layers, an integrated hydrologic steady state model (IHM) of the groundwater prospective LNKB area was created. It consisted of the three aquifers, separated by two aquitards. The simulated period was six hydrologic years. The steady-state model comprised mean measurement of six hydrologic years. The steady-state model was calibrated by trial and error method, using the vertical (VK, VKCB) and horizontal (HK) hydraulic conductivities as calibration variables.

After model calibration, the fluxes IN and OUT of the model were calculated. It was observed that, the total inflow components to the model was $194.10 \text{ mm yr}^{-1}$, out of which, $194.06 \text{ mm yr}^{-1}$ (99.9%) came from the UZF gross recharge component of which $194.03 \text{ mm yr}^{-1}$ was lost through ET, resulting into only 0.03 mm yr^{-1} as groundwater recharge through the unsaturated zone.

Key words: Kalahari Karoo Basin; Lokalane-Ncojane Karoo Basin; 3D Stratigraphy model; 3D hydrostratigraphy model; integrated hydrologic model.

ACKNOWLEDGEMENTS

I would like to address my first gratitude to the Government of the Kingdom of the Netherlands, for granting me the Scholarship through the Netherlands Fellowship Programme, which has been the only financial support to accomplish my study at ITC. I also convey my gratitude to the Government of Tanzania, through its Ministry of Water, for granting me the permission to pursue this study, and complying with the NUFIC terms and condition for the scholarship.

I am delighted to address my sincere acknowledgement to my first Supervisor, Dr Maciek Lubczynski, who has worked with me hand to hand, and gave me directives on how to tackle this project. His technical advice and encouragement gave me strength to believe that the goals of this study would be met. I am also thankful to my second supervisor, Drs Robert Becht, for giving me freedom to do this project the way I wanted.

My special appreciation goes to Moiteela Lekula (PhD candidate) at ITC, who has been a good advisor on my work and ensured the availability of all the datasets used in this research, (Thanks mate!), Mr. Richard Winston of the United States Geological Survey for his technical support and advice on the use of Modflow-NWT and Modflow Model Muse software, his quick response to the questions and on fixing the bugs for the UZF package ensured timely completion of my steady state modelling works.

I am also grateful to the Course Director of the Department of Water Resources and Environmental Management, " Mr Arno van Lieshout" and all members of staff in the department for their esteemed collaboration for the entire period of my study at ITC. I extend my kind regards to my fellow students on the groundwater stream for working as a team, whenever we faced any challenges, Mr Patrick Nyarugwe (Kuzman) and Mehreteab Yohannes Weldemichael, "It is done mates"!! Also to my good friends over the entire period of my study at ITC, Mr. Sammy Njuki and Amos Tabalia, for sharing together the happy moments during my study.

Lastly, but not least, my sincere regards go to my dear wife and children, for their moral support and being tolerant with my absence for the entire period of 18 month. Salma, it has been challenging, but thanks that you have survived!! See you soon.

TABLE OF CONTENTS

1.	introduction	1
1.1.	Background of the study	1
1.2.	Objective of the study	2
1.2.1.	Main objective	2
1.2.2.	Specific objective.....	2
1.2.3.	Main research question (s).....	2
1.2.4.	Specific research questions	2
1.3.	Hypothesis	2
1.4.	Novelty of the study	2
1.5.	Study area.....	3
1.5.1.	Location.....	3
1.5.2.	Climate.....	3
1.5.3.	Topography and drainage.....	4
1.5.4.	Land use and land cover	5
1.6.	Geology	5
1.6.1.	Geological setting.....	5
1.6.2.	Pre Karoo Group.....	6
1.6.3.	Dwyka Group.....	6
1.6.4.	Ecca Group (Middle Karoo).....	7
1.6.5.	Beaufort Group (Middle Karoo).....	7
1.6.6.	Lebung Group.....	7
1.6.7.	Stormberg Lava Group.....	7
1.6.8.	Kalahari Group	8
1.7.	Hydrogeology	8
1.7.1.	Groundwater flow.....	8
1.7.2.	Hydraulic conductivity	8
1.7.3.	Water quality.....	9
2.	research methods	11
2.1.	Introduction	11
2.2.	Development of the Stratigraphic and hydrostratigraphic KKB model	12
2.2.1.	Data collection.....	12
2.2.2.	Data processing.....	13
2.3.	LNKB - driving forces and state variables	14
2.3.1.	Precipitation.....	14
2.3.2.	Potential evapotranspiration	15
2.3.3.	Interception.....	16
2.3.4.	Infiltration rate	16
2.3.5.	Heads distribution.....	17
2.4.	Conceptual model of the LNKB.....	19
2.4.1.	Hydro-stratigraphic units.....	19
2.4.2.	Flow systems pattern, flow direction and rates.....	20
2.4.3.	Preliminary water balance	20
2.4.4.	External and internal model physical boundary.....	20

2.5.	Numerical model of the LNKB.....	21
2.5.1.	General concepts	21
2.5.2.	Grid design	21
2.5.3.	Software selection.....	21
2.5.4.	The Unsaturated Zone Flow (UZF) Package	21
2.5.5.	Structural model.....	22
2.5.6.	Layer groups	22
2.5.7.	Driving forces.....	22
2.5.8.	System parameterization.....	23
2.5.9.	State variables	23
2.5.10.	Boundary conditions	23
2.5.1.	Time discretization	24
2.6.	Numerical model calibration.....	24
2.6.1.	General concepts	24
2.6.2.	Sensitivity analysis.....	25
2.6.3.	Water budget	25
3.	results and discussions	27
3.1.	Structural modelling.....	27
3.1.1.	Stratigraphic cross-sections	27
3.2.	Hydro-stratigraphic cross-sections	30
3.3.	3D Stratigraphic model	34
3.3.1.	Thickness of hydrostratigraphic layers	35
3.3.2.	Comparison with available geological information	41
3.4.	Numerical groundwater model of the LNKB.....	44
3.4.1.	Driving forces.....	44
3.4.2.	Model hydrostratigraphy	46
3.4.3.	Calibration parameters	46
3.4.4.	Error assessment.....	48
3.4.5.	Sensitivity analysis of the parameters	50
3.4.6.	Water budget	51
3.4.7.	Annual recharge estimation.....	53
3.4.8.	Spatial variability of the groundwater fluxes in the LNKB.....	53
3.5.	Water resources evaluation	54
3.6.	Comparison with other studies	55
3.6.1.	Horizontal hydraulic conductivity.....	55
3.6.2.	Net recharge	55
3.6.3.	Water balance	55
3.7.	Limitations of the study	56
4.	Conclusion and recommendations	57
4.1.	Conclusion	57
4.2.	Recommendations.....	57

LIST OF FIGURES

Figure 1: Location map of the study area.....	3
Figure 2: Daily precipitation and temperature at Ghanzi Airport stations.....	4
Figure 3 Digital elevation model (DEM) of the study area.	5
Figure 4: Major and minor structures in Botswana, with geology excluding Kalahari Sand.....	6
Figure 5: Steps followed leading to: left panel - hydro-stratigraphic model of the KKB; right panel - groundwater model of the LNKB.	12
Figure 6: Borehole logs, main structures and cross-section lines.	14
Figure 7: Averaged rainfall intensity within 1 st Oct 2004-30 th Sept 2010 period in (LNKB).	15
Figure 8: Spatial position of piezometric points with single time measurements and time series measurement data in LNKB.....	17
Figure 9: Time series of daily heads and precipitation.....	19
Figure (10):Conceptual model of the LNKB modified after (Rahube, 2003).....	22
Figure: (11) Boundary conditions for the groundwater flow model.	24
Figure 12: Stratigraphic cross-section A-B as shown on Figure 6.....	27
Figure 13: Stratigraphic cross-section C-D as shown in Figure 6.....	27
Figure 14: Stratigraphic-cross section E-F as shown in Figure 6.....	28
Figure 15: Stratigraphic cross-section G-H as shown in Figure 6.	28
Figure 16: Stratigraphic-cross I-J as shown in Figure 6.....	29
Figure 17: Stratigraphic cross-section K-L as shown in Figure 6.....	29
Figure 18: Stratigraphic-cross section M-N as shown in Figure 6.....	30
Figure 19: Hydro-stratigraphic cross-section A-B as shown in Figure 6.....	30
Figure 20: Hydro-stratigraphic cross-section C-D as shown in Figure 6.....	31
Figure 21: Hydro-stratigraphic cross-section E-F as shown ion Figure 6.....	31
Figure 22: Hydro-stratigraphic cross-section K-L as shown in Figure 6.....	32
Figure 23: Hydro-stratigraphic cross-section through point K-L as shown on Figure 6.....	32
Figure 24: Hydro-stratigraphic cross-section M-N as shown in Figure 6.	33
Figure 25: Hydro-stratigraphic cross-section through point O-P as shown on Figure 6.	33
Figure 26: 3D Lithostratigraphic model of the KKB.....	34
Figure 27: 3D Stratigraphic model of the KKB.	35
Figure 28: Spatial thickness variation of the Kalahari Sand layer.	36
Figure 29: Spatial thickness variation of the Stormberg Basalt layer.....	37
Figure 30: Spatial thickness variation of the Ntane Sandstone layer.....	38
Figure 31: Spatial thickness variation of the Mosolotsane-Kwetla Mudstone-Siltstone layer.....	39
Figure 32: Spatial thickness variation of the Ecca Sandstone layer.....	40
Figure 33: Modelled Kalahari thickness over the known KKB geology of Botswana.....	41
Figure 34: Modelled Basalt (Volcanic) thickness over the known KKB geology of Botswana.....	42
Figure 35: Modelled Ntane Sandstone thickness over the known KKB geology of Botswana.	43
Figure 36: Modelled Mosolotsane-Kwetla thickness over the known KKB geology of Botswana.	43
Figure 37: Modelled Ecca thickness over the known KKB geology of Botswana.	44
Figure 38: Infiltration rate (m day ⁻¹) zones based on the variable precipitation in the area.	45
Figure 39: Rainfall in the LNKB with the resulting infiltration rates.....	45
Figure 40: Relationship between Precipitation, PET and mean temperature in LNKB area.	46
Figure 41: Horizontal hydraulic conductivity (m day ⁻¹) of the Kalahari Sand aquifer.....	47
Figure 42: Horizontal hydraulic conductivity (m day ⁻¹) of the Ntane Sandstone aquifer.....	47

Figure 43: Vertical hydraulic conductivity (VKCB) in (m day^{-1}) for M-K Mudstone aquitard.....	47
Figure 44: Horizontal hydraulic conductivity (m day^{-1}) of the Eccca Sandstone aquifer	48
Figure 45: Head distribution in Eccca Sandstone aquifer after steady-state model calibration.	48
Figure 46: Scatter plot of observed and simulated heads after steady-state calibration.....	49
Figure 47: Sensitivity of model parameters under steady-state calibration.	50
Figure 48: Sensitivity of the UZF parameters and GHB conductances under steady-state calibration.....	50
Figure 49: Schematized water budget ($\text{m}^3 \text{d}^{-1}$) per each saturated layer obtained in steady state calibration	52
Figure 50: Schematized water budget ($\text{m}^3 \text{d}^{-1}$) for entire LNKB aquifer system after steady-state calibration.	53
Figure 51: Averaged UZF gross recharge in mm d^{-1} for the period 1 st Oct 2004 to 30 th Sept 2010.	54
Figure 52: Averaged UZF- ET_g in mm d^{-1} for the period 1 st Oct 2004 to 30 th Sept 2010.....	54

LIST OF TABLES

Table 1: Karoo stratigraphic units-adapted from (Smith 1984)	8
Table 2: Karoo stratigraphic units-Adapted from Smith 1984.....	19
Table 3: The thickness interval for the hydro-stratigraphy layers in the KKB and their lithology.	40
Table 4: Error assessment of heads after Steady-State calibration	49
Table 5: Volumetric water budget ($\text{m}^3 \text{ day}^{-1}$) of the individual aquifers after steady state calibration.....	51
Table 6 : Volumetric water budget ($\text{m}^3 \text{ day}^{-1}$) for composite model after steady state calibration.....	52

LIST OF ACRONYMS

KKB	Kalahari Karoo Basin
LNKB	Lokalane-Ncojane Karoo Basin
m a.s.l	meter above sea level
DWA	Department of Water Affairs
3D	Three dimensions
BNWMP	Botswana National Water Master Plan.
BNWMPR	Botswana National Water supply Master Plan Review
UZF	Unsaturated Zone Flow
MODFLOW-NWT	Modular finite-difference groundwater-flow model-Newtonian Solver Modflow
SW-NE	South West - North East
FAO	Food Association Organization
ADAS	Automatic Data Acquisition System
PET	Potential Evapotranspiration
DEM	Digital Elevation Model
DWA	Department of Water Affairs
WB	Water Budget
GHB	General Head boundary

1. INTRODUCTION

1.1. Background of the study

There is an ever increasing demand of water in the world, to satisfy cultural, societal and economic needs. These demands can be fulfilled by either groundwater or surface water sources; however, comparing the two, groundwater is wider distributed and safer. Groundwater flow and storage is restricted to aquifers and is governed by laws and equations which facilitate groundwater hydrologists, engineers and planners with powerful tools such as hydrological models, to forecast the behaviour of a regional aquifer systems in response to stresses, e.g. wellfield abstractions, (Bear, 2012). Groundwater resources have to be protected and monitored for their sustainability. Over-exploitation and unreasonable utilization of groundwater resources cause serious problems including pollution and aquifer depletion, which can restrict the sustainable development of society but also destruct ecological system equilibrium.

The Kalahari Karoo area falls under the semi-arid climate. Water resources management in such climate is particularly difficult because years with good rains resulting in recharge are followed by several years of "normal" low rains without any recharges, (Obakeng, 2007). Mean recharge of about 5 mm yr⁻¹ is suggested by de Vries et al., (2000) in the Eastern Fringe, where annual rainfall exceeds 400 mm. Towards the Central Kalahari, recharge decreases to 1 mm yr⁻¹. A high retention storage due to large thickness of unsaturated zone (Kalahari Sand >60 m) and high evapotranspiration, result in very little water passing through the root zone to become recharge, (de Vries et al., 2000).

According to Obakeng(2007), almost all Kalahari infiltrating water is taken up by vegetation (the rest is evaporated while surface runoff is negligible) making recharge to deep aquifers only a small portion of the total precipitation. This is also pointed out by Lubczynski, (2009), who discusses possibility of certain plant species, particularly trees to access groundwater or capillary fringe by plant tap-root systems, while Obakeng (2007), confirmed this by using LiCl tracer on various acacia trees. He tested rooting depth of 19 Kalahari trees by LiCl to determine their rooting depth which varied from 8 m to 70 m depth.

This study focused on understanding the 3D hydro-stratigraphy model of the Kalahari Karoo Basin (KKB) and the structural influence on the spatial extent of the hydro-stratigraphic units, which helped in constructing the conceptual model of the Lokalane-Ncojane Karoo Basin (LNKB) earlier addressed by (Rahube, 2003) as Ncojane-Lokalane Basin. The LNKB is located in western side of the KKB. In the LNKB, two productive aquifers are known, Ntane Sandstone (Lebung Group) and Ecca Group of the Karoo Super Group. This study updates the work by Rahube, (2003). The boundary of the LNKB was extended more on the west, towards Namibia, in order to delineate water divide, interpreted from the constructed structural model.

This research leads to understanding of the spatial extent of the potential aquifers in the LNKB, to quantification of groundwater storages and characterisation of structural influence upon the groundwater recharge and aquifer flow.

Problem definition

Groundwater is the only source of portable water in the Kalahari Karoo Basin. The Karoo sediments (Lebung and Ecca group) have proved to be good aquifers in large part of the Kalahari Basin-Botswana. The Ntane Sandstone of the Lebung group makes these strata more consistent and potentially the most productive aquifers in Botswana (BNWMP, 1991). According to Botswana National Water Master Plan Review estimates, 65% of the national water demand is met through supply from groundwater resources (BNWMPR, 2006), while Schmoll & Organization, (2006), estimates 80% of the supply coming from groundwater. However, hydrogeological systems of the KKB have been negatively stressed. Water level in the area has continuously been declining while the projected water demand for 2006-2035 linearly increases (BNWMPR, 2006).

For proper understanding of the flow systems in the KKB, there is a need to understand the 3D hydro-stratigraphy of the KKB, including its vertical and horizontal heterogeneities to select prospective with regard to groundwater resources area. For that selected area, i.e. LNKB, hydrological model had to be done to evaluate groundwater recharge, groundwater flow and groundwater resources.

1.2. Objective of the study**1.2.1. Main objective**

To evaluate groundwater recharge and groundwater resources in the Lokalane-Ncojane Karoo Basin (LNKB)

1.2.2. Specific objective

- i) To develop the 3D hydro-stratigraphic model of (KKB)
- ii) Using the KKB model, to define domain and conceptual model of the LNKB
- iii) To calibrate steady-state flow model of the LNKB
- iv) To estimate recharge and groundwater resources in the LNKB area

1.2.3. Main research question (s)

What are the recharge and groundwater resources of the Ncojane-Lokalane Karoo Basin (LNKB)?

1.2.4. Specific research questions

- i) How can the 3D stratigraphy of the KKB be presented?
- ii) What is the domain and conceptual model of the LNKB?
- iii) What is the water balance of the steady - state calibrated model of the LNKB?
- iv) What is the estimated net recharge and groundwater resource in the LNKB?

1.3. Hypothesis

A well calibrated steady-state model, accounting for surface-groundwater interactions, can reliably quantify recharge and groundwater resources of the LNKB.

1.4. Novelty of the study

The clear understanding of the 3D stratigraphic model of the Kalahari Basin, which will lead to a realistic conceptual model of the LNKB, is the novelty of this study, as it has never been studied in details. Moreover; estimation of recharge by the use of an integrated model in the LNKB adds more value to this study, as this approach has never been applied in the area.

1.5. Study area

1.5.1. Location

The Kalahari Karoo Basin (KKB) extends from the North-Eastern part of Botswana to Namibia in the South - Western side. The area covers about 325,210.5 km² extending from 1850000 m to 2700000 m Easting and -2920000 m to -2295000 m Nothings. This is the area extent which was used for developing the 3D Stratigraphic model in this study, while for groundwater flow model (LNKB), area extent used was 47,829 km², which is only 14.7 % of KKB, (Figure 1).

1.5.2. Climate

The climate of KKB is characterised by semi-arid conditions with rainfall restricted to the summer period, which is from November to April, with winter period from May to October. The rainfall is predominantly convectonal, characterised by highly localised, high intensity thunderstorms/showers and hailstorms that are generally short lived, (Rahube, 2003), cited from (Botswana National Atlas, 2001).

The area experiences seasonal temperature variations, with the highest temperature occurring during the summer and the coldest during the winter (The winter period is cold and dry, while summer is hot and wet). The mean maximum monthly temperature varies between 27 °C to 35 °C, with the minimum monthly temperature varying between 4 °C to 10 °C. However, there are temperature variations within 24-hour period due to high temperature during the day and low temperature during the night. Observations on the Ghanzi station which is nearby LNKB show that, the higher temperature is associated with the higher rainfall, (Figure 2).

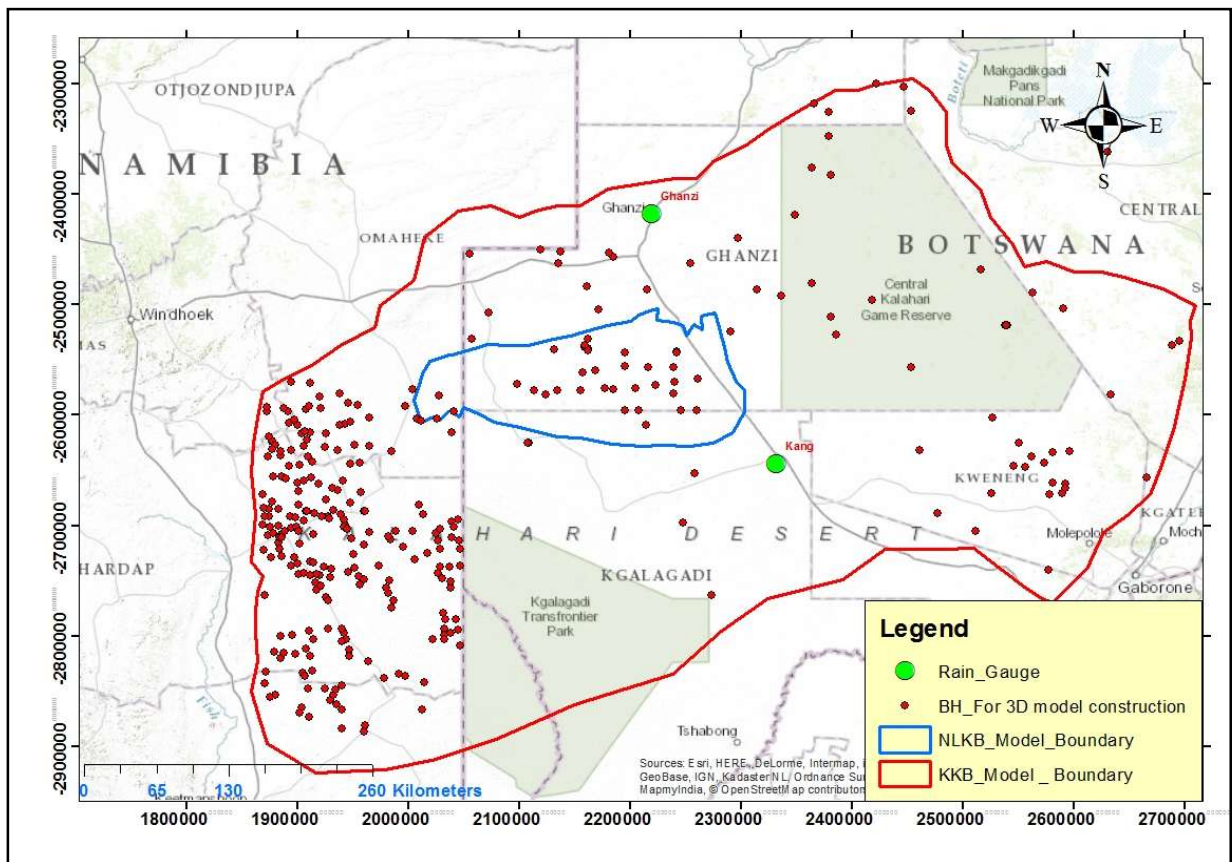


Figure 1: Location map of the study area.

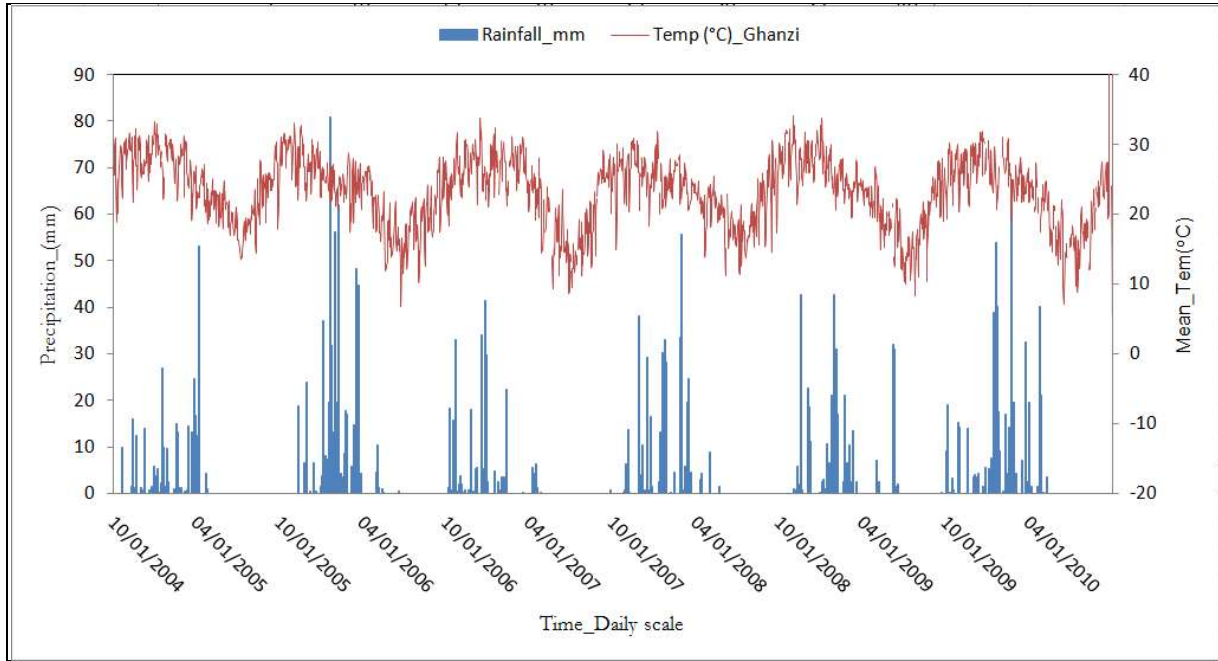


Figure 2: Daily precipitation and temperature at Ghanzi Airport stations

1.5.3. Topography and drainage

The KKB is characterized by a flat, slightly undulating topography with an elevation range from 913 to 1516 m a.s.l. (Figure 3), with a latitudinal distance of about 284,468 m, which results in a very low eastward topographic gradient approximated to 0.00086.

The LNKB is located in the Western part of the KKB (Figure 3). The area lays just South of Ghanzi Ridge, which is a prominent topographic feature, running from the SW-NE and is an elevated sequence of meta-sedimentary rocks that form part of the Ghanzi-Chobe Belt (Figure 4). The area is characterised by a gently undulating relief in which fossil dunes and pans are the main geomorphologic features. The LNKB area has a maximum altitude of 1304 m in the west and there is a general decline trend to the East to the elevation of 1059 m. The Western side is the recharge area, while the Eastern is the discharge side. The discharged water drains towards the KKB. No surface water bodies are present in the LNKB, with only temporary streams using internal drainage system.

The Southwest Botswana Basin (hereafter referred as LNKB) is one of the seven Karoo sub-basins in Botswana. This sedimentary Basin attains a depth > 15 km to the west of the Kalahari Line, (Figure 4). The Basin is divided into two-sub basins, namely the northern Ncojane Sub Basin and southern Nossop Sub Basin. This division is along an inferred south-western extension of another regional structural feature known as the Makgadikgadi Line (Figure 4). This feature delineates a major northeast trending fault zone that runs from the Tshane Complex across Botswana into Zimbabwe. Part of the Ghanzi-Chobe Fold Belt runs through the study area in the northwest and this fold belt is comprised of tightly folded meta-sedimentary rocks of Quartzite extending from Namibia via Botswana to Zambia in the northeast, (Figure 4). The thick arenaceous sedimentary sequence of the Ghanzi Group within the fold belt forms the Ghanzi Ridge and the Kgwebe Formation, which outcrops further northeast, forming the basal sequence of the Ghanzi Group, (Smith, 1984).

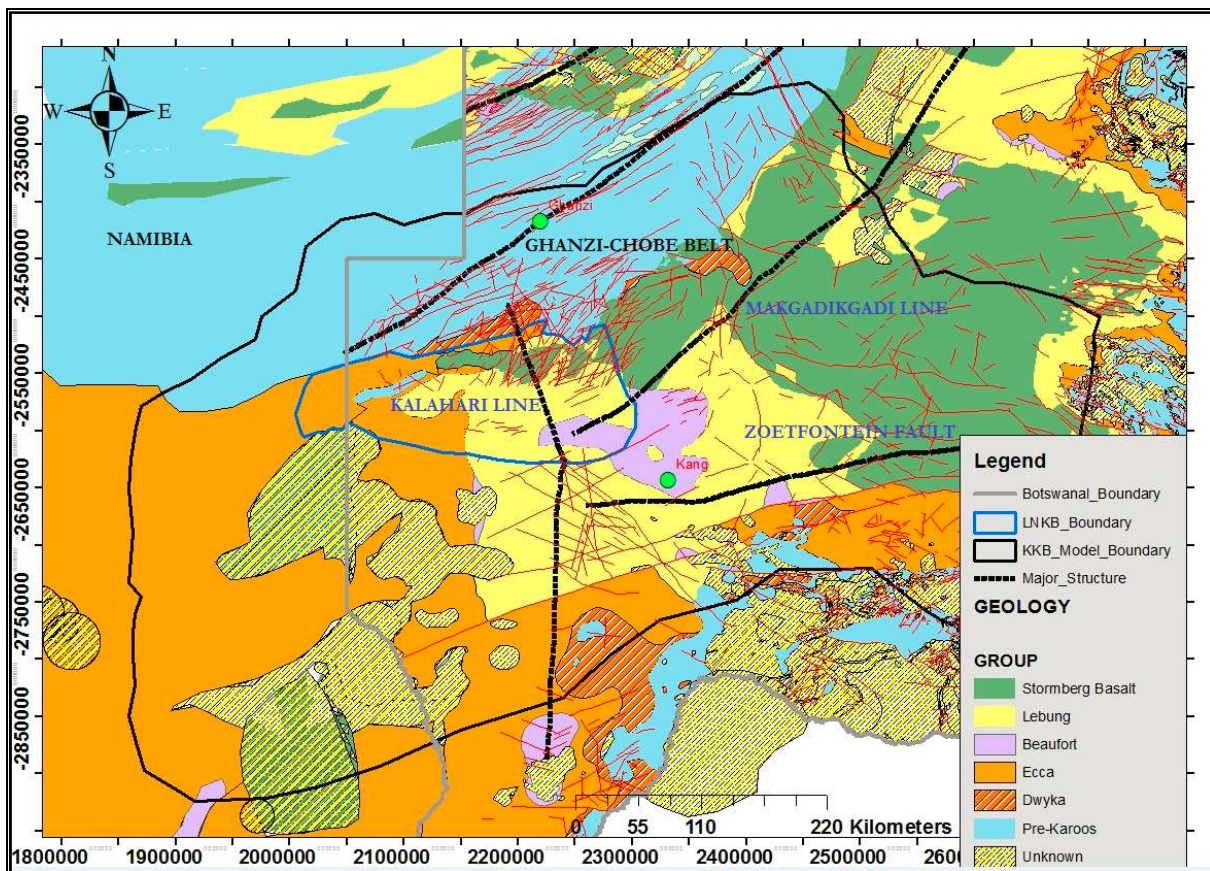


Figure 4: Major and minor structures in Botswana, with geology excluding Kalahari Sand.

1.6.2. Pre Karoo Group

These are Proterozoic in age with two group of rocks, which are Transvaal (interbedded reddish, grey and purple quartzite, carbonaceous siltstone and shale, cherty, limestone, ironstone and volcanic). The second group is Waterberg group (Reddish siliciclastic sedimentary rocks, mostly quartzite sandstone and conglomerate). These rock type are not discussed in details as they are not in the interest of this study.

1.6.3. Dwyka Group

The Dwyka group is the Basal unit of the Karoo Super group and is represented by the Dukwi Formation. This formation rests un-comfortably on Proterozoic Transvaal and Waterberg Super group as well as Archaean basement strata. This unit is not considered in the groundwater flow evaluation, and rather considered as part of the basement in the hydrogeological layers.

1.6.4. Ecca Group (Middle Karoo)

The Ecca Group is divided into three separate conformable Formations, namely the Bori, Kweneng and Boritse in respective order from oldest to youngest.

- i) The Bori Formation overlies conformably the Dwyka Formation and is thought to be an accumulation of mud deposited from suspension in a post glacial lake, indicating a waning of the early Karoo glacial depositional environment. This unit is considered part of the basement in this study and not potential groundwater resource.
- ii) The Kweneng Formation (Middle Ecca) is the transition from the argillaceous units of the Bori Formation to grits and coarse sandstones. It is characterised by massive, poorly bedded, coarse to medium grain quartz-feldspathic gritty arkoses becoming finer grained and silty towards the base. This is also considered part of the basement in this study.
- iii) The Boritse (Upper Ecca) consists of an alternating sequence of fine to coarse grained feldspathic sandstone, alternating with carbonaceous mudstones, muddy siltstones and silty mudstone intercalations, dull and bright coals and coaly carbonaceous mudstones. The coaly carbonaceous mudstones are in places siderites and pyritic with pyrite nodules and veins, while the bright coal bands may have calcite veins. This is the fifth layer in the groundwater flow model of the LNKB.

1.6.5. Beaufort Group (Middle Karoo)

The Beaufort Group of the Karoo is represented on the southern margins of the Kalahari Basin by the Kwetla Formation. This unit follows conformably from the Ecca and is characterised by a largely argillaceous non-carbonaceous multi-coloured, (yellow, brown, green, greenish grey, purple, cream, white and light grey) sequence of mudstones and subordinate siltstone, with minor fine to coarse grained sandstone intercalations. Together with Mosolotsane Mudstone, It forms the fourth layer Mosolotsane-Kwetla in the groundwater flow model of the LNKB, which is an aquitard, confining the Ecca aquifer.

1.6.6. Lebung Group.

Throughout Botswana the Lebung Group lies unconformably on the uppermost Ecca Group and Kwetla Formation. Lebung strata are subdivided into two formations, the lower Mosolotsane Formation and the upper Ntane Sandstone Formation. The Ntane Sandstone Formation is the most area consistent, the most widely understood and the most predictable aquifer in the Karoo sequence, and thus forms the principal target for groundwater development in many regions of the country, especially the Central and Eastern part of Botswana. In this study, Ntane Sandstone forms the third hydro geologic layer (aquitard) of the LNKB. Moreover, the Mosolotsane Formation is the lowermost subdivision of the sequence of continental sediments and volcanic that comprises the Lebung group. It's mostly mudstones -siltstones with occasionally intercalations of coarse sandstones. In this study, the Mosolotsane was combined with the Kwetla unit of Beaufort Group, to form a fourth hydro geologic layer (aquitard) of the LNKB.

1.6.7. Stormberg Lava Group

This group forms the uppermost unit of the Karoo Super group and has been formally designated the Ramoselwana Volcanic Formation, (Smith, 1984).The 'Stormberg lava' or 'Stormberg Basalt' generally means the same unit in this report. The Stormberg strata consist of a very extensive, and often very thick, sequence of tholeiitic flood Basalts which mark the end of the Karoo sedimentary succession. The Basalt is black to greenish grey, but reddish brown in the amygdaloidal zones. Only a small part of the Eastern LNKB constitute this layer (aquitard),which forms the second hydro geologic layer, confining the Ntane Sandstone aquifer.

1.6.8. Kalahari Group.

This is the Post-Karoo superficial deposits of the Kalahari Group (commonly termed ‘Kalahari Beds’ or ‘Kalahari Sands’) which are extremely widespread in the area with considerable thickness of more than 60 m. This unit comprises a discordant and highly variable sequence of loose to poorly consolidated sand, silcrete and calcrete intercalations of variable proportions, subordinate to minor Ferricrete, silcretized/calcretized sandstones and mudstones,(Smith, 1984). In the LNKB, this unit forms the first layer, mainly unconfined and considered to be unsaturated zone.

1.7. Hydrogeology

The hydrogeological regime of the area is significantly influenced by the spatial distribution of the geological units of the Karoo and their lithological and structural characteristics. A summary of the litho-stratigraphy of the area is shown in (Table 1) below.

Table 1: Karoo stratigraphic units-adapted from (Smith 1984)

AGE	SUPER-GROUP	GROUP	FORMATION	LITHOLOGICAL DESCRIPTION		
CENOZOIC		Kalahari	<i>Kalahari Beds</i>	Loose sands, cretes, calcareous sandstone and mudstone.	Post Karoo	
		Stormberg	Ramoselwana Volcanics	Crystalline, massive amygdaloidal basalts	Karoo	
			Ntane	Fine to medium grained, clean, friable sandstone, brownish red/pink. Often calcretised in zones.		
		Lebung	Mosolotsane	Red/brown greenish mudstones and siltstones with fine to medium, occasionally coarse, intercalated sandstones. Basal conglomerate in places.		
		Beaufort	Kwetla	Grey mudstones and siltstones with minor sandstones. Non-carbonaceous. Occasionally arenaceous.		
			Boritse	Fine to coarse, white, feldspathic sandstone interbedded with coal, carbonaceous mudstone and siltstone.		
			Kweneng	Predominantly medium to coarse grained feldspathic sandstone, grits with subordinate siltstone and mudstone. Minor coals.		
			Ecca	Bori		Dark, micaceous siltstone/mudstone and minor sandstone.
						Purple siltstone and very fine sandstone.
						Massive, dark grey, sandy mudstone and siltstone.
						Purple mudstone rythmites/varvites with dropstones.
MESOZOIC	KAROO	Dwyka	Dukwi	Tillite, conglomerate with quartzite/granite clasts in sandstone matrix.	Karoo	
PROTEROZOIC	WATERBERG			Reddish siliciclastic sedimentary rocks, mostly quartzitic sandstone and conglomerate.	Pre-Karoo	
	TRANSVAAL			Interbedded reddish, grey and purple quartzite, carbonaceous siltstone and shale, chert, limestone, ironstone and volcanics.		

1.7.1. Groundwater flow

The Ntane sandstone of the Lebung Group and the Ecca Group sediments host the main aquifers of the KKB, however water strikes within minor aquifers have also been recorded in other lithological groups. There is limited data on these minor aquifers due to their secluded and localised nature (WCS, 2001). Groundwater inflow into the model is from direct diffused recharge and a horizontal flux component from the Ecca in the West, (Namibian side).Groundwater outflow from both aquifers is through the horizontal flow in the East of the model boundary.

1.7.2. Hydraulic conductivity

Rahube, (2003), came up with the horizontal hydraulic conductivities ranging from 0.08-1.8 m day⁻¹ and 0.01-0.5 m day⁻¹ for Ntane and Ecca aquifers respectively. He also assumed the vertical horizontal conductivities to one-tenth of the horizontal hydraulic conductivities. However, Ambayo, (2005),suggested the values for vertical hydraulic (K_v) conductivities for different lithology in the LNKB which were 0.61 m day⁻¹ for Ntane aquifer, 0.17 m day⁻¹ for Basalt, 0.21 m day⁻¹ for Mosolotsane Mudstone and 0.54 m day⁻¹ for the aquifer. These were used as initial inputs to estimate the horizontal and vertical hydraulic conductivities of the LNKB groundwater flow model.

1.7.3. Water quality

The groundwater of Western Central Kalahari Basin, hereafter called LNKB is largely used for domestic purposes. Therefore, evaluation of its quality is inevitable. In general, the water has dominant cations of Ca^{2+} , Na^+ and Mg^{2+} and dominant anions are HCO_3^- and Cl^- . The distribution of these cations and anions is apparently governed by the regional flow configuration, (WCS, 2012). The hydrochemistry data indicates that the Ecca and the Ntane Sandstone aquifers contain very fresh groundwater, with TDS values ranging between 400-700 mg l^{-1} and between 500-1000 mg l^{-1} respectively, (WCS, 2012).

2. RESEARCH METHODS

2.1. Introduction

In order to answer the research questions, the methodology applied were summarized in Figure 5. The methodology consists of two major steps: 1) development of the 3D hydro-stratigraphic model of the KKB; 2) development of the conceptual and numerical groundwater model of the LNKB.

Four data types can be used to study the vertical and horizontal heterogeneity nature of the subsurface. These data type include; remote sensing (RS), geophysical, geological and structural data. The use of all data types simplifies the interpolation method for a continuous 3D stratigraphic model which describe the geometry of geology (Calcagno et., al 2008). Models of geological bodies should be easy to edit and update to integrate new data(Kaufmann & Martin, 2009).

The Kalahari Karoo Basin area lacks a complete developed stratigraphic model. Only small portions of this area have the stratigraphic model, mostly conceptualized, but not developed in details. Nxumalo (2011), MSc thesis dealt with the stratigraphic and Basin modelling of the Gemsbok Sub-basin. He came out with a 3D schematic geological model of the western part of Kalahari Botswana and Eastern Namibia. Bordy et., al(2010), discuss the sedimentology of Mosolotsane formation (Lebung Group) of the upper Triassic of the Kalahari Botswana, hence came up with the lithological analysis of one formation in the Basin. Likewise, different reports by Wellfield Consulting Services deal with specific locations in their studies as mentioned in the introduction part. All these studies cannot be used to represent the stratigraphy model of the whole KKB.

The Rock Works 14th version software was used for data processing and hydro-stratigraphic modelling. Rockworks 14th version is the third latest version of Rock Ware's flagship software program. It is standard software in the petroleum, environmental, geotechnical and mining industries for sub surface data visualization. It has popular tools which include maps, logs, fence diagrams, solid models and volumetric. With this software, the 3D stratigraphy of the KKB was deduced. Sections and thicknesses of different lithological units were calculated for the entire KKB.

Surface-groundwater exchange occurs through the flux exchange between surface water and groundwater systems. For the case of LNKB, this happens through the unsaturated zone and infiltration to or exfiltration from saturated zone. However, due to deep water table in the LNKB area, groundwater exfiltration is impossible, and hence the surface leakage in the groundwater flow model is expected to be zero for the Steady-State flow. The head differences govern the flow direction, which is generally eastwards.

The assessment of groundwater recharge and groundwater resources in the Lokalane-Ncojane Karoo Basin, (LNKB) has been already a focus of interest of several studies which are geological, hydro-geological and also modelling studies. However, all these modelling studies used standalone models and focused more on assessing the recharges, with very little being done regarding groundwater storage and groundwater resources.

The first complex study including groundwater of the LNKB was carried out by (WCS, 2001), on the Hunhukwe/Lokalane Groundwater Survey Project. In this study, among other objectives, the Ntane Sandstone aquifer was evaluated using a steady state numerical model. Chilume (2001), came up with a one layer model of the Ntane Sandstone aquifer, which was later extended to two aquifer layers model

(Ntane Sandstone & Ecca Sandstone) by (Rahube 2003). Ambayo, (2005) studied the spatial and temporal groundwater recharge in the area, using GIS and 1D reservoir modelling method.

In this research the integrated hydrologic model MODFLOW-NWT under Model Muse utilising UZF1 Package which interfaces surface with groundwater fluxes. This model is a Newton formulation of MODFLOW-2005 (Niswonger et al., 2011). The developed Newton formulation has advantage that it keeps all model cells active within a simulation and thus solving the nonlinearity problems (drying and wetting) observed in MODFLOW-2005 which had been a common source of convergence failures (Niswonger et al., 2011).

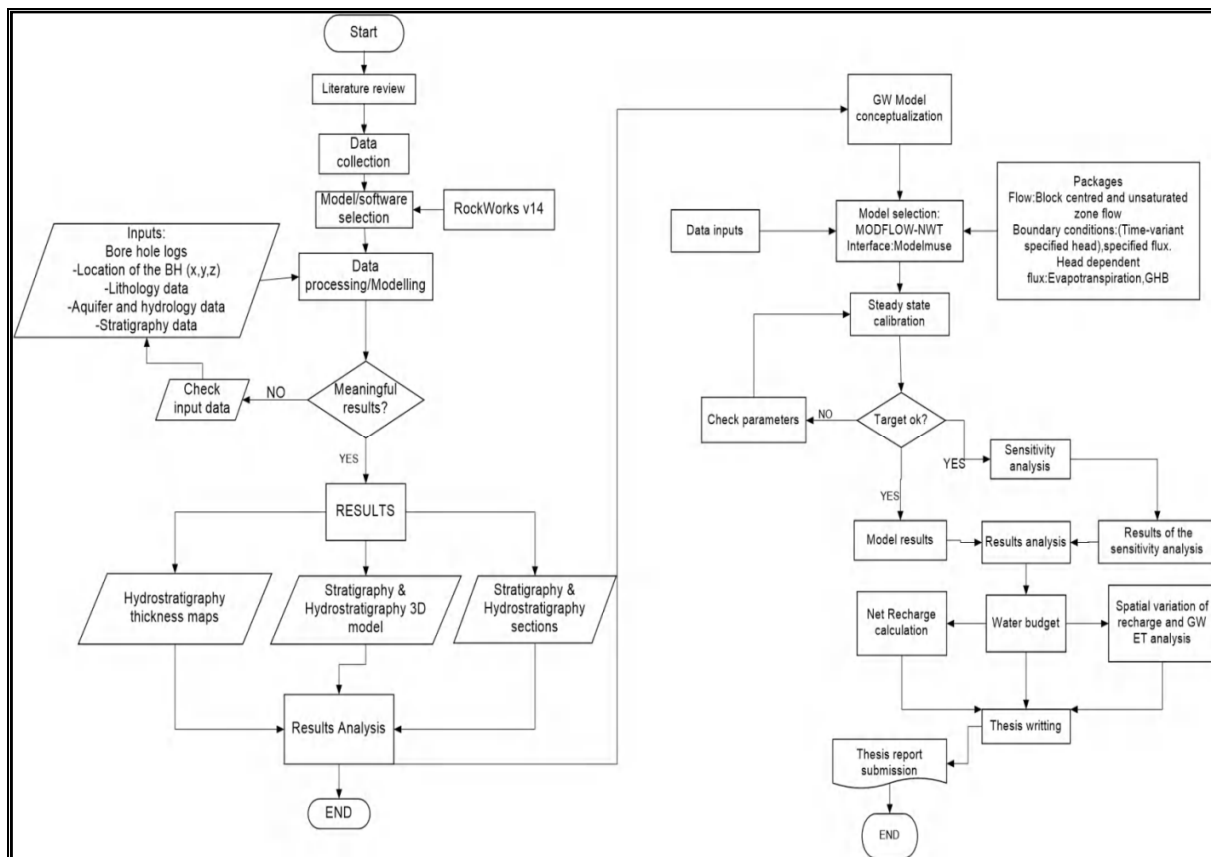


Figure 5: Steps followed leading to: left panel - hydro-stratigraphic model of the KKB; right panel - groundwater model of the LNK.

2.2. Development of the Stratigraphic and hydrostratigraphic KKB model

The methods used to achieve the research objectives and answering the research questions regarding the 3D stratigraphic model of the area are summarized in (Figure 5). The method is composed of five basic steps (left panel of Figure 5), namely: Data Collection, Model Selection, Stratigraphic and Hydrostratigraphic Modelling, Model Results and Results Analysis.

2.2.1. Data collection

In this study, the geological model was developed using the available borehole logs and descriptions. The borehole data available in the KKB area were found enough to construct a 3D stratigraphic model as suggested by (Wu et al., 2005). A total of 229 borehole data logs were used for the models development. Databases for stratigraphy and hydrostratigraphy units were established. Stratigraphy and

hydrostratigraphy interval descriptions of the boreholes, borehole location and elevations were collected. The DEM of 90 m resolution was used to extract the point elevation values for each borehole.

2.2.2. Data processing

Both stratigraphic and hydro-stratigraphic models were built by interpolating surface layers from the borehole logs. The borehole locations, elevation and down-hole intervals, were imported in the software and surface interpolation by Kriging method was performed.

Seven cross sections were drawn in the study area, NW-SE & SW-NE, (Figure 6). Consideration of the major structures was important when positioning the cross-sections. The cross-sections were drawn perpendicular to the structural units in order to extract all the necessary information for the lithological heterogeneity.

The 3D stratigraphic and hydro-stratigraphic models were developed. For the stratigraphic model, individual lithological units were drawn from the post Karoo (Kalahari Beds) Stratigraphy, Karoo Stratigraphy (Stormberg Basalt, Ntane Sandstone, and Mosolotsane Mudstones, Kwetla, Ecca and Dwyka) and the Pre- Karoo unit which combined all the Pre-Karoo lithological units. For the purpose of hydro-stratigraphic model, Mosolotsane and Kwetla Mudstone were combined to form one hydro-stratigraphic layer, with the last unit being the Ecca (Boritse). All layers below the Ecca was considered to be the basement unit and was not included in the development of the hydro-stratigraphy sections.

The process of developing the stratigraphic and hydro-stratigraphic models involves the interpolation of a grid model of the upper and lower surface of each of the stratigraphic units using the user-selected gridding method, (Lewandowski, 2015). For this study, the surface thicknesses were interpolated and subtracted one after the other, with the DEM being the top layer.

The stratigraphy, followed by hydro-stratigraphy cross-sections for KKB was drawn independently in which, for the stratigraphy cross-sections, Mosolotsane and Kwetla litho-units were treated independently. In hydro-stratigraphic cross-sections, the Mosolotsane and Kwetla Mudstone units were combined to form a single layer. The thickness of each hydro-stratigraphic layer was exported as X, Y Z data. The exported data was plotted in Arc GIS and points were interpolated to obtain the raster maps of the hydro-stratigraphic units (Kalahari beds, Stormberg Basalt (Volcanic), Ntane, Mosolotsane - Kwetla and Ecca-Boritse). The X, Y, Z data were also gridded in surfer software to obtain thickness contours for each hydro-stratigraphy layer. The contour thickness maps were validated against the known geology of Botswana to observe if the modelled thickness of each lithological unit coincides with the respective geology. Only five layers (Kalahari beds, Basalt, Ntane Sandstone, Mosolotsane-Kwetla Mudstone and Ecca Sandstone) which were used in the groundwater flow model construction were considered.

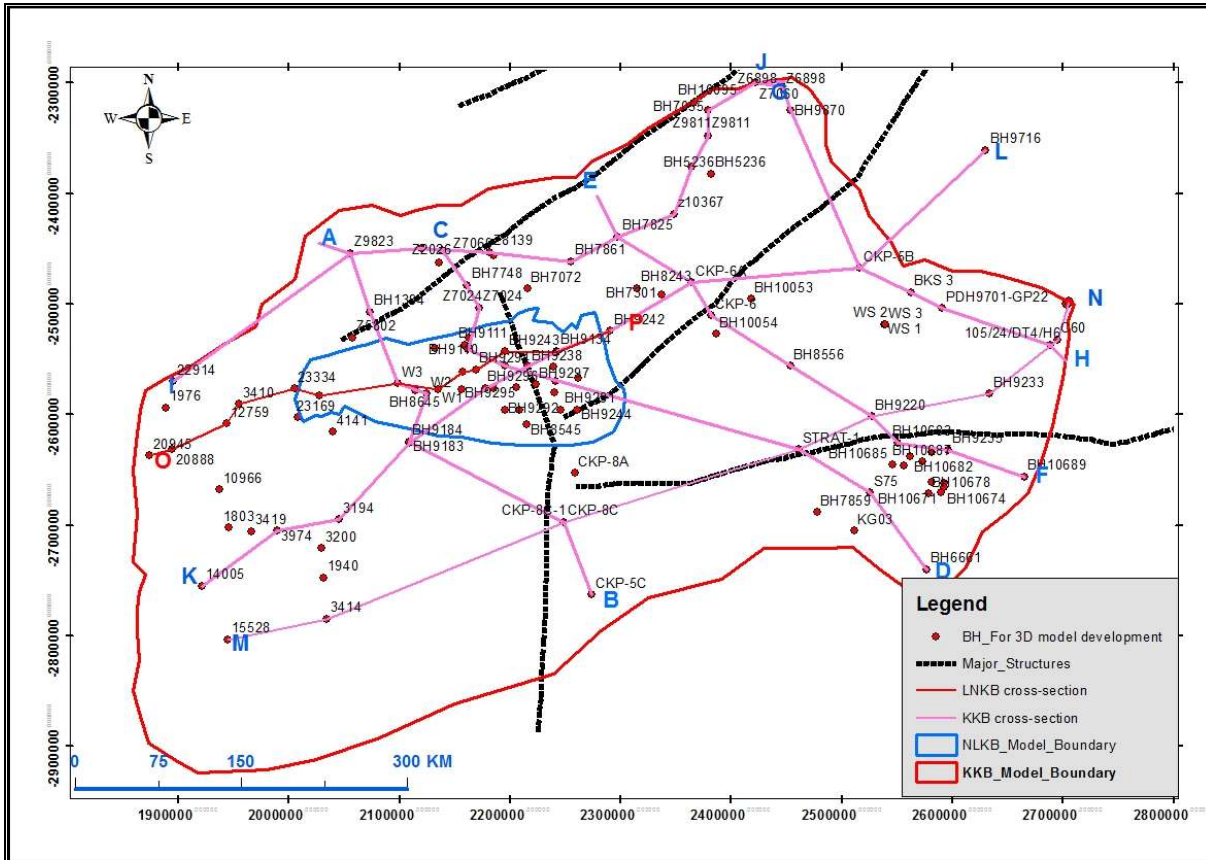


Figure 6: Borehole logs, main structures and cross-section lines.

2.3. LNKB - driving forces and state variables

The external boundaries of the LNKB were delineated based on the KKB model. The no flow boundary set on the northern part of the model was due to geological contact, while for the western side, the no flow boundary was set based on the interpreted water divide after structural model of the hydro-stratigraphic layers. For the southern boundary, a no flow was assigned based on the groundwater flow direction, in which the boundary was delineated parallel to the flow. In the eastern end, which is the discharge side, a general head boundary was set to allow discharge of groundwater to the Central Kalahari Basin.

The variable used for the state was the hydraulic heads which were 19 in total, out of which 15 piezometers had single time readings and only 4 piezometers had the time variable readings. The driving forces to the LNKB numerical model included precipitation and evapotranspiration.

2.3.1. Precipitation

The daily precipitation was used as one of the driving forces. The data used for this model were collected from the Ghanzi and Kang gauging station. The rainfall was considered to vary spatially in the area. Due to this, different zones of rainfall intensity were obtained from correlation of TRMM and gauge data. The average rainfall raster map of temporal scale from 1st Oct 2004 to 30th Sept 2010 with 0.25 degree spatial resolution was sourced from the advisor to this research. The raster map was re-sampled to 1 km and clipped using the LNKB model boundary. Five different zones of rainfall intensities were obtained, ranging from 1.04 to 1.482 mm day⁻¹ (Figure 7).

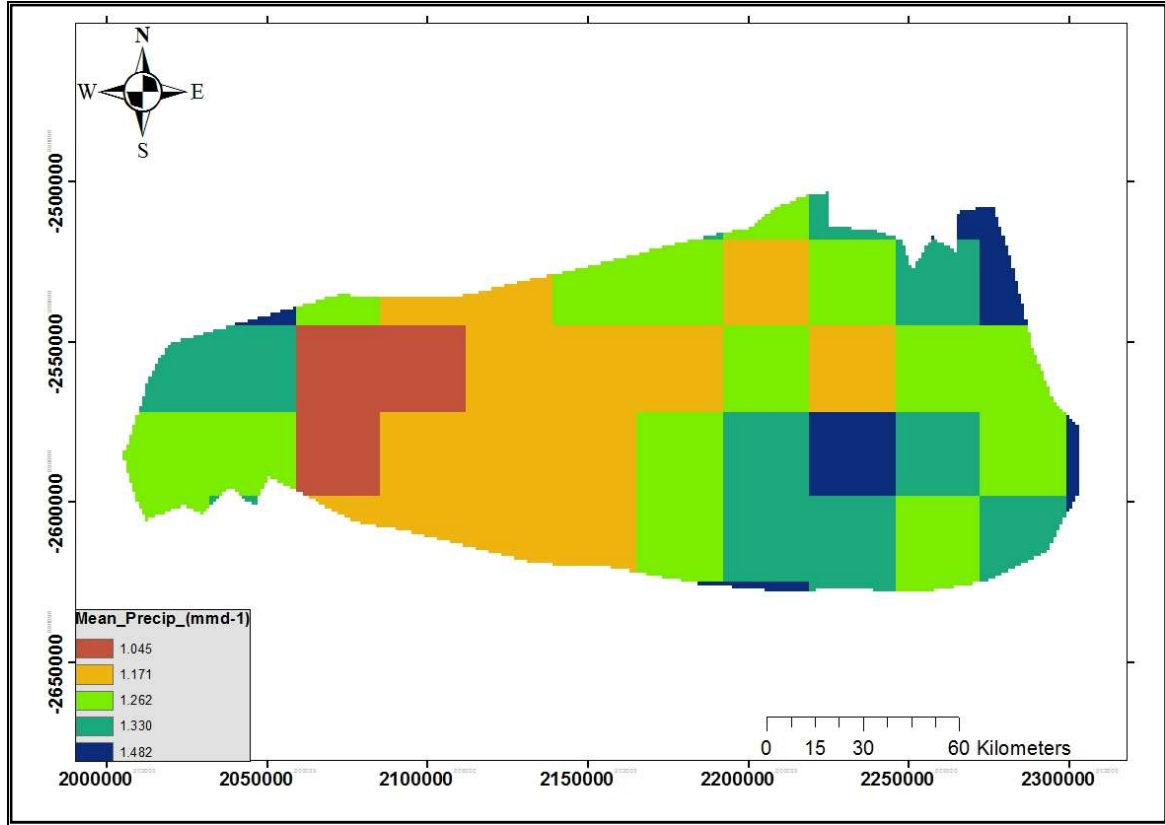


Figure 7: Averaged rainfall intensity within 1st Oct 2004-30th Sept 2010 period in (LNKB).

2.3.2. Potential evapotranspiration

The amount of evaporation that would occur if a sufficient water source is available is what is referred as potential evapotranspiration (PET). The PET, next to precipitation, is another driving force of the model developed. The PET was calculated using the single crop FAO methodology of Penman-Monteith. Equation 1.

$$PET = Kc * ETo \quad (1)$$

where by

PET= Potential evapotranspiration,

Kc = Crop coefficient

ETo = Reference evapotranspiration.

The ETo for the LNKb was estimated by the original Hargreaves method (equation 2), using the ADAS data in adaptation of the original Penman method as suggested in the FAO irrigation and Drainage paper, no. 56 by (Richard et al., 1998). The Hargreaves method was designed to suit the estimation of crop reference evapotranspiration, in situations when data is limited and only minimum and maximum air temperature data are available. Because of insufficient data, this method was adopted for this study.

$$ETo = 0.0023 * (T_{mean} + 17.8) * (T_{max} - T_{min})^{0.5} * Ra \quad (2)$$

Where T_{mean} , T_{max} and T_{min} are the daily mean, maximum and minimum air temperature ($^{\circ}C$), R_a is the total incoming extra-terrestrial solar radiation in the same units as evaporation. It was calculated using temperature data ($^{\circ}C$), latitude (in degrees) and the Julian day (J) as an input to estimate incoming solar energy, Equation 3.

$$Ra = \frac{24 \times 60}{\pi} G_{SC} * d_r * [\omega_s * \sin(\phi) * \sin(\delta) + \cos(\phi) * \cos(\delta) * (\omega_s)] \quad (3)$$

d_r is the relative distance between the earth and the sun given by:

$$d_r = 1 + 0.033 \cos \left[\frac{2\pi}{365} * J \right] \quad (4)$$

δ is the solar declination (radians) defined by:

$$\delta = 0409 \sin \left[\frac{2\pi}{365} * J - 1.39 \right] \quad (5)$$

ω_s is the sunset hour angle (radians), given by

$$\omega_s = \arccos [-\tan(\phi) * \tan(\delta)] \quad (6)$$

The obtained ETO was converted into PET using the crop coefficient approach, in which 81% of the area is covered by grass. The grass coefficient (Kc) value used was 0.75, while the Kc values representing trees and shrubs used was 1.0. The Kc values were assigned following to (Richard et., al 1998). The weighted average of the Kc value was calculated and a value of 0.8 obtained. The ETO was converted to PET, following Equation 1 .

2.3.3. Interception

This refers to precipitation that does not reach the soil, but instead is intercepted by the leaves and branches of plants and the forest floor. As explained in the Landcover section, the Kalahari area has mostly four savannah vegetation which are tree savannah, shrub savannah, mixed savannah and grass savannah, (Science, 2004). The Landcover map was classified into two classes, which are grass and other vegetation, (shrubs and other tree species). The interception for grass was as 6.9 % of rainfall following (Corbett & Crouse, 1968). The interception of the other group of vegetation was assumed 11.2% of rainfall based on the only available acacia interception estimated of the *Acacia auriculiformis* as estimated in Wang et al., (2007), for the month of March. The area ratio for grass and other vegetation after classification was 0.81 to 0.19 respectively. The interception was then calculated following the Equation 7.

$$I = RF * (I_g * Area_g + I_{other} * Area_{other}) \quad (7)$$

Where I is canopy interception (mm day⁻¹), RF is rainfall (mm), I_g and I_{other} are interception loss rates of grass and other land use cover respectively (%). $Area_g$ and $Area_{other}$ are ratio of area covered by grass and other land cover respectively. The weighted interception value for the study period from 1st Oct 2004 to 30th Sept 2010 was calculated from these two vegetation cover. The interception rate was considered uniform for the area, because of a uniform vegetation cover which is Mostly grass and shrubs as suggested by Obakeng, (2007).

2.3.4. Infiltration rate

In the Unsaturated Zone Flow (UZF) Package, infiltration rate is calculated from the difference between precipitation and interception rates estimated in Section 2.3.1 and 2.3.3 respectively. The infiltrating water is converted to water content, and the water content is set to the saturated water content when the specified infiltration rate in the UZF package exceeds the saturated hydraulic conductivity, (Niswonger et al., 2011). Because of variable precipitation zones, different infiltration rates were applied to the model. A total of five different infiltration rate zones, were obtained after subtracting the intercepted rainfall in the area. This means, in this study, the infiltration rate was considered to vary spatially due to variable rainfall intensity.

2.3.5. Heads distribution

Heads are state variables that are used in the model calibration. There are 15 single time head measurement applied for steady state model calibration and 4 monitoring points with time series data (Figure 8). The single time measurements were obtained from the previous studies which were determined based on water-levels measurement in piezometers and were all recorded in the year 2005, which is within the study periods of this research.

In LNKB there are only four groundwater monitoring points with monthly data (Figure 9 a-d) extending from 1st October 2004 until 30th September 2010. In piezometer BH 7763 and BH 7764, there is a slight rise in water table between Nov 2005 and March 2006, which might be caused by a noticeable precipitation that occurred in the same period. However, this rise of water table occurs between May-December in piezometer BH 7761 and BH 7768 reflecting a delayed recharge phenomenon. A slight change of about 0.1-0.15 m groundwater level is observed as an outcome of the increased rainfall in both Piezometers.

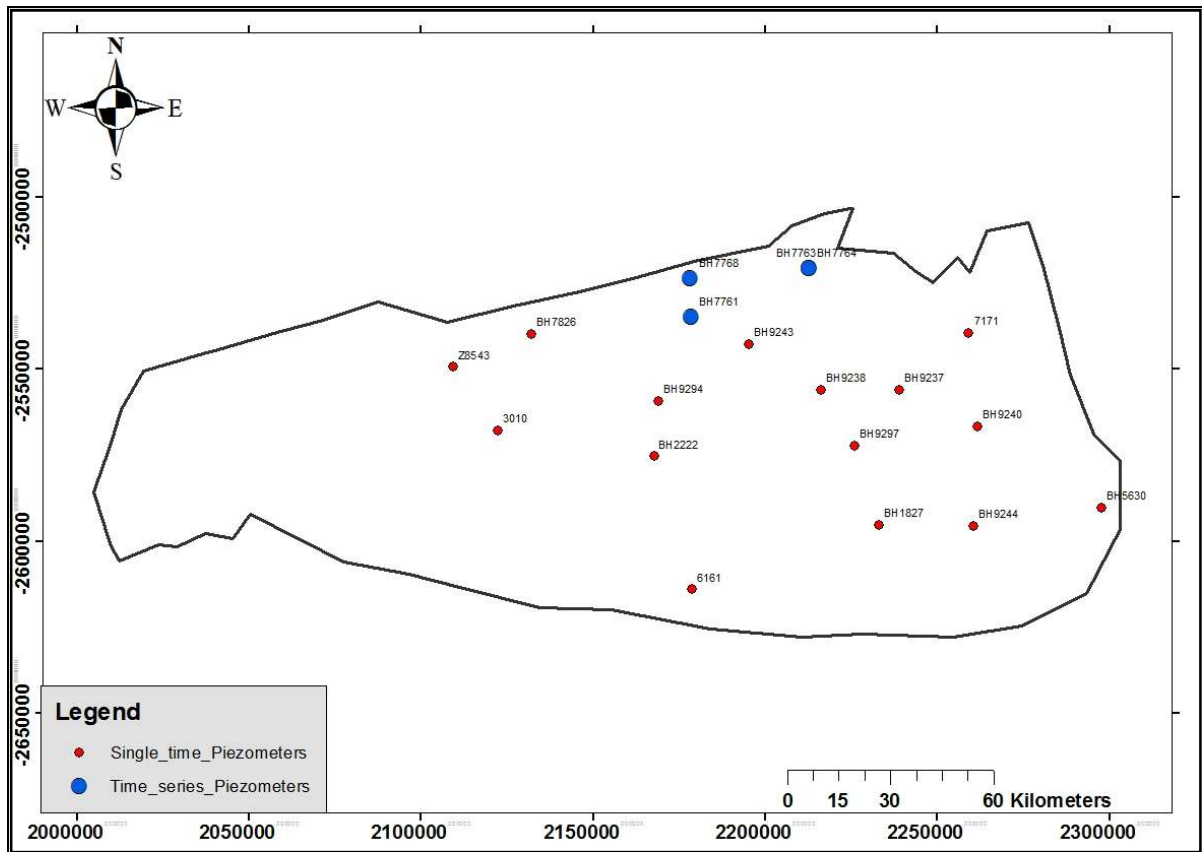
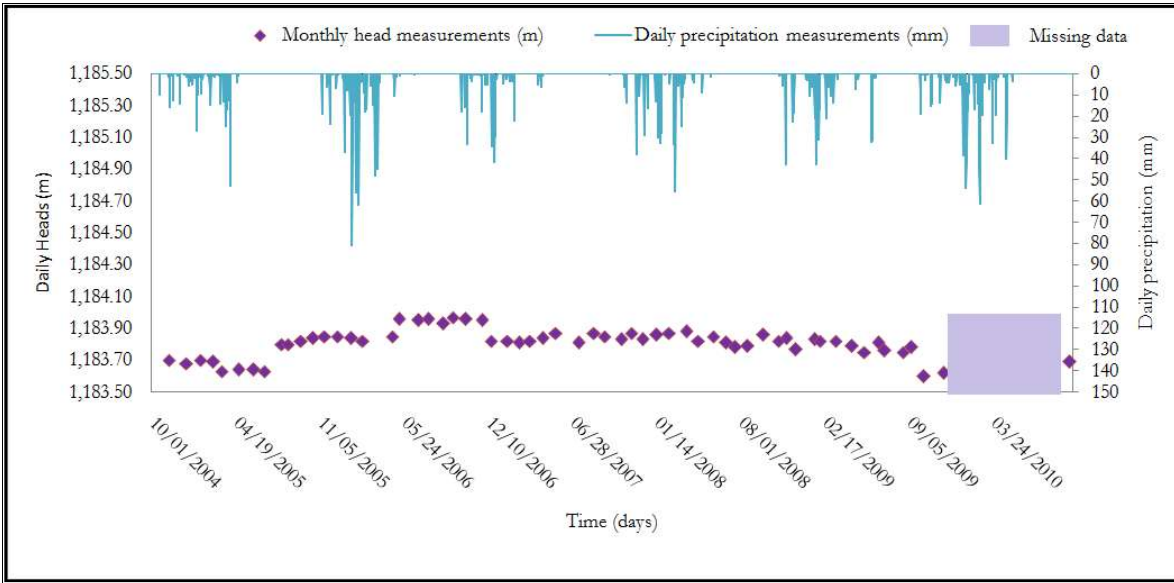
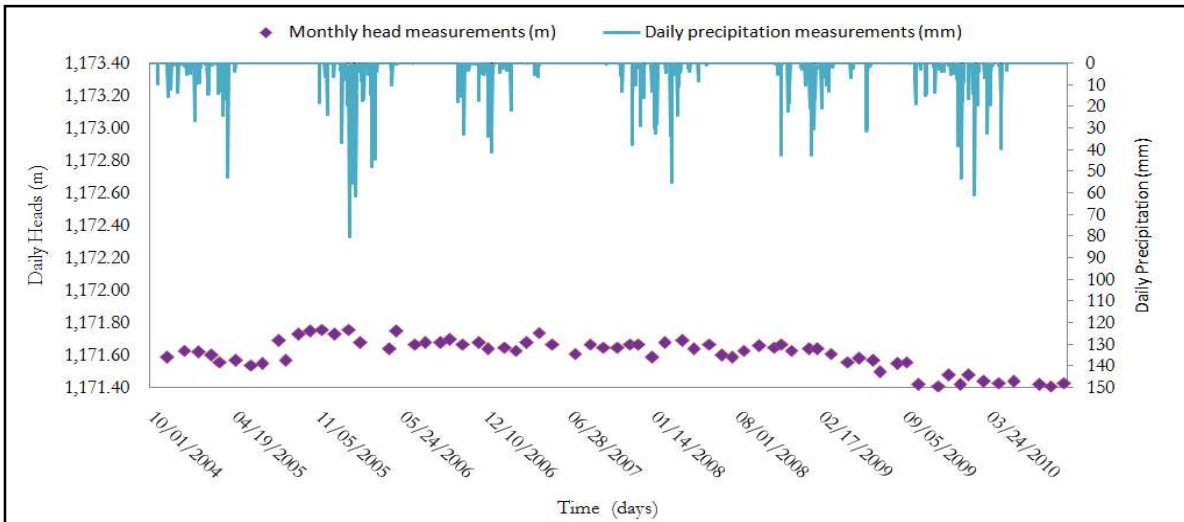


Figure 8: Spatial position of piezometric points with single time measurements and time series measurement data in LNKB

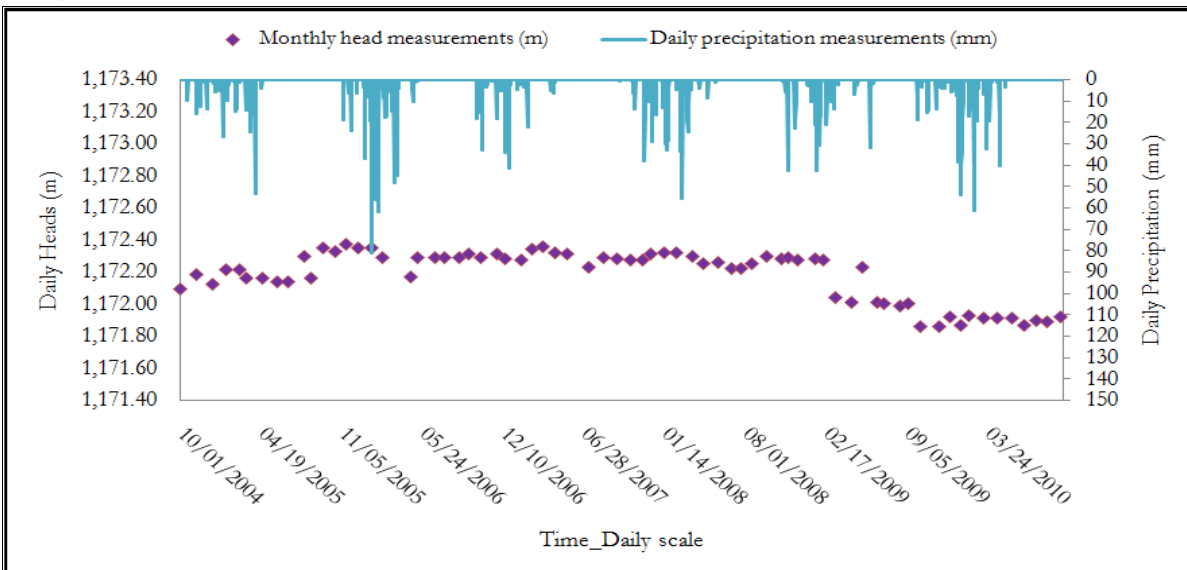
a) Piezometer BH 7768



b) Piezometer BH 7763



c) Piezometer BH 7764.



d) Piezometer BH 7761.

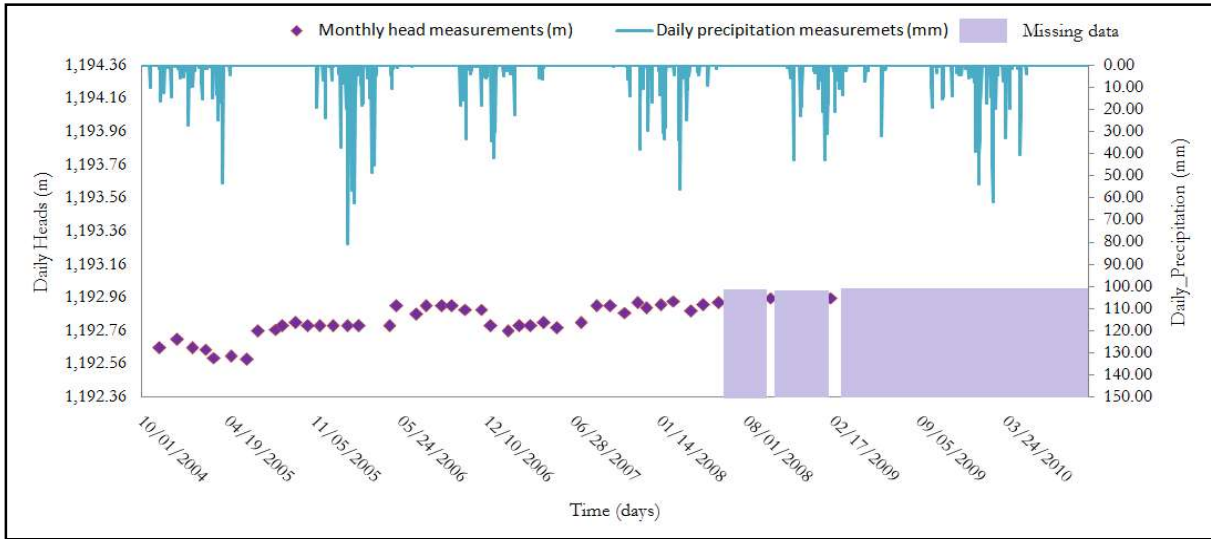


Figure 9: Time series of daily heads and precipitation.

2.4. Conceptual model of the LNKB

The reason behind constructing a conceptual model is to have a pictorial representation of the system (Figure 9). The conceptual model helps to determine the dimensions of the numerical model and design the grids,(Anderson & Woessner, 1992). In the conceptual model, all the model parameters are stated. Below is the explanation of each parameter.

2.4.1. Hydro-stratigraphic units

Five hydrostratigraphic layers were recognized in the LNKB consisting of 3 aquifers and 2 aquitards. The Kalahari Beds (unsaturated zone) as 1st layer, Stormberg Basalt (Volcanic) (2nd layer) which is the aquitard below the Kalahari aquifer. The Ntane Sandstone is the 3rd layer, the Mosolotsane-Kwetla Mudstone (aquitard) forms the 4th layer, and finally there is Ecqa aquifer, which consists of the Boritse, Kweneng and Bori formation. Only the Boritse unit was evaluated in this study, as the entirely productive boreholes end in this unit. Table 2 shows the hydro-stratigraphy used for developing the numerical model of LNKB edited from (Smith, 1984).

Table 2: Karoo stratigraphic units-Adapted from Smith 1984.

AGE	SUPER-GROUP	GROUP	FORMATION	LAYER DESCRIPTION	
CENOZOIC		Kalahari	<i>Kalahari Beds</i>	1 st layer aquifer, unsaturated zone.	Post Karoo
MESOZOIC	KAROO	Stormberg	Ramoselwana Volcanics	2 nd layer, confining - aquitard	Karoo
		Lebung	Ntane	3 rd layer - aquifer	
		Lebung/Beaufort	Mosolotsane - Kwetla	4 th layer confining - aquitard	
		Ecqa	Boritse	5 th layer -aquifer	

2.4.2. Flow systems pattern, flow direction and rates

There are no surface water bodies in the area. Groundwater flow direction is towards the Eastern direction towards the central part of Kalahari Basin. The gentle slope of the basin, with an approximated gradient of 0.00086 as explained in 1.6.3, matches groundwater gradient.

2.4.3. Preliminary water balance

Part of the water that falls as precipitation evaporates and some of that water infiltrates into the aquifer system. A high infiltration rate and high retention storage, with high transpiration, makes very little water to pass through the root zone to contribute to the aquifer recharge (de Vries et al., 2000). The recharged water either is discharged by groundwater evapotranspiration or flow down gradient, either in Ntane or in Ecqa aquifers to the eastern discharge boundary of LNKB. In addition, some negligible well abstraction are present but were not simulated in this model.

2.4.4. External and internal model physical boundary

For a groundwater modelling exercise, the boundary conditions choice is an important aspect because the boundaries affect the flow in both steady-state and transient (not part of this study) flow conditions. The physical boundaries are the most robust and defensive type of perimeter or internal boundary as they represent physical features that are easily identified in the field, (Anderson & Woessner, 1992).

In this study, internal physical boundaries were not considered in the model. However, for the external physical boundaries, for the Kalahari aquifer, in the western side, a no flow boundary was assigned. This means, there is no groundwater flow across this boundary. The no flow boundary on the side was assigned based on the water divide on the western end observed after construction of the structural model of the hydro-stratigraphic layers. The northern Kalahari boundary was assigned a no flow boundary, based on geological contact. The northern part of the LNKB is bordered with the Dwyka Karoo rocks on the NE side and Quartzite rocks of Ghanzi ridge in the NW side, with the Kalahari sand being very thin or absent in that area. Likewise, a no flow was assigned in the southern part of the Kalahari aquifer based on the flow direction of the groundwater in the LNKB. Since groundwater flow is from West to East, the model boundary was delineated parallel to the flow in southern part, making a no flow boundary condition suitable.

The eastern boundary being the discharge side was assigned a general head boundary (GHB). A GHB is head dependent flow boundary defined by two cell values, which are hydraulic conductance ($\text{m}^2 \text{d}^{-1}$) and hydraulic head at the boundary (m), governed by Equation 8 below;

$$Q_b = C_b (h_b - h) \quad (8)$$

where ; Q_b is the flow through the general head boundary ($\text{m}^3 \text{d}^{-1}$), C_b is the hydraulic conductance ($\text{m}^2 \text{d}^{-1}$), h_b is the hydraulic head at the boundary (m) and h is hydraulic head in the aquifer. Eventhough, with the nature of the Kalahari sand, the lateral groundwater movement is considered very limited, hence physical boundaries on this layer were considered non critical.

The western and northern boundary condition for the Ntane aquifer were all set to no-flow boundary delineated coinciding with the geological boundary of the Ntane aquifer. However, the southern boundary was simulated with a no flow based on the groundwater flow direction. At the discharge point on the eastern part, a general head boundary (GHB) was applied.

For the Ecqa aquifer, a no flow boundary was assigned in the northern part due to a geological boundary of the Ecqa group, with the southern boundary simulated with a no flow due to the groundwater flow direction, which is parallel to the model boundary. However, the Ecqa aquifer is deep seated towards the East, leading to groundwater flow towards this direction, and water discharges to the Central Kalahari

through GHB applied at the eastern side. The western boundary is simulated with a no flow boundary due to a water divide observed after the structural layers construction.

For the aquitards i.e. Stormberg Basalt and Mosolotsane-Kwetla Mudstone, a no flow boundary was applied for both sides of the layer boundary.

2.5. Numerical model of the LNKB

2.5.1. General concepts

In numerical modelling, the groundwater flow can be simulated in two methods, which are steady-state and transient flows. There is no change in aquifer storage with time in the steady state conditions, while in the transient condition the aquifer storage changes with time. The flow of an incompressible three dimensional groundwater system through a porous medium under a confined environment is governed by Equation 9, while for the confined layer presented in Equation 10.

$$\frac{\partial}{\partial x} \left(K_x \frac{\partial h}{\partial x} \right) + \frac{\partial}{\partial y} \left(K_y \frac{\partial h}{\partial y} \right) + \frac{\partial}{\partial z} \left(K_z \frac{\partial h}{\partial z} \right) + W = S_s \frac{\partial h}{\partial t} \quad [T^{-1}] \quad (9)$$

$$\frac{\partial}{\partial x} \left(K_x h \frac{\partial h}{\partial x} \right) + \frac{\partial}{\partial y} \left(K_y h \frac{\partial h}{\partial y} \right) + \frac{\partial}{\partial z} \left(K_z h \frac{\partial h}{\partial z} \right) + R = S_y \frac{\partial h}{\partial t} \quad [LT^{-1}] \quad (10)$$

Where:

K is hydraulic conductivity in x, y and z directions [LT⁻¹]; x, y, z are orthogonal Cartesian coordinates [L]; h is a piezometric head [L]; W = R is a source or sink [T⁻¹]; S_s is a specific storage [L⁻¹] and t is time [T].

2.5.2. Grid design

The model was constructed using a uniform grid design of 1 km by 1 km. The grid network has 149 rows and 321 columns with a total of 47,829 grid cells. The alignment was done with the projected coordinate systems WGS_1984_ARC_System_Zone_10.

2.5.3. Software selection

The MODFLOW-NWT model under ModelMuse interface was used to simulate the interaction between surface and groundwater interactions. The presence of the UZF package in this model enables the link between ground and surface water, through the unsaturated zone. Since the model developed is an integrated model, MODFLOW-NWT was found to suit the purpose of this study.

2.5.4. The Unsaturated Zone Flow (UZF) Package

The unsaturated zone is a transitional boundary of flux exchange between surface water and groundwater systems. Non-linear relationship governs the water flow through and the storage within the unsaturated zone which makes the calculation of the flow more complicated (Ely & Kahle, 2012). Even though, the development of technology in terms of software and hardware has helped to simplify the complications.

The UZF package in MODFLOW-NWT simulates the water flow and storage within the unsaturated zone, segregating the groundwater recharge and evapotranspiration from surface infiltrating water, and accounts for land surface run off to streams and lakes, (Ely & Kahle, 2012). Inputs to the UZF package include evapotranspiration demand, infiltration rate, extinction depth and extinction water content. The evapotranspiration demand and infiltration rate were estimated in sub sections 2.2.4 and 2.2.6 respectively.

The extinction depth (depth below which ET cannot be removed), was set to 70 m. The depth was set considering the maximum root depth of vegetation within the study area as suggested by, (Obakeng, 2007).

He concluded that, several tree species in the Kalahari Desert are able to extend their roots to great depths of more than 70 m. The extinction depth was considered constant throughout the LNKB area. Also, the extinction water content, i.e. water content below which ET cannot be removed from the unsaturated zone, was fixed to 0.1. The rest of the parameters in the package were accepted as default.

2.5.5. Structural model

The structural model was constructed from the borehole logs, selected from the data base prepared. A cross section (O-P) was drawn across LNKB, Figure 6). The DEM of 90 m resolution downloaded from <https://lta.cr.usgs.gov/SRTM1Arc> website of USGS, (2015) was used to define the model top. Model bottoms of aquifers and aquitard were defined from the sections obtained in the RockWorks, interpolated and imported in ModelMuse. In this case, the ASCII files of the bottoms of each layer unit were imported.

2.5.6. Layer groups

The layer groups are defined by five types of layer structures when the UZF and Upstream Weighting (UPW) packages are activated. From the constructed structural model, the Kalahari Beds form the first unconfined layer; Stormberg Basalt (volcanic) form the second confining, spatially limited layer and Ntane Sandstone form the third layer also spatially limited layer, which is partly confined by Basalt in the Eastern side.

The Kwetla and Mosolotsane Mudstone were considered the fourth confining layer at the top of the Ecca aquifer which is the fifth layer; (Figure 9).The first layer is the convertible, in which the heads in the model cells determine status of the cells. The cells are considered to be in confined or unconfined states when the heads are, respectively, above or below the cell tops. In the confined layer structure, the heads are always above the cell tops. The non-simulated confining layers, (second and fourth) use the vertical hydraulic conductivity of the confining bed (VKCB) to calculate the conductance between the two layers.

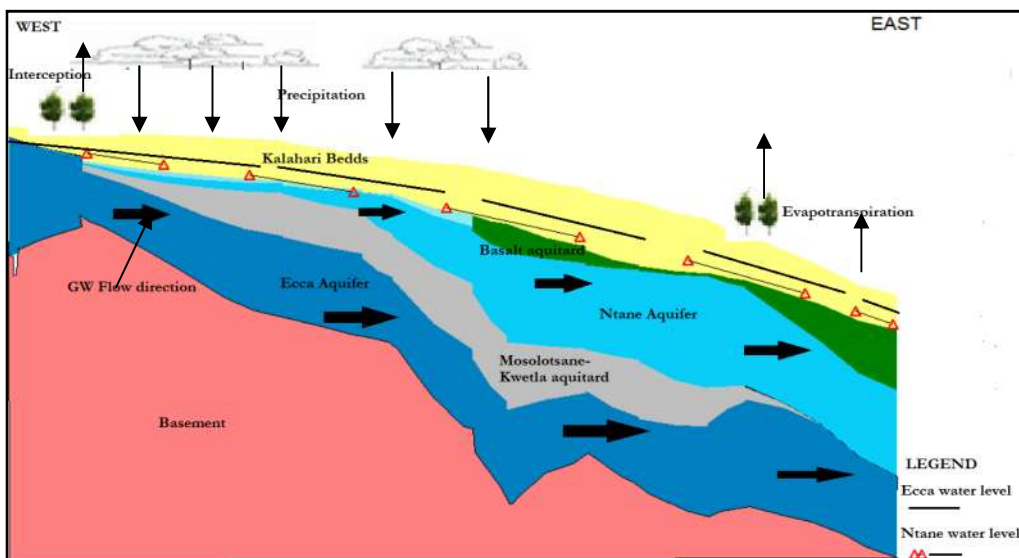


Figure (10):Conceptual model of the LNKB modified after (Rahube, 2003).

2.5.7. Driving forces

The driving forces to the model differ from one type of the model to another, depending on the purpose of that model. In this model type, the driving forces to the model included; precipitation, potential evapotranspiration (PET) and interception. These are all described in subsections 2:3:1, 2:3:2 and 2:3:3 respectively. According to (Nossent et la., 2014), he points out that, on top of the effect of

parameterisation of the model, the driving forces also play a big role on the model, hence have to be estimated accurately.

2.5.8. System parameterization

The flow packages were selected for the groundwater flow model. For simulating the flow in the unsaturated zone, Upstream Weighting (UPW) and UZF packages were selected. In the steady-state condition, the zone parameters of horizontal and vertical hydraulic conductivities (HK and VK) of the aquifer layers and the vertical hydraulic conductivity of the confining bed (VKCB) were defined in the UPW package. The recharge and discharge location (NUZTOP) were set on top layer with the VK (IUZFOPT) specified. UZF was set to simulate evapotranspiration (IETFLG), print summary of the UZF budget terms (IFTUNIT) and calculate surface leakage. The number of trailing waves (NTRAIL2) and the number of wave sets (NSETS2) were accepted by default which is 15 and 20, respectively.

The maximum unsaturated vertical hydraulic conductivity was set equal to 0.55 m d^{-1} , initial unsaturated water content set to $0.03 \text{ m}^3 \text{ m}^{-3}$, residual water content equal to $0.02 \text{ m}^3 \text{ m}^{-3}$, saturated water content was $0.45 \text{ m}^3 \text{ m}^{-3}$ and for the Brooks Corey Epsilon a value of 3 was set for the system. However, the land surface was set equal to the model top, which was the DEM. In the steady state calibration, the HK, VK and VKCB zones for the confined, unconfined and confining beds were established. The HK values for the Ntane and Ecca aquifers from Rahube, (2003), were used as initial values to start up the calibration, which ranged from $0.08 - 1.8 \text{ m day}^{-1}$ and $0.01-0.13 \text{ m day}^{-1}$ for Ntane and Ecca aquifers respectively. The conductances of the GHB were assigned to 15 m d^{-1} , 30 m d^{-1} and 20 m d^{-1} for Kalahari, Ntane and Ecca layers respectively.

2.5.9. State variables

In this study, the state variables were the groundwater heads. The initial hydraulic heads used were interpolated from the 19 observation heads in the project, which were also individually used during calibration process. The task was difficult due to the fact that, the area has deep water table and extinction depth of $70 \text{ m}+$ which caused difficulties in the model convergence.

2.5.10. Boundary conditions

The no flow boundary was set for external boundary, with a general head boundary (GHB) at the discharge area (Figure 11) in the Eastern side. The reasons for assigning the flow boundaries in the LNKB are explained in details in 2.4.4.

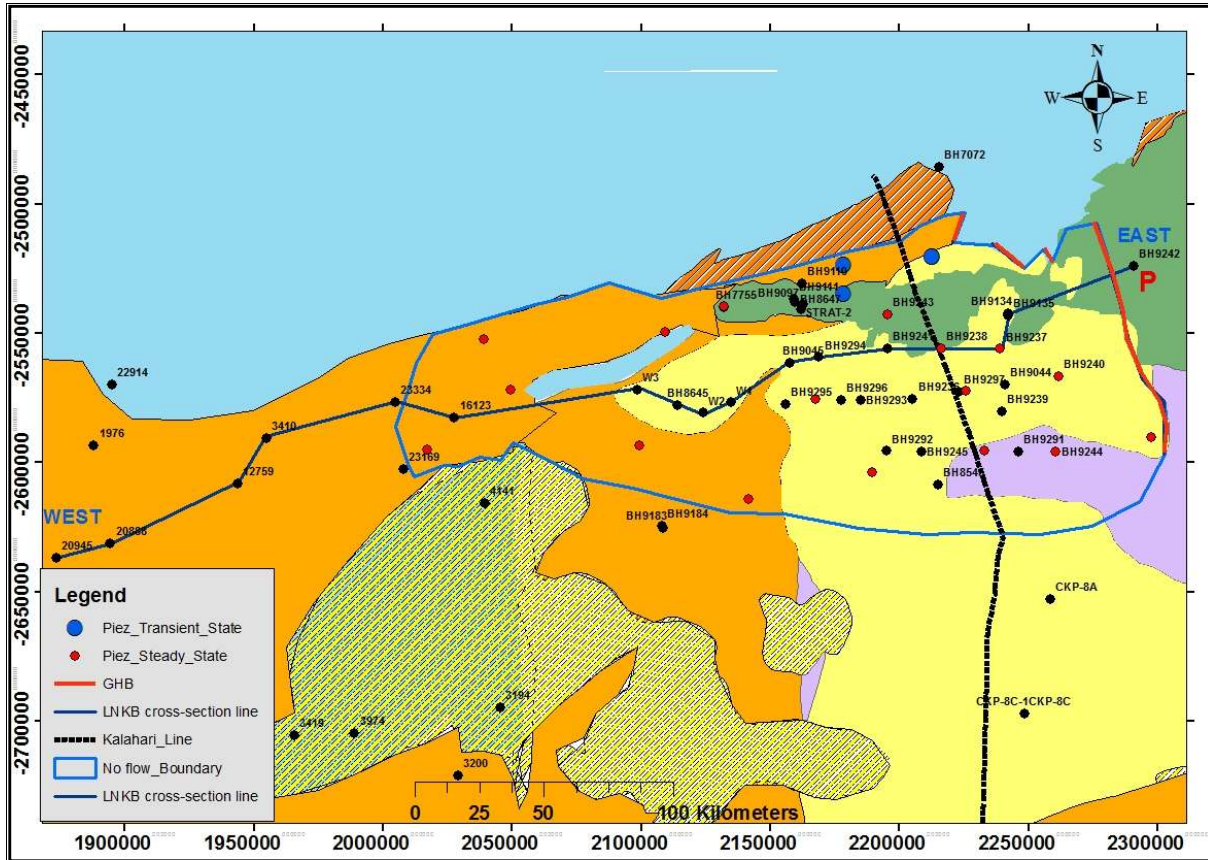


Figure: (11) Boundary conditions for the groundwater flow model.

2.5.1. Time discretization

The units of the model were set to meters for length and days for time. The time frame of the steady-state model simulation was six hydrologic years from 1st October 2004 to 30th September 2010. The data for this period was averaged to get one input value for all the data needed by the steady-state model. The achieved solution of groundwater heads of the calibrated steady state model were assessed for errors.

2.6. Numerical model calibration.

2.6.1. General concepts

Model calibration was done to find the good match between the observed and simulated heads. Only steady state calibration was performed. The MODFLOW-NWT which has the Newtonian solver was selected and used for the computations in the study. This solver is compatible with the Upstream Weighting (UPW) package. The maximum number of iterations was set to 1000, and other settings were accepted as default, with the model complexity fixed to simple.

During calibration process, the parameters (in this case the hydraulic conductivities) were adjusted by trial and error approach, until the simulated and observed heads had good match. The average driving forces for the specified time frame (1st Oct 2004-30th Sept 2010) were calculated, which in this regard involved precipitation, evapotranspiration and interception.

Despite the fact that, calibration could be done in automated way, using PEST, the trial and error method was adopted as it incorporates site specific knowledge and ensures gained insight of model behaviour during calibration (Hassan et al., 2014). During model calibration, it was taken into account that, it is difficult to get

the exact values of the parameters because of the uncertainties which are associated with the groundwater models. Such sources of the uncertainties may include model parameters, a conceptual model, observation data and boundary conditions, (J. Wu & Zeng, 2013). Even though, these effects of uncertainties on calibrated model was studied using an approach of sensitivity analysis, as suggested by (Bear & Cheng, 2010). After recognizing the more sensitive parameters in the model, they were treated with special attention during the calibration process. An accuracy assessment was done to observe the accurate determination of the most sensitive parameters.

To assess the reliability of the calibrated parameters, the mean error (ME), mean absolute error (MAE) and root mean square error (RMSE) were used as given in equations (11), (12) and (13) respectively. According to Anderson & Woessner (1992), the magnitude of changes in heads in a model domain determines the maximum acceptable value of calibration criterion. Regarding water balance, the calibration was assessed by discrepancy between total inflows and outflow which, calculated as ratio of the difference between total inflow and outflow to the total inflow or outflow. Anderson & Woessner, (1992) considered an error of 1% to be acceptable, though a value lower than that is desired.

$$ME = \frac{1}{N} \sum (H_{obs} - H_{sim}) \quad (11)$$

$$MAE = \frac{1}{N} \sum |H_{obs} - H_{sim}| \quad (12)$$

$$RMSE = \sqrt{\frac{1}{N} \sum (H_{obs} - H_{sim})^2} \quad (13)$$

2.6.2. Sensitivity analysis

Two sensitivity analyses were performed, in which the first analysis was to investigate the effect of the calibration parameters which included HK, VK and VKCB. The analysis was performed using the RMSE variation as the parameters changed. The changes on the parameters were made from -30% through 0% to 30% increase or decrease of the proposed parameter values. The same approach was used to assess the sensitivity of the UZF parameters and general head conductances to the model and finally the results were analyzed.

2.6.3. Water budget

In the Modflow-NWT run under ModelMuse, there are two possibilities of getting the water budget of the model. In the first option, the listing file is used, which gives the water budget for the composite model. The water budget from this file is volumetric ($m^3 \text{ day}^{-1}$), and does not give the budget for the individual aquifers in the model.

The second option is by the use of Zone budget, (Winston, 2009). This overcomes the short comings observed in the first option. When this option is used, the model calculates the water budget for individual aquifer, hence giving a picture on the potentiality of each aquifer. Moreover, together with the water budget of the individual aquifers, this option also calculates the water budget for the composite model. Implementation of the second option is through ZONE BUDGET which is under Post processors in the MODFLOW Packages and Programs main window. The ZONE BUDGET tool was used to calculate and retrieve the water budgets of the Kalahari beds, Ntane and Ecqa aquifers as well as the composite water balance for the whole Ncojane-Lokalane Karoo Basin (LNKB). To explain the general water balance for the basin, Equation (14) solves and explains all the components involved in the system

$$Q_{Lin} + P = ET + Q_{Lout} + \Delta S \quad (14)$$

Where: P is the precipitation rate, ET is the total evapotranspiration as per Equation 15, Q_{Lout} and Q_{Lin} are the lateral outflow and inflows through a general head boundary and ΔS is the change in storage in steady state equal to zero.

$$ET = ET_g + ET_{uz} + I \quad (15)$$

" I " is the canopy interception, ET_{uz} is the unsaturated evapotranspiration and ET_g is the groundwater evapotranspiration. In the steady-state model solution, ET_{uz} is zero. Likewise, the water balance of the land surface and the unsaturated zone is expressed in equation (16) below;

$$P + Exf_{gw} = I + Ro + R_g + ET_{uz} + \Delta S \quad (16)$$

The Ro which is the total runoff into the streams was considered zero in this case, R_g is the gross recharge (uzf recharge) and ΔS is zero as the simulated flow is steady state. Exf_{gw} , which is groundwater exfiltration was also not regarded as relevant; the water table in the area is deep; so the chance for groundwater exfiltration to occur is very limited. For the groundwater exfiltration to occur, the simulated heads should be above the land surface, which is not possible in this area. Re-writing equation (16);

$$P = I + R_g \quad (17)$$

Equation (15) can further be re-written to include the aspect of actual infiltration (Pe) and the gross recharge (R_g) in the unsaturated zone as follows;

$$P + Exf_{gw} = I + Pe \quad (18)$$

$$Pe = R_g + ET_{uz} \pm \Delta S \quad (19)$$

For steady state flow, $Pe = R_g$

The water balance of the saturated zone is expressed in Equation 20

$$Q_{Lout} + R_g + Q_{slin} + Q_{Vin} = ET_g + Exf_{gw} + Q_w + Q_{Lout} + Q_{slout} \pm \Delta S_g + Q_{Vout} \quad (20)$$

Where, Q_{slin} is the stream leakage into the groundwater, Q_{slout} is the groundwater leakage into the stream, ΔS_g is the change in the groundwater storage and Q_w is well discharge. In this case, Q_{slin} and Q_{slout} are zero. Likewise, Exf_{gw} , Q_w and ΔS_g are also zero.

The net recharge in the Basin was assessed from the gross recharge as the inflow component and the groundwater exfiltration and ET as the outflow components, following (Hassan et al., 2014) Equation 21 below.

$$R_n = R_g - Exf_{gw} - ET_g \quad (21)$$

R_n is the net recharge, R_g is the gross (total) recharge, Exf_{gw} is the groundwater exfiltration and ET_g is the groundwater evapotranspiration. In order to avoid confusions, Exf_{gw} is considered zero and this is calculated as the surface leakage factor by the model.

3. RESULTS AND DISCUSSIONS

3.1. Structural modelling

3.1.1. Stratigraphic cross-sections

Stratigraphic cross-sections presented in Figure 12 - 18, follow nomenclature of the Karoo stratigraphic units Smith, (1984). The NW-SE cross-sections (A-B, C-D, E-F, and G-H) and SW-NE (I-J, K-L, M-N) were drawn, following the cross-section lines marked in (Figure 6). The obtained sections are presented below.

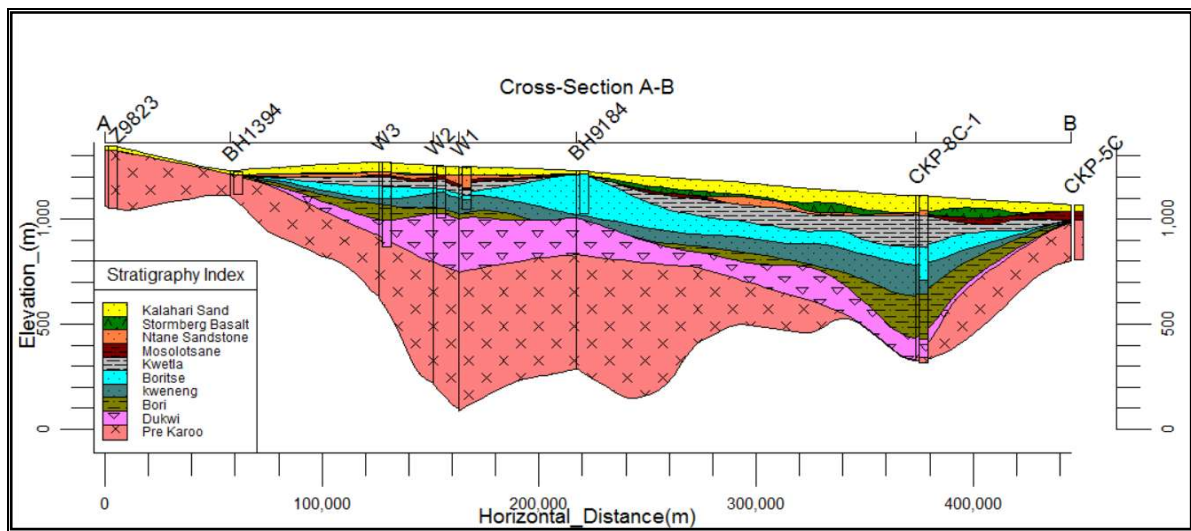


Figure 12: Stratigraphic cross-section A-B as shown on Figure 6.

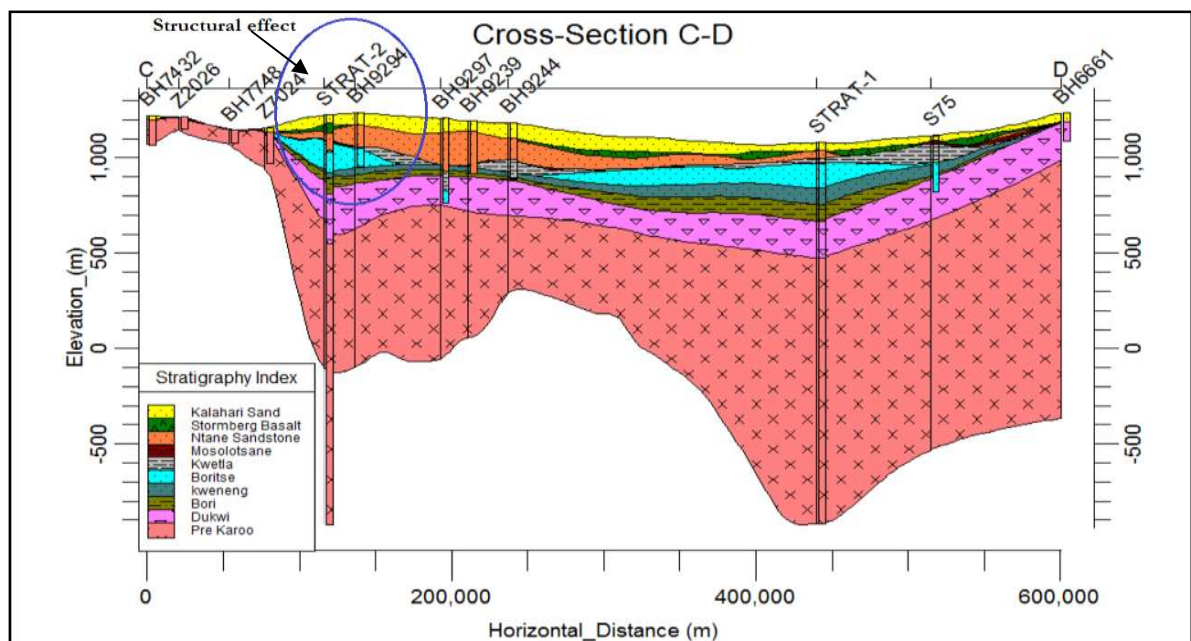


Figure 13: Stratigraphic cross-section C-D as shown in Figure 6.

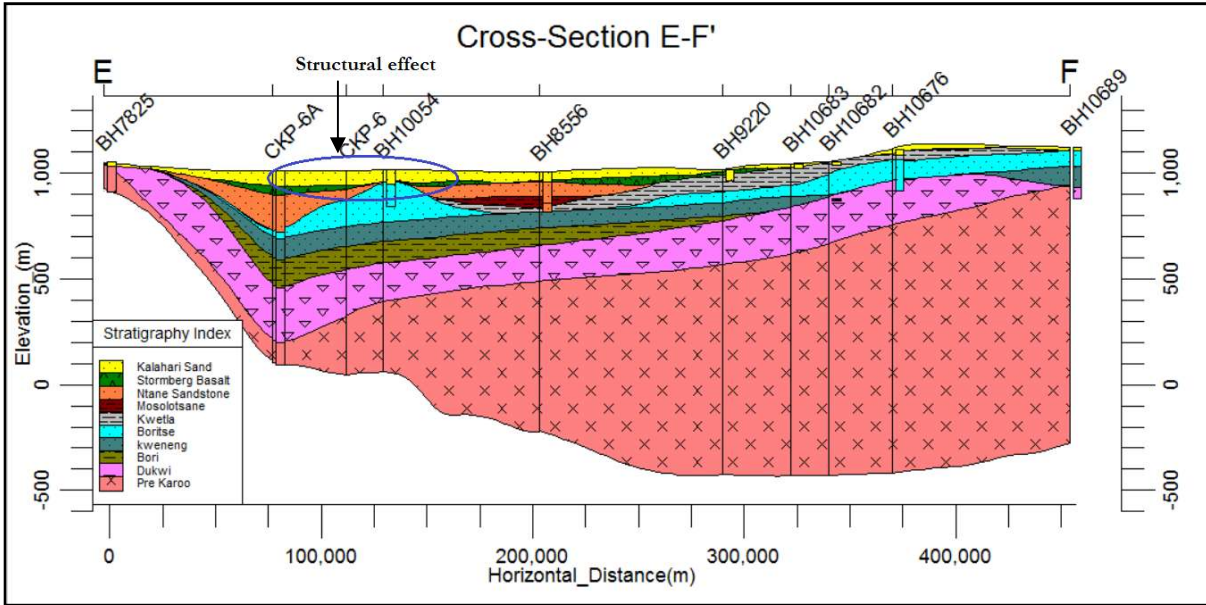


Figure 14: Stratigraphic-cross section E-F as shown in Figure 6.

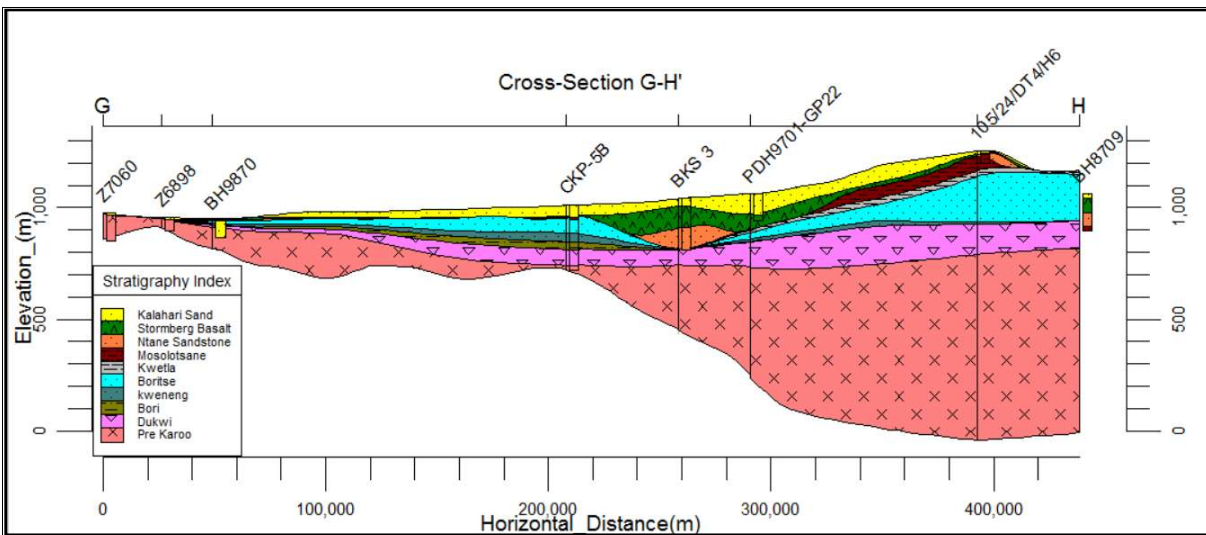


Figure 15: Stratigraphic cross-section G-H as shown in Figure 6.

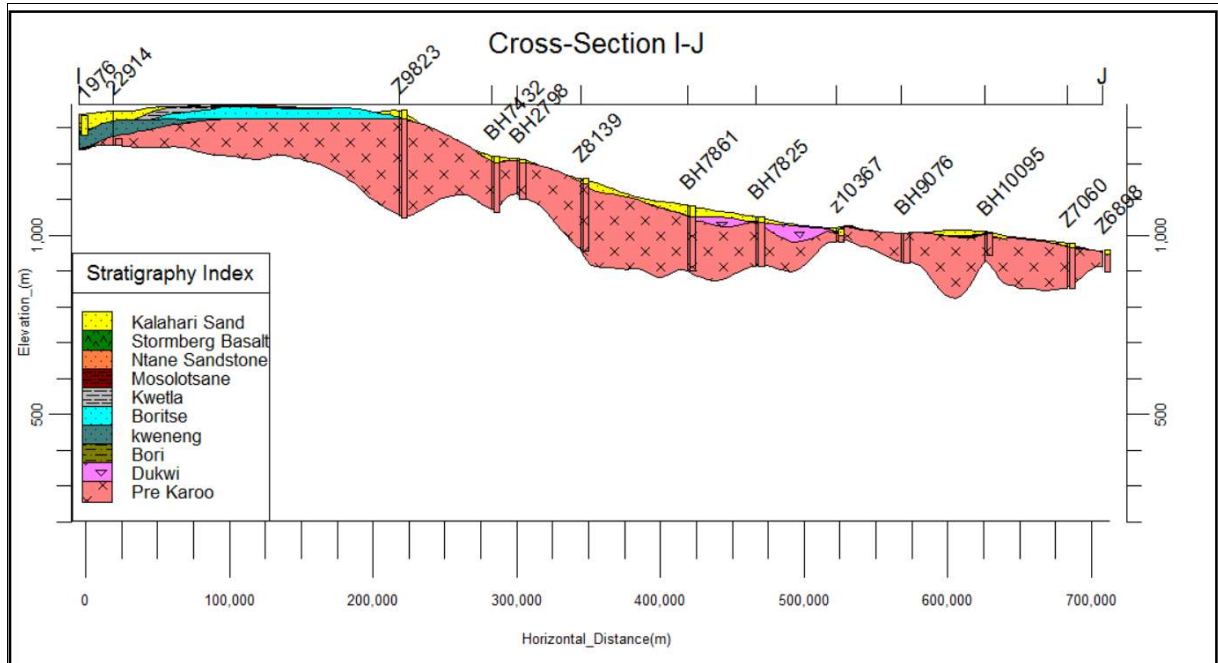


Figure 16: Stratigraphic-cross I-J as shown in Figure 6.

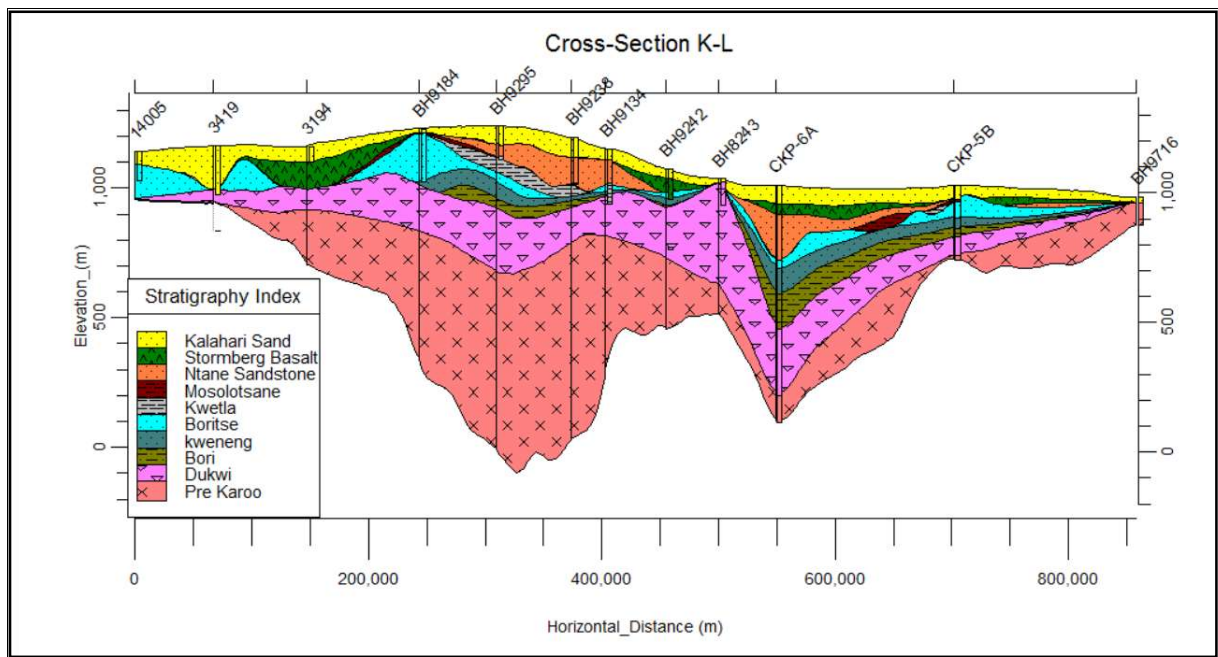


Figure 17: Stratigraphic cross-section K-L as shown in Figure 6.

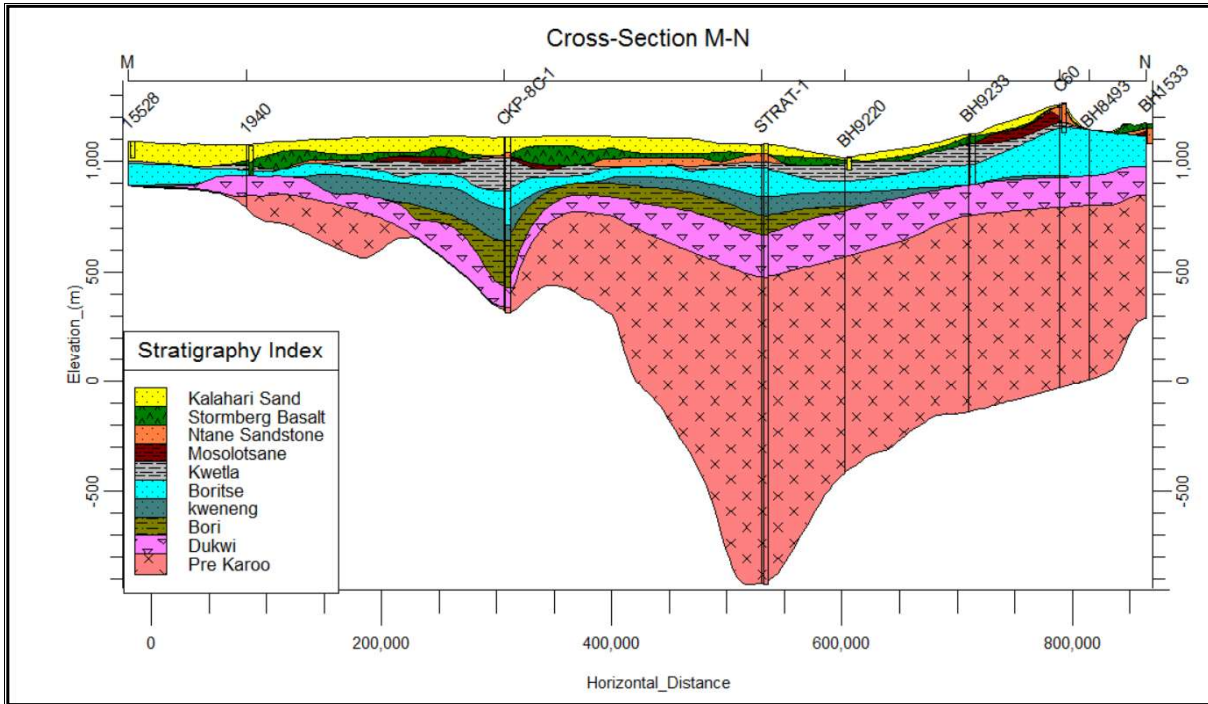


Figure 18: Stratigraphic-cross section M-N as shown in Figure 6.

Generally, all NW - SE sections which are A-B, C-D, E-F and G-H present the non- deformed Karoo strata, while the SW-NE sections (I-J, K-L, M-N) are reflecting the deformed Karoo strata, affected by the major structures. The presented cross-sections, well depict and confirm basin type of the structure analysed.

3.2. Hydro-stratigraphic cross-sections

The same cross-section lines marked in (Figure 6) were used to create and present hydrostratigraphic cross-sections of the KKB.

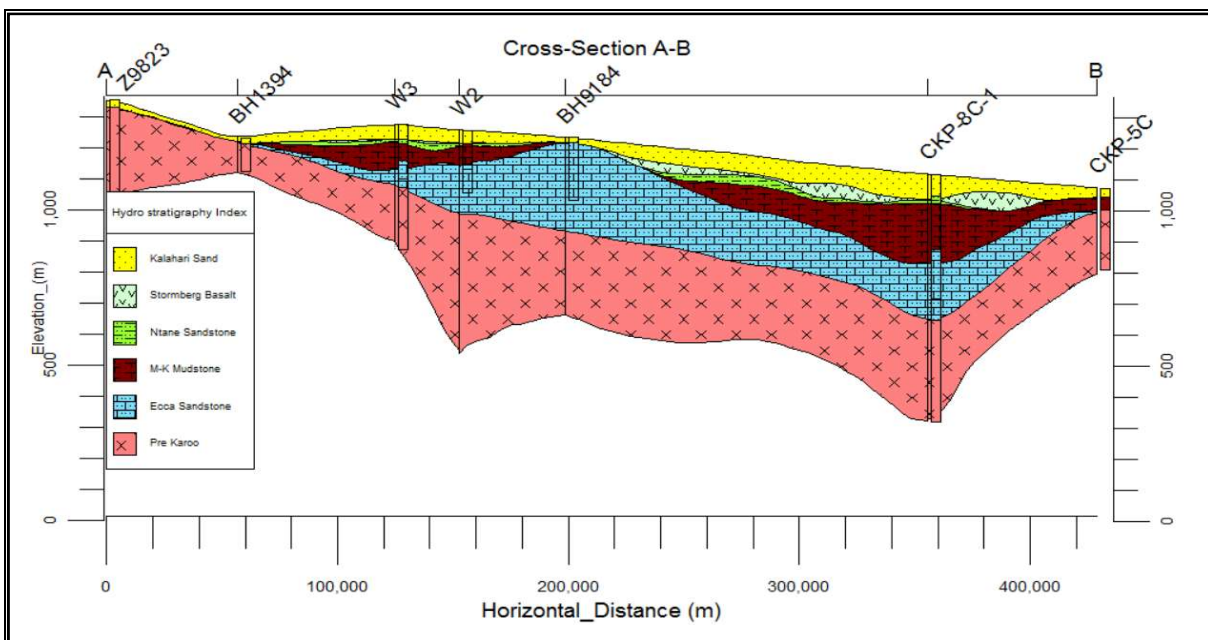


Figure 19: Hydro-stratigraphic cross-section A-B as shown in Figure 6.

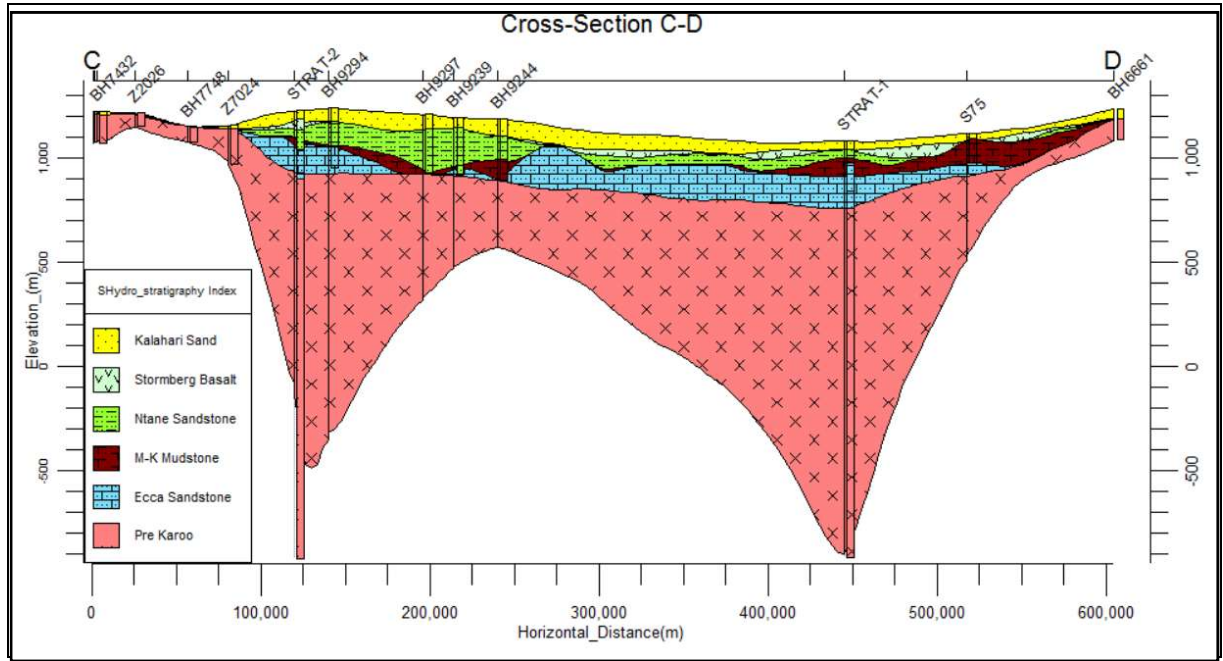


Figure 20: Hydro-stratigraphic cross-section C-D as shown in Figure 6.

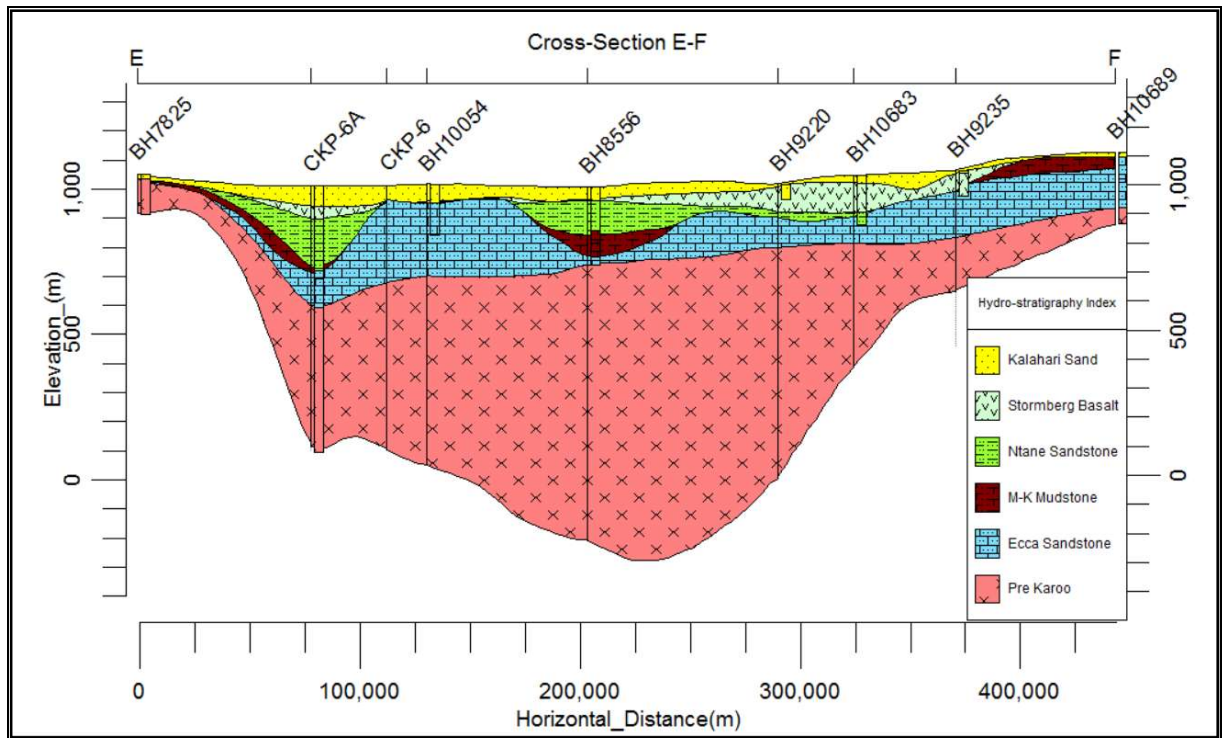


Figure 21: Hydro-stratigraphic cross-section E-F as shown in Figure 6

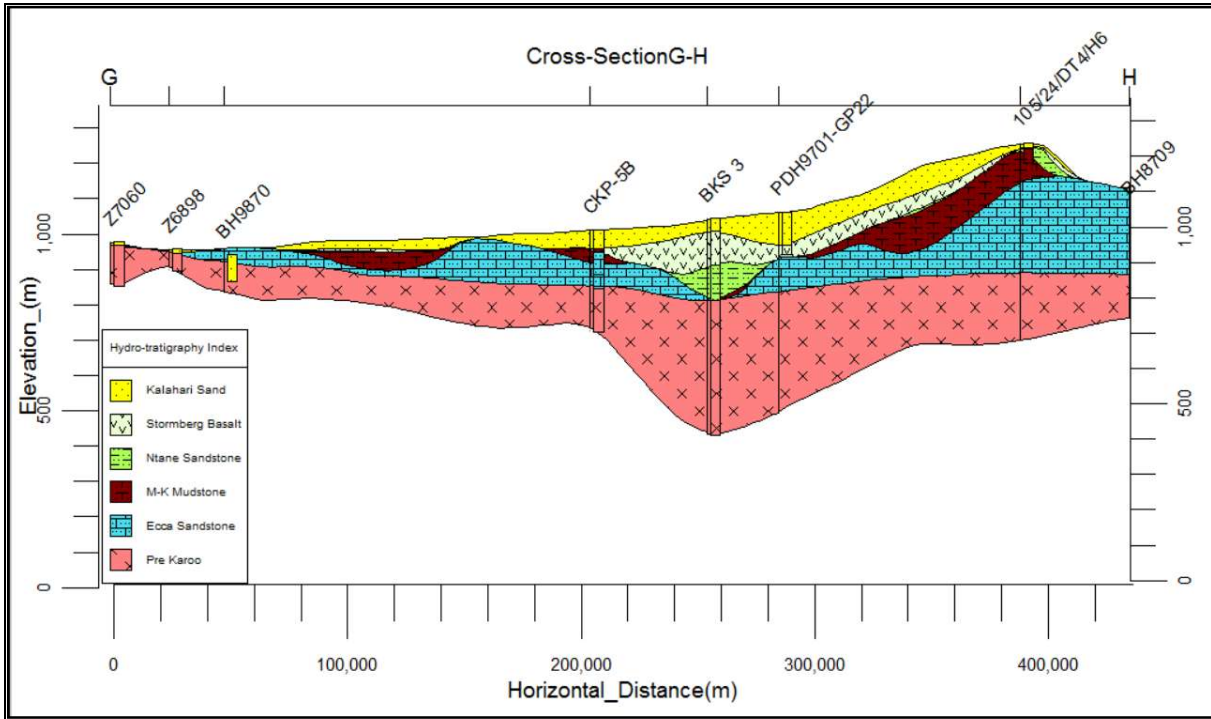


Figure 22: Hydro-stratigraphic cross-section K-L as shown in Figure 6.

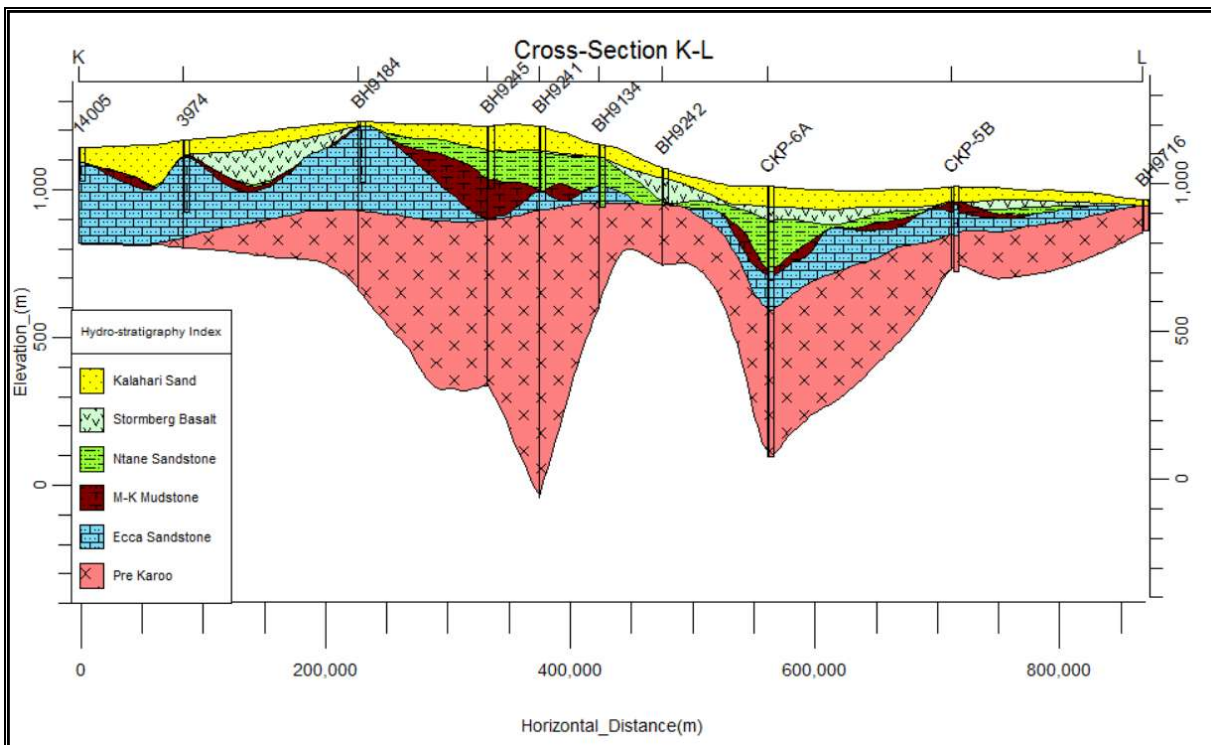


Figure 23: Hydro-stratigraphic cross-section through point K-L as shown on Figure 6.

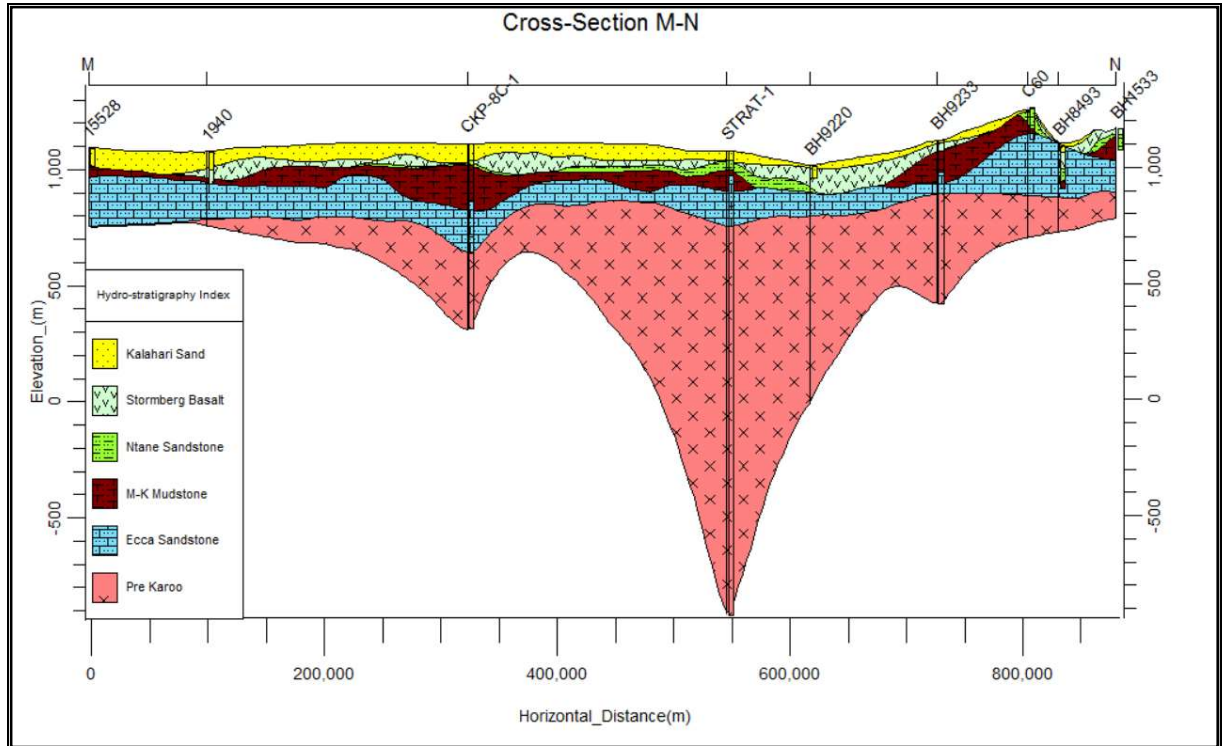


Figure 24: Hydro-stratigraphic cross-section M-N as shown in Figure 6.

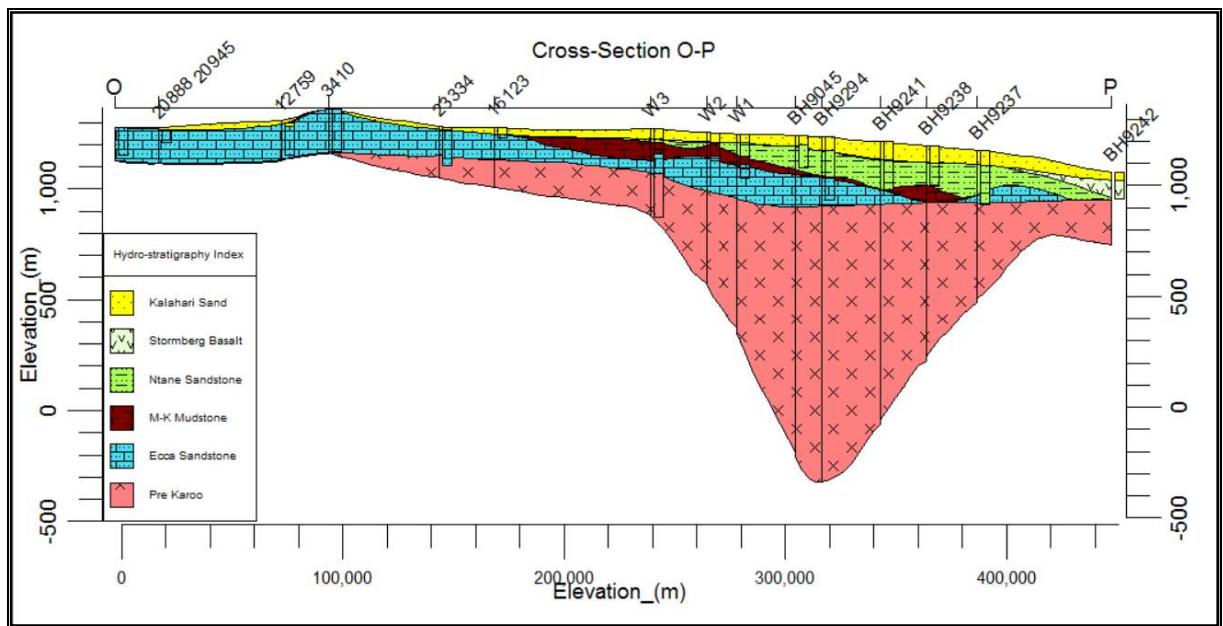


Figure 25: Hydro-stratigraphic cross-section through point O-P as shown on Figure 6.

From the hydro-stratigraphic sections presented above, it can be concluded that, two hydrostratigraphic layers, Kalahari Sand and Ecca Sandstone have generally spatially continuous extent. In contrast, the Stormberg Basalt, Ntane Sandstone and M-K Mudstone layers are spatially limited. These layers are observed to pinch out in all the cross-sections drawn above. Remarkable is, that towards east, first Ntane Sandstone wedges and then M-K Mudstone, creating recharge condition to Ecca Sandstone which over there is overlain only by relatively thin Kalahari Sand (Figure 24). The Mosolotsane-Kwetla Mudstone aquitard, which separates Ntane and Ecca aquifers, is observed to be continuous in the southern part of the KKB with a very thin layer around BH 1940 as presented in Figure 24. In contrast, the Ntane and

Ecca aquifers are in hydraulic contact in the places where Mosolotsane-Kwetla Mudstone layer is missing as observed in Figures 19, 20, 21, 22 and 23, with Figure 25 presenting the structural layers of the LNKb drawn through the cross-section line O-P in Figure 6. The pre Karoo layer is considered the basement in all the hydrostratigraphic layers, which show variable thicknesses as the result of structural deformations.

3.3. 3D Stratigraphic model

Solid modelling is a true 3-dimensional gridding process, used to create a " box" of regularly-spaced nodes from an irregular-spaced data, (Lewandowski, 2015). The RockWorks utilities Solid/Model tool creates solid models from X, Y, Z data listed in the datasheet or in an external ASCII file. The borehole manager Lithology, (Profile, Section, Fence and Model) create the solid models from lithology, interval-or point sample quantitative data or fracture data in the respective data tabs.

Once the software knows the dimensions of the study area, the program divides it into three-dimensional cells or "voxels," their dimensions automatically or user-determined. Each voxel is defined by its corner points or nodes. Each node is assigned the appropriate X, Y, and Z location coordinates according to its relative placement within the study area. Interpolation of the surfaces was done using the Kriging method as explained in the subsection (2:1). With the solid model, we can see execute distribution of the lithology and stratigraphy. The lithological distribution can be displayed as a 2- dimensional section (multiple slices) or profile (1 slice). In this study, for the presentation purpose, mainly the 2-dimension section approach was used.

The 3D stratigraphic and hydrostratigraphic model outputs were produced and presented in Figure 26 and 27. The 3D models, show, that the layers in the western side of the study area are thinner and elevated as compared to the layers in the eastern side. This reflects the structural effect on the study area, especially along the Kalahari line, which cuts across the LNKb in the North-South direction. The western side of the Kalahari line is uplifted while the eastern side downthrown.

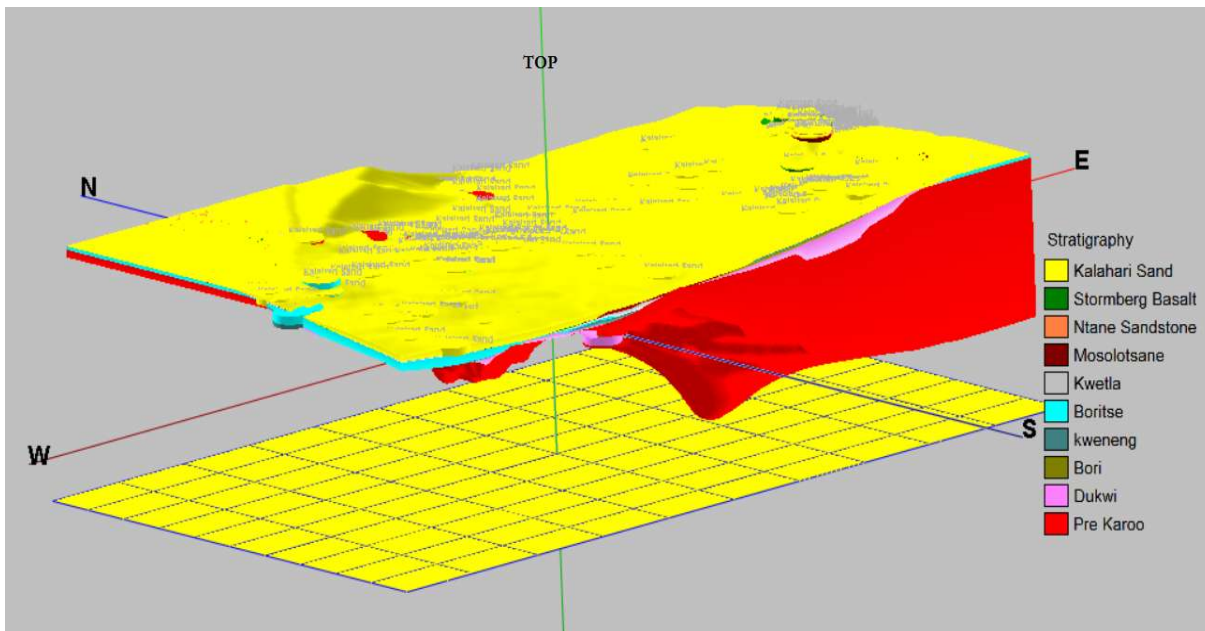


Figure 26: 3D Lithostratigraphic model of the KKB

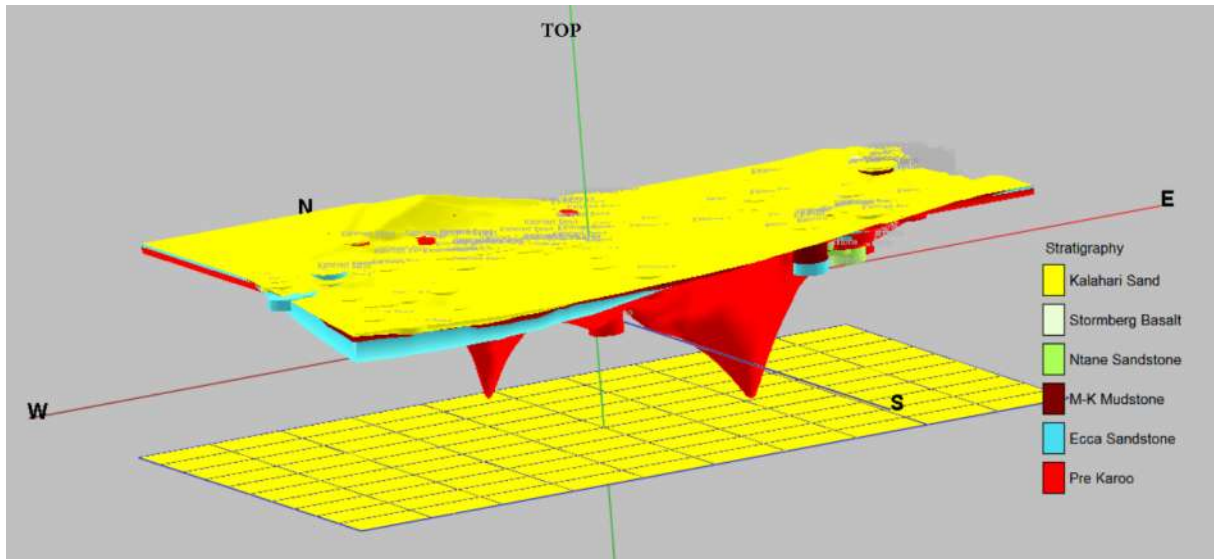


Figure 27: 3D Stratigraphic model of the KKB.

3.3.1. Thickness of hydrostratigraphic layers

After interpolation of the each lithological thickness defined by hydro-stratigraphic layers, classified raster images of thickness each lithological layer were obtained. Figures 28 - 32 show spatial thickness variability of each hydro-stratigraphic layer of the Kalahari Karoo Basin, with a summarized thickness values per hydrostratigraphic layer presented in Table 3. Lastly, the modelled hydro-stratigraphic thicknesses were validated against the known geology of Botswana.

3.3.1.1. Kalahari group (Kalahari Sand)

The Kalahari Sand is the uppermost loose sand (mainly, unsaturated zone). It is composed of relatively homogeneous sandy material, varying in thickness, colour, composition and grain size. It is represented by loose to poorly consolidated fine sand and silt of various colours ranging from orange, white, yellow, brown, cream greyish brown, with frequent minor sand, silt, and clay intercalated lenses, (Smith, 1984). This is a post-Karoo eolian sand unit of the Cenozoic age. It is considered the uppermost hydro-stratigraphic layer in the numerical groundwater of LNKB forming mainly the unsaturated zone and fragmentarily the unconfined aquifer, where water table of the Ntane Sandstone aquifer occurs.

The thickness of Kalahari Sand is highly non uniform because in some areas sand is washed out by eolian processes. It is thicker along the SW-NE line, parallel to the Makgadikgadi line, with a range from 0 m-189 m. The unit follows the trend of the Karoo formations, while narrowed in the non-Karoo formations. It is thin (50 m) area to the South of Zoetfontein Fault and along the Ghanzi-Chobe Belt, but the thickest in the SW corner of the KKB; (Figure 28). The thickness of the Kalahari Sand layer is extremely important factor constraining recharge to groundwater as the sand beds determines the downward percolation of water from the surface but also evapotranspiration from groundwater (ET_g) and unsaturated zone (ET_u), i.e. the thinner the beds the higher the possibility of groundwater recharge, but also ET.

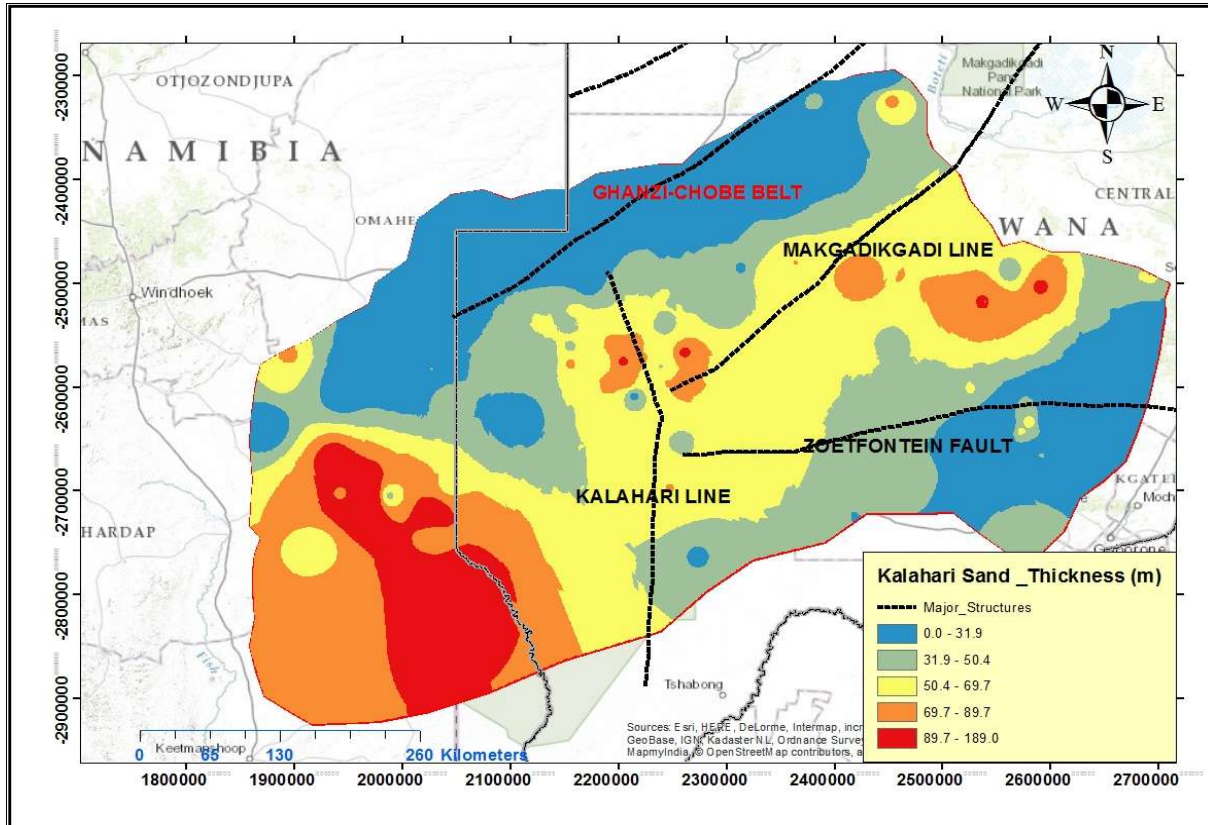


Figure 28: Spatial thickness variation of the Kalahari Sand layer.

3.3.1.2. Stormberg Basalt (Volcanic)

Stormberg Basalt is crystalline, massive amygdaloidal basalts. It is the topmost layer of the Karoo sequence, sitting on top of the Ntane sandstone and below the Kalahari group. The Stormberg Basalt is located, in the eastern part of Kalahari Line and north of the Zoetfontein Fault, with the thickness range from 0 m to 329 m, (Figure 29). The Makgadikgadi Line cuts across this lithological unit marking the depositional environment being within the structurally controlled regime. As elsewhere in the Botswana, there is very likely to be considered local variation in the basalt thickness as a result of structural movement as well as the uneven depositional surface, (WCS, 2012).

Where uplifting has occurred, resulting in horst structures, the Stormberg Basalt has been eroded and its thickness reduced (WCS, 2012). Where significant downthrown-faulting (> 200 m) has occurred, leading to grabbed structures, which forms groundwater flow barriers. Generally the Stormberg Basalt does not constitute an aquifer in the KKB; although some water strikes have been encountered in some boreholes due to faulting and fracturing. These structures are however believed to be localised and not hydraulically connected. Where the structures are deep, propagating into the Ntane Sandstone below, they can form potential groundwater recharge zones, (WCS, 2013). The Stormberg Basalt forms the second hydrostratigraphic layer, considered as an aquitard.

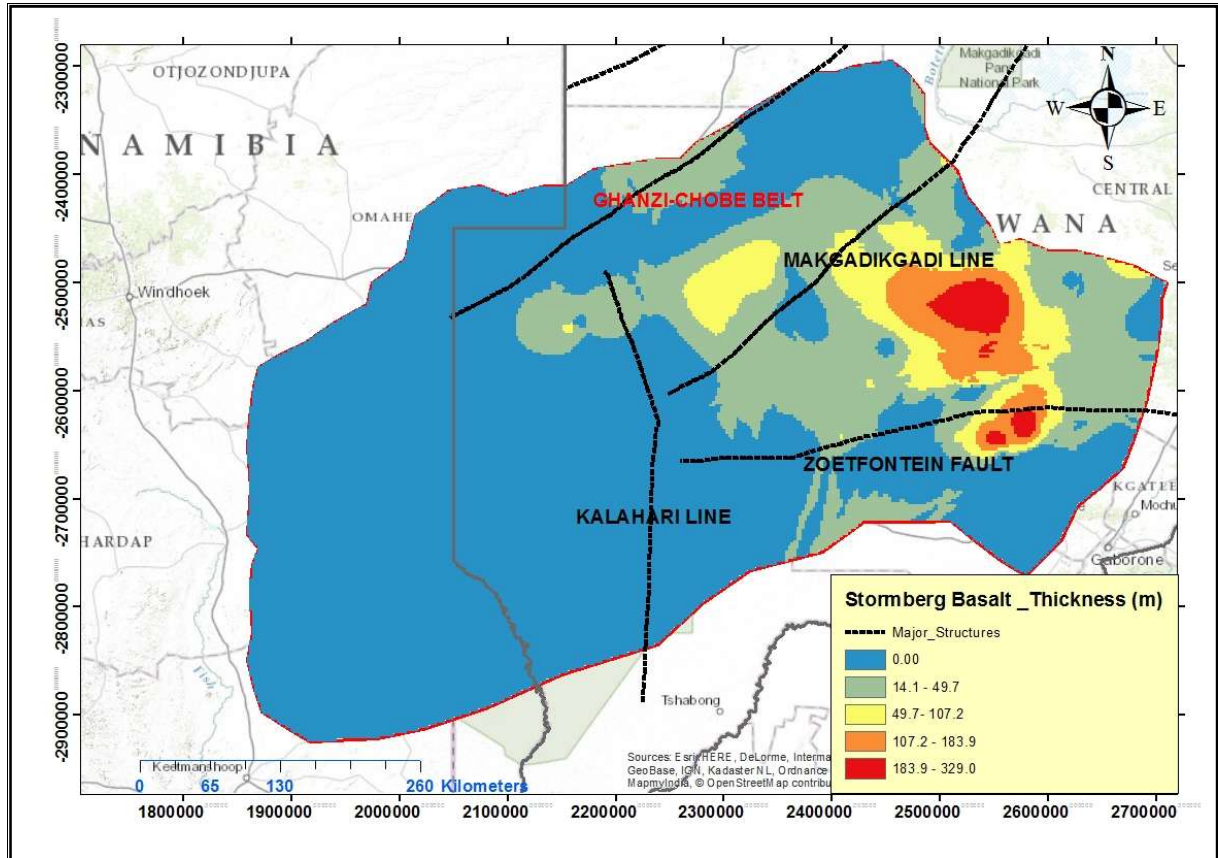


Figure 29: Spatial thickness variation of the Stormberg Basalt layer.

3.3.1.3. Ntane Sandstone

The Ntane Sandstones are fine to medium grained, clean, brownish red/pink, often calcretized in zones. Its thickness is irregular and eroded in some points. It is thickest at the central part of the KKB, at the eastern side of the Kalahari line. As observed in the Figure 30 South-Western part of the KKB. The calculated thickness of Ntane Sandstone ranges from 0 to 518 m, (Figure 30). Water strikes in this layer occurs at its side, just below the Basalt unit, if present (WCS, 2013). The Ntane Sandstone is the third hydro-stratigraphic layer in the LNKB numerical model, forming productive aquifer.

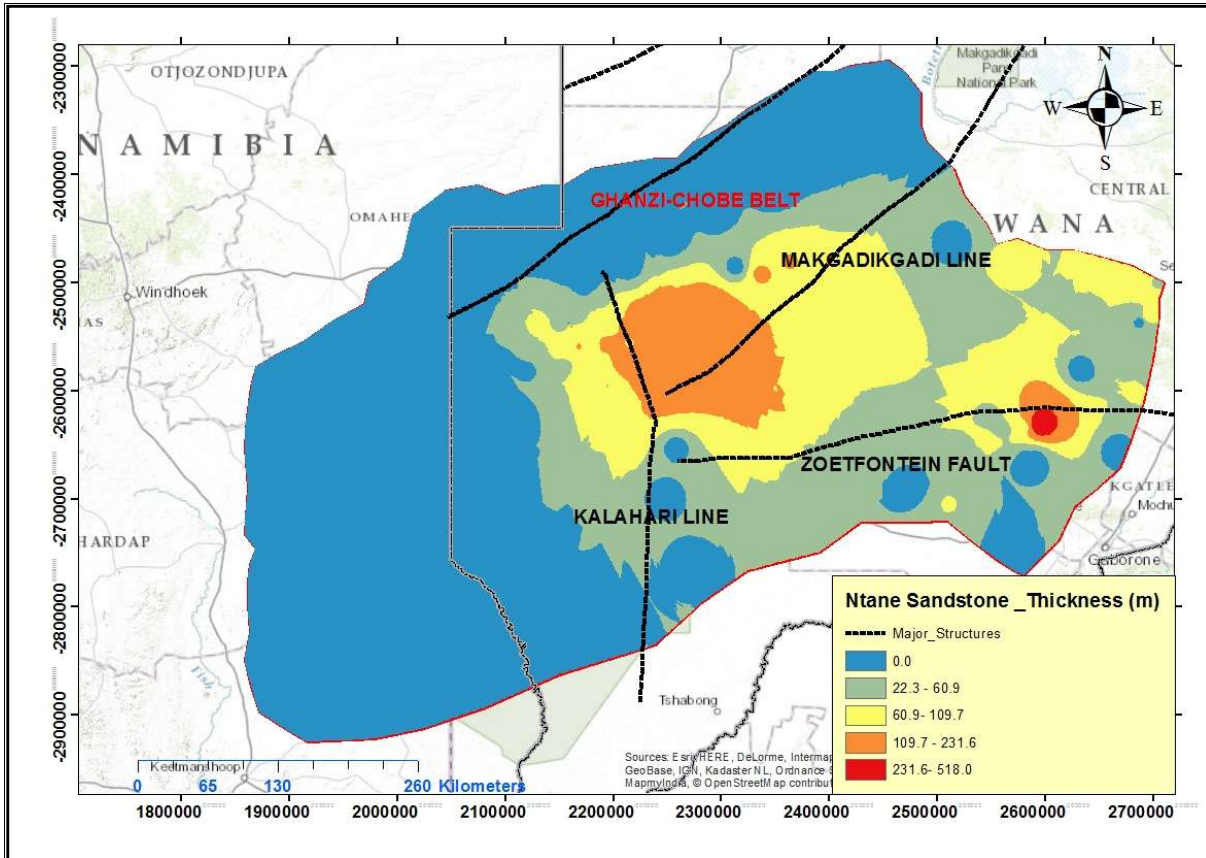


Figure 30: Spatial thickness variation of the Ntane Sandstone layer.

3.3.1.4. Mosolotsane -Kwetla Mudstone and Siltstone

The Mosolotsane-Kwetla (M-K) Mudstone and Siltstone hydrostratigraphic layer is underlying the Ntane Sandstone. This layer is formed by two lithological units, which are Mosolotsane of Lebung Group and Kwetla of Beaufort Group. The M-K layer is formed by red/brown greenish mudstones and siltstones with fine to medium, occasionally coarse, intercalated sandstones, with basal conglomerate in places, (Smith, 1984). The layer varies from impermeable to semi-permeable and is mostly observed in the southern side of the Makgadikgadi Line and localized in some places western side of the Kalahari Line. The low permeability nature of this layer, ensures a very low to no vertical water exchange between the Ntane and deeper Ecca aquifers as pointed out by (DWA, 2000), cited from (WCS, 2013). This layer forms a fourth aquitard layer in the numerical model of the LNKb, with the thickness ranging from 0 to 282 m (Figure 31).

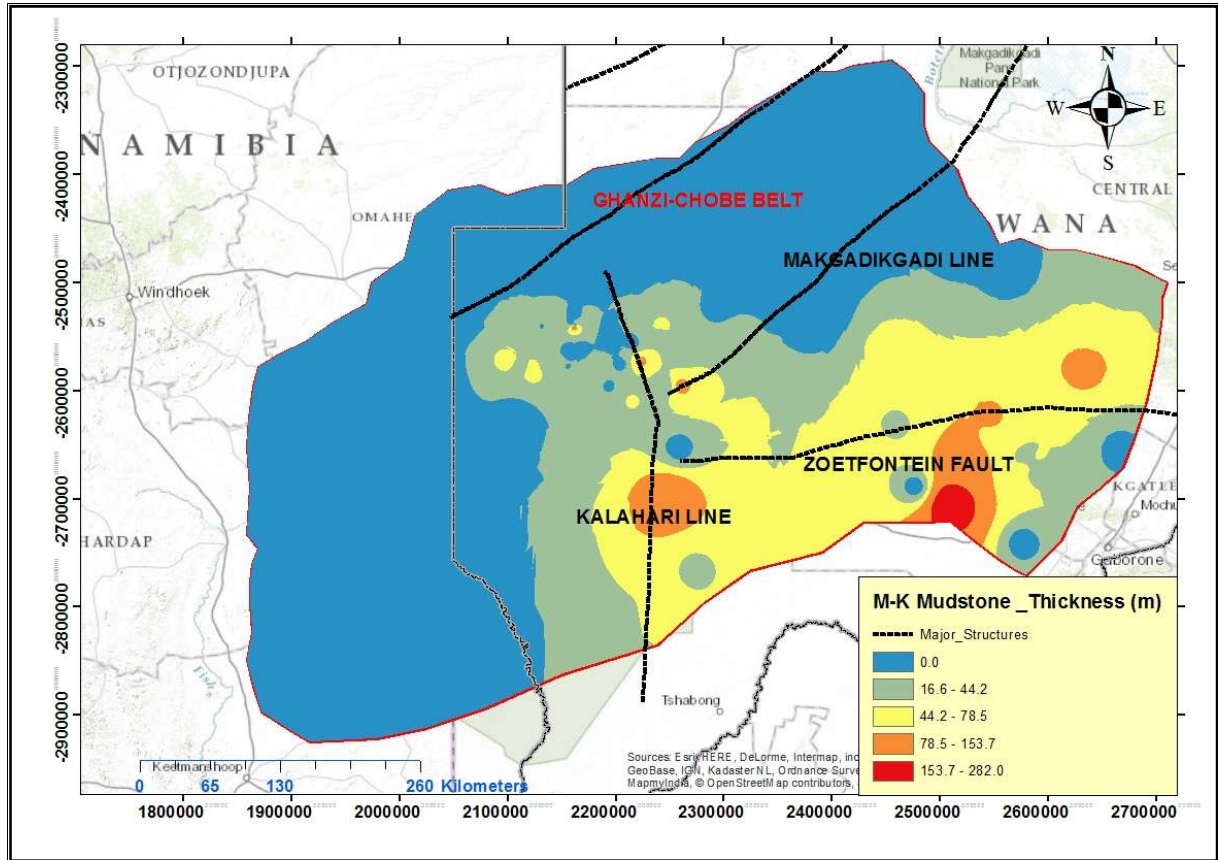


Figure 31: Spatial thickness variation of the Mosolotsane-Kwetla Mudstone-Siltstone layer.

3.3.1.5. Ecca Group.

The Ecca group is sub divided into three formations, which are Boritse, Kweneng and Bori. The Boritse Formation consists of an alternating sequence of fine to coarse grained feldspathic sandstone, alternating with carbonaceous mudstones, muddy siltstones and silty mudstone intercalations, dull and bright coals and coaly carbonaceous mudstones. The unit underlies the Kwetla formations in the South Eastern and North eastern part of the KKB. The thickness of this formation ranges from 0 m to 275 m and being continuous over the large part of the area, (Figure 32). It is a known productive aquifer in the KKB so far, from the Ecca group as most of the drilled production boreholes have not gone beyond this unit. For this study, The Ecca Sandstone forms the fifth hydrostratigraphic unit, considered in the LNKB numerical model as an aquifer, and below it is the basement. Only The Boritse formation of the Ecca Group is considered for the fifth layer, with Kweneng and Bori units being part of the basement.

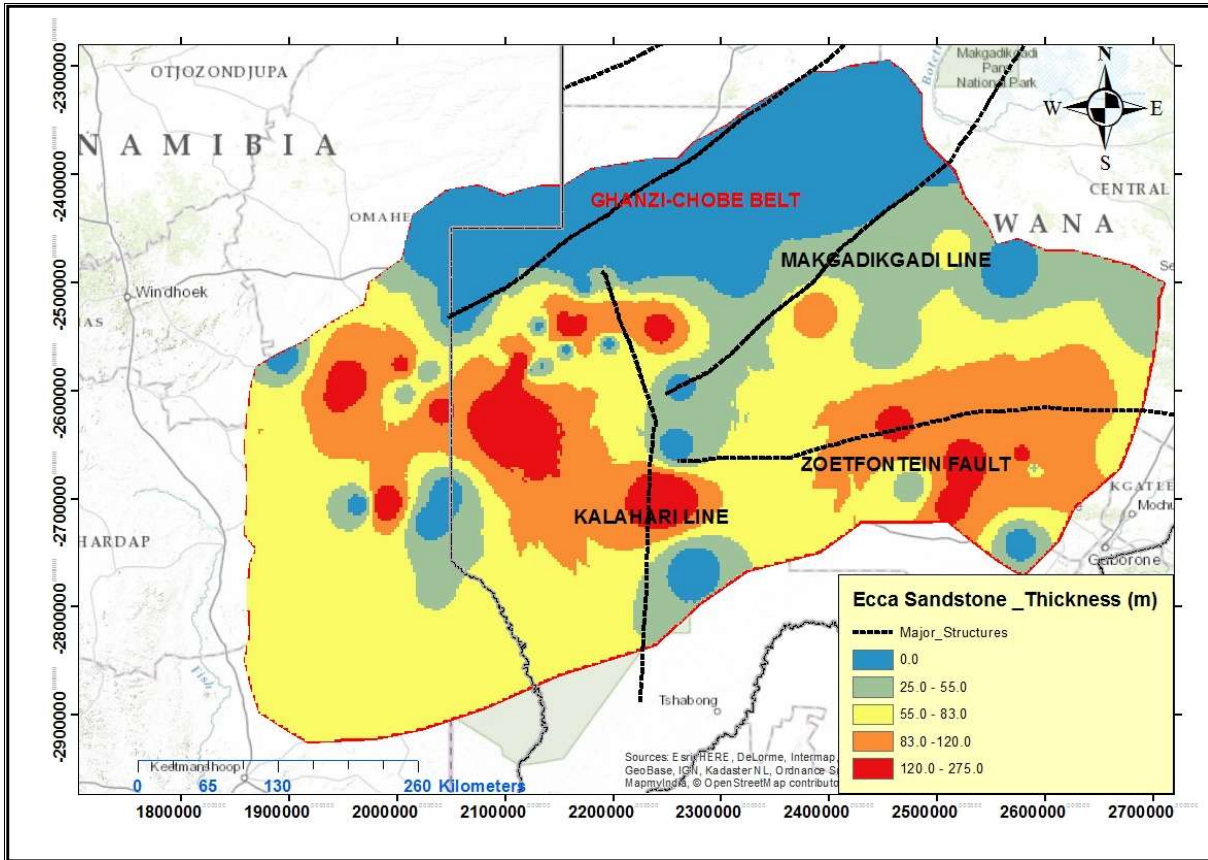


Figure 32: Spatial thickness variation of the Ecca Sandstone layer

The summarized thicknesses for the hydrostratigraphic layers are tabulated in Table 3, with the lithological descriptions for each layer.

Table 3: Interval thicknesses for hydro-stratigraphy layers in the KKB with their lithologies.

Name/Group	Interpolated depth_(m)	Descriptions/Group formation
Kalahari Sand	0 - 189	Loose sands, calcrete, calcareous Sandstone and Mudstone.
Stormberg Basalt	0 - 329	Crystalline, massive amygdaloidal basalts
Ntane Sandstone	0 - 230	Fine to medium grained, clean, friable sandstone, brownish red/pink. Often calcretised in zones.
M-K Mudstone and Siltstone	0-282	Grey mudstones and siltstones with minor sandstones. Non-carbonaceous. Occasionally arenaceous.
Ecca Sandstone	0-275	Fine to coarse, white, feldspathic sandstone interbedded with coal, carbonaceous mudstone and siltstone.

3.3.2. Comparison with available geological information

The modelled layer thicknesses of the Kalahari Karoo Basin were correlated with the known regional geology of Botswana. Figures 33 to 36 present the modelled thickness of Kalahari Sand, Stormberg Basalt, Ntane Sandstone, M-K Mudstone & Siltstone and Ecca Sandstone in contour form over the known geology map.

3.3.2.1. Kalahari Sand

This is the uppermost unit modelled. The Kalahari Sand covers the entire KKB, with variable thickness as observed in Figure 33. However, the unit is thicker along the Karoo Formations and thinner over the pre-Karoo units. Comparing the Kalahari Sand hydrostratigraphic layer it seems to be the thickest in the areas where Stormberg Basalt and Ntane Sandstone are present underneath.

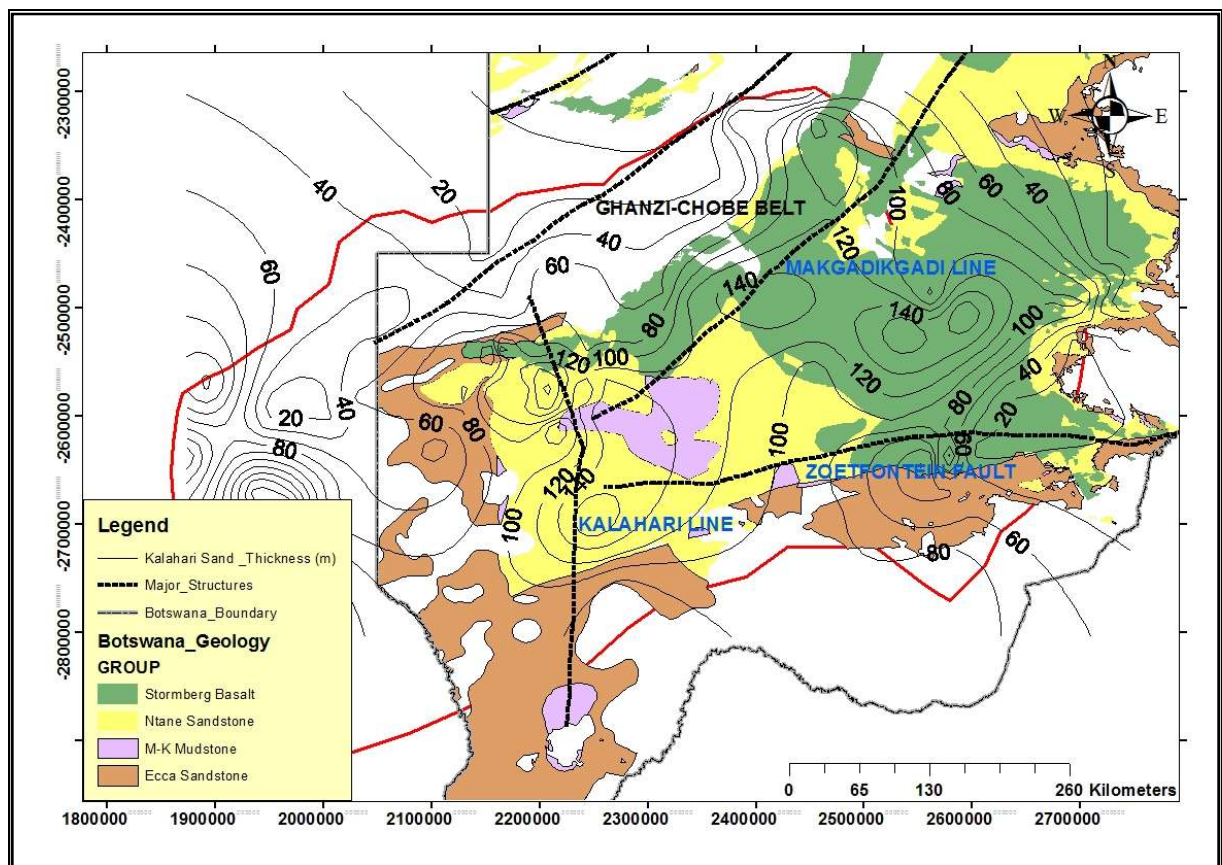


Figure 33: Modelled Kalahari thickness over the known KKB geology of Botswana.

3.3.2.2. Stormberg Basalt

The modelled thickness of the Stormberg Basalt layer coincides with the known geology as observed in Figure 33. This unit is found within structural deformed regimes in which Zoetfontein Fault and Makgadikgadi Line strike through it (Figure 34). The north eastern side of the KKB reveals thickest zone of the Stormberg Basalt layer.

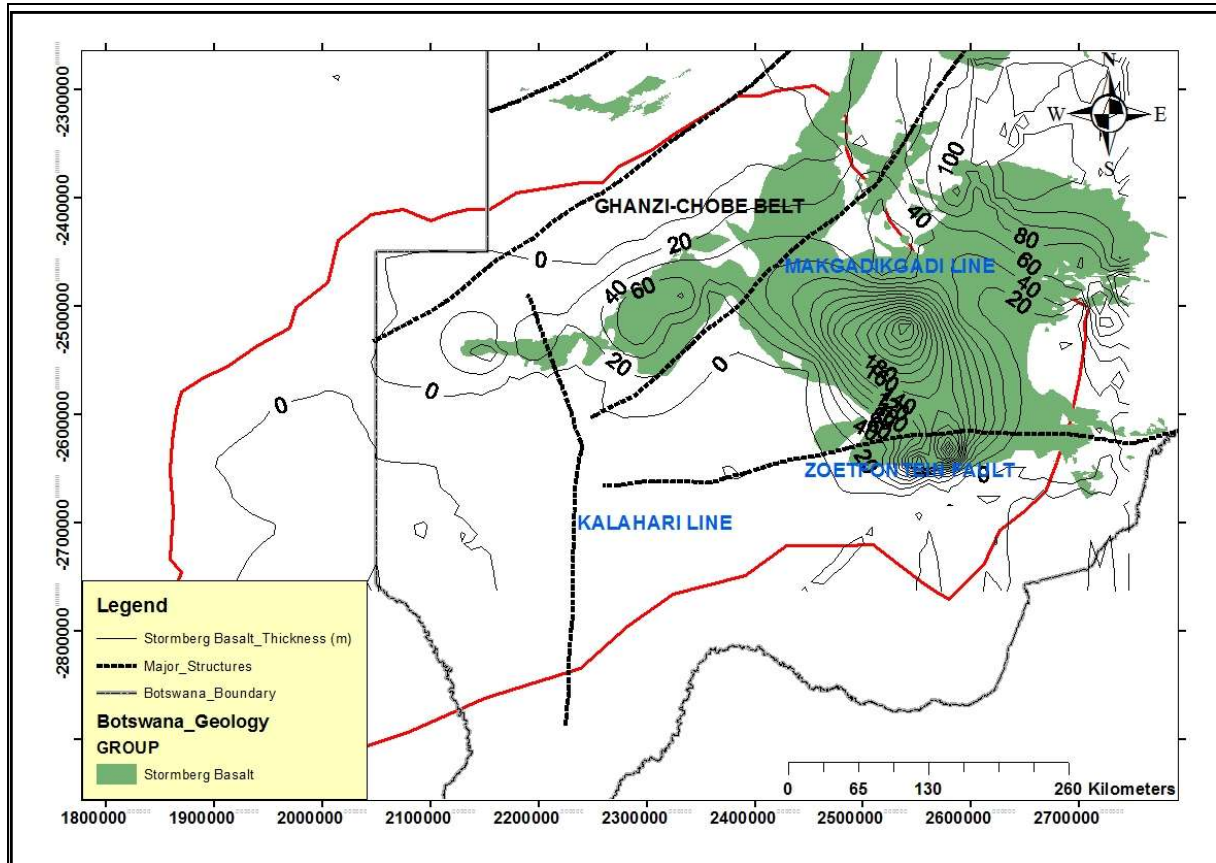


Figure 34: Modelled Basalt (Volcanic) thickness over the known KKB geology of Botswana.

3.3.2.3. Ntane Sandstone

The modelled thickness of Ntane Sandstone shows some discrepancies as compared to the known geology of Botswana. In some locations the modelled thicknesses show presence of the Ntane Sandstone, while the known geology does not show presence of this unit. In this case, modelled thickness is considered more accurate because the modelling of this study used all recent boreholes, with more data than it was available for constructing geological map of Botswana. Remarkable is that, wherever there is the Stormberg Basalt layer, the Ntane Sandstone is also, almost always found below (Figure 35). Which was also pointed out by (WCS, 2012).

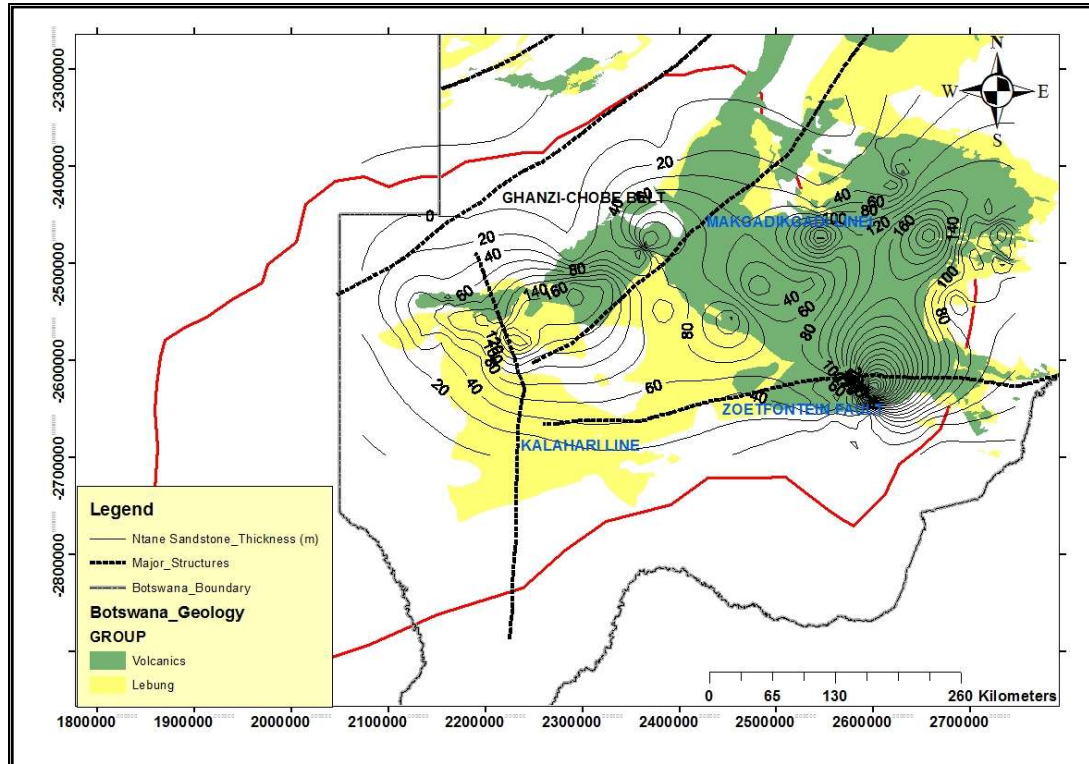


Figure 35: Modelled Ntane Sandstone thickness over the known KKB geology of Botswana.

3.3.2.4. Mosolotsane-Kwetla (M-K) Mudstone and Siltstone

The Mosolotsane Mudstone of the Lebung group and Kwetla Mudstone of the Beaufort group were combined together to form one hydrostratigraphic layer (aquitar). The modelled thickness is presented in Figure 36 below.

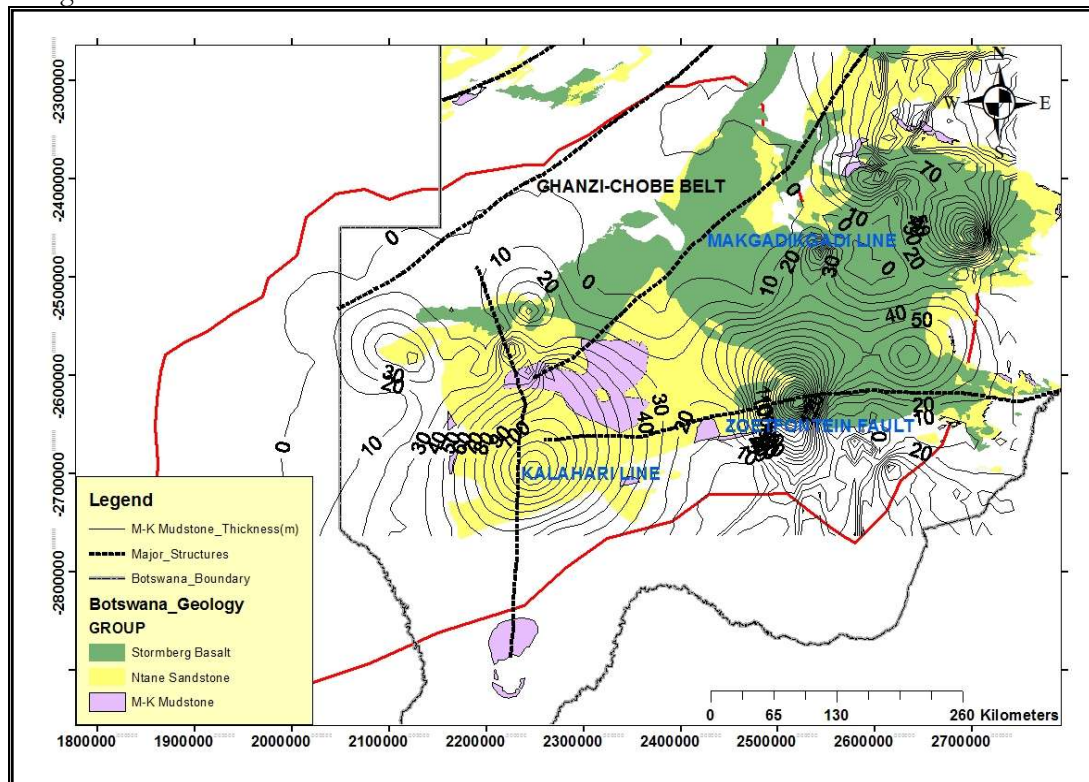


Figure 36: Modelled Mosolotsane-Kwetla thickness over the known KKB geology of Botswana.

The Beaufort Group of the Karoo is represented on the southern margins of the Kalahari Basin with variable thickness. The modelled thickness coincides with the known geology of the area as observed in Figure 36.

3.3.2.5. Ecca Sandstone

The Ecca Sandstone extends nearly throughout the whole KKB. The modelled thickness match with the geology as presented in Figure 37 below. Eventhough, the Ecca Sandstone is also observed in the northern part where the geology does not show any Karoo formations. All in all, comparing the figures 35, 36 and 37, it can be confirmed that the Ntane Sandstone and Ecca Sandstone unit are in direct contact in some regions of the KKB, which is also confirmed reflected by the cross-sections presented in Figures 19, 20, 21, 22 and 23.

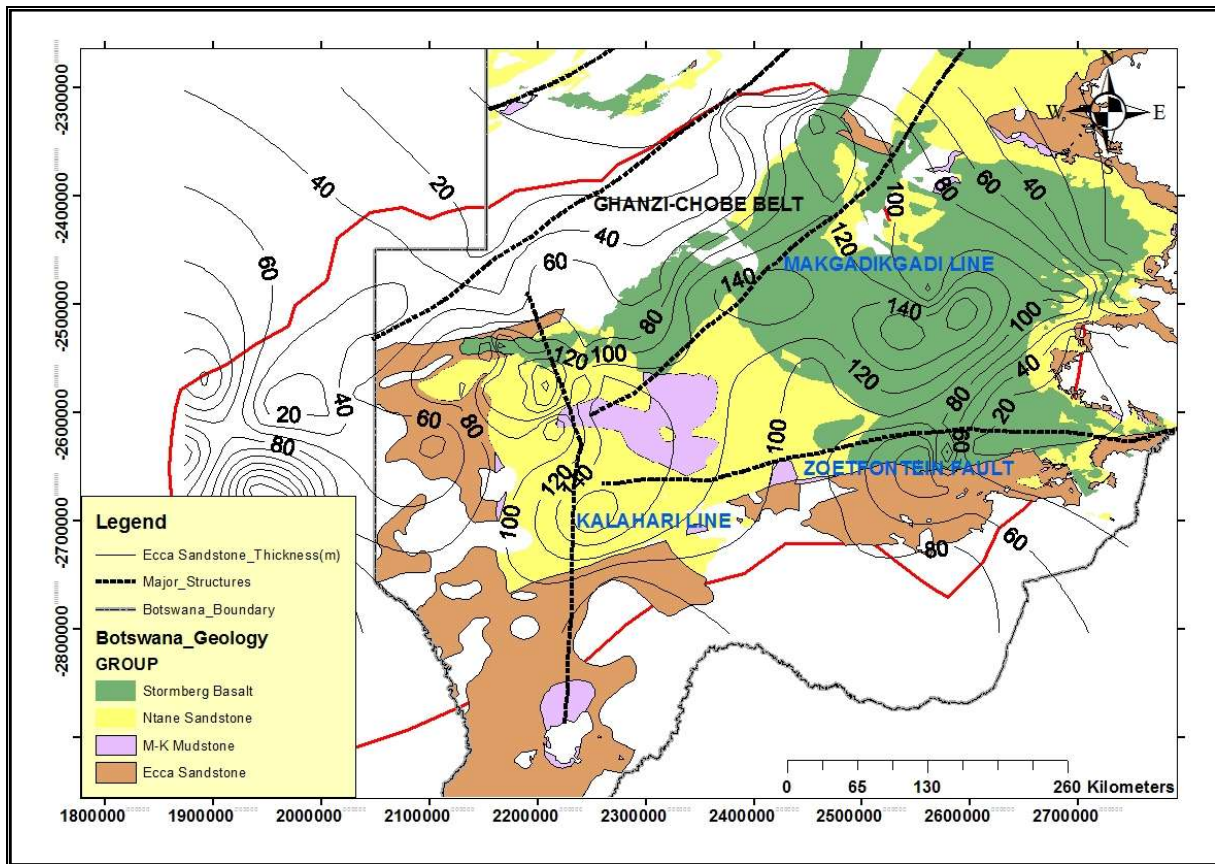


Figure 37: Modelled Ecca thickness over the known KKB geology of Botswana.

3.4. Numerical groundwater model of the LNKB

3.4.1. Driving forces

The driving forces to the numerical groundwater model of LNKB included precipitation, interception and evapotranspiration which were estimated as explained in 2.3.1, 2.3.2 and 2.3.3. The overall estimated interception rate was $0.000208 \text{ m day}^{-1}$ calculated as the weighted average which was contributed by acacia tree specie which represented the other vegetation (shrubs and trees) and grassland occupying large areas and was kept constant for the entire LNKB. The average precipitation as presented in Figure 7, were 0.00133 , 0.00171 , 0.001262 , 0.001040 and $0.001482 \text{ m day}^{-1}$ for Zone 1 to 5 respectively. After subtracting interception rate from rainfall, the resulting infiltration rates were 0.001123 , 0.000964 , 0.001055 , 0.000838 and $0.001275 \text{ m day}^{-1}$ which were used as model inputs (Figure 38). The temporally

varying precipitation and infiltration rates with the intercepted precipitation are presented on Figure 39. The variable precipitation in LNKB resulted into variable interception rates and hence variable infiltration rates.

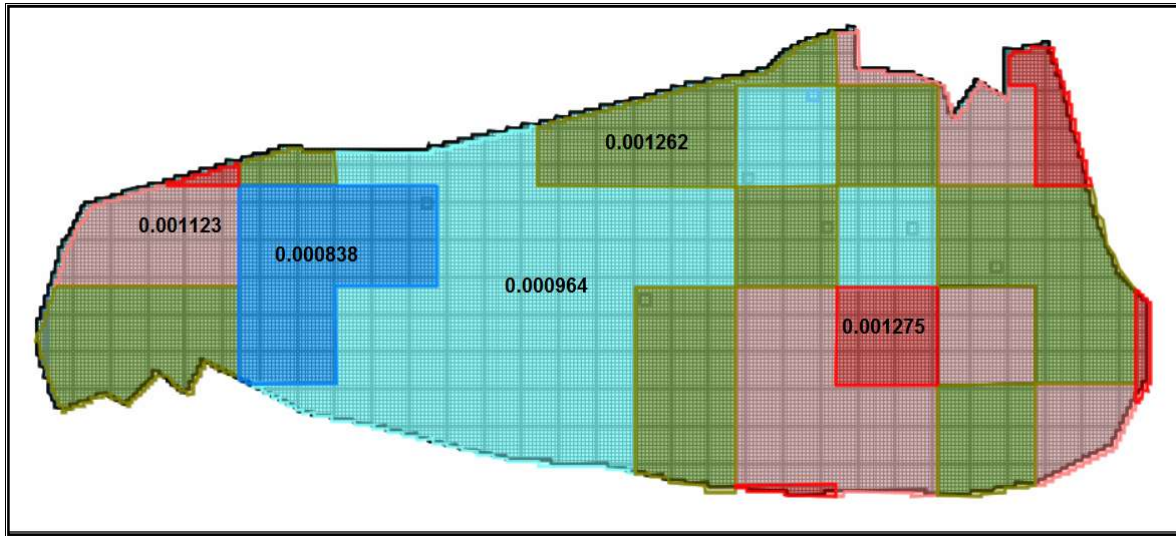


Figure 38: Infiltration rate (m day^{-1}) zones based on the variable precipitation in the area.

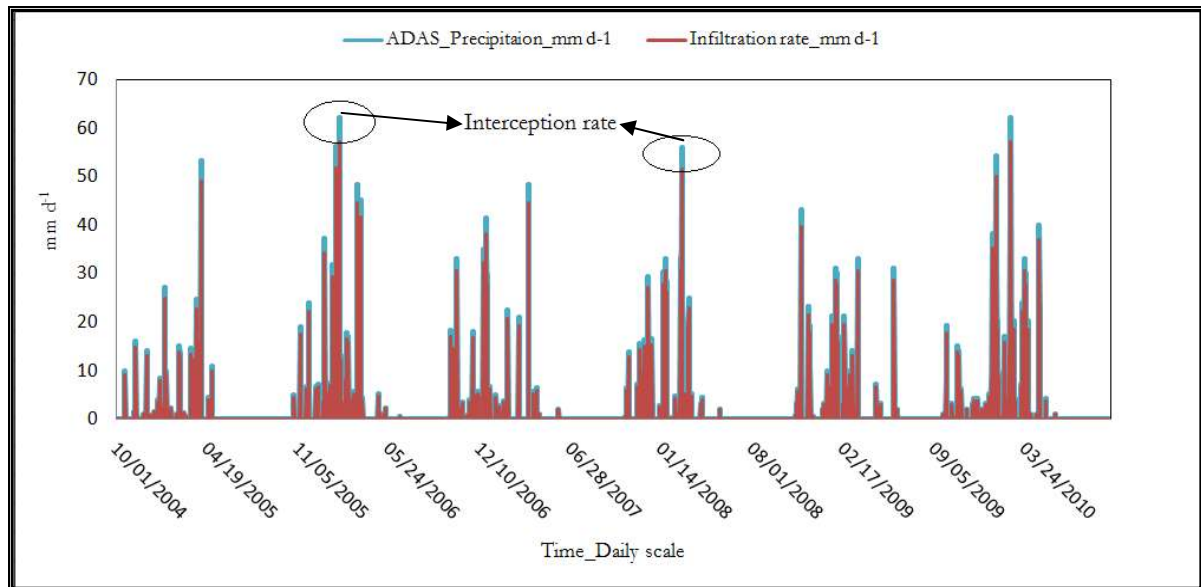


Figure 39: Rainfall in the LNKB with the resulting infiltration rates.

The potential evapotranspiration was calculated using the single crop FAO methodology of Penman-Monteith as explained in section 2.3.2. (Equation 1), with the ET_0 estimated by Hargreaves method (Equation 2). From the calculated time series of PET, the minimum was 0.48 mm day^{-1} , the maximum 5.07 mm day^{-1} and the mean 3.25 mm day^{-1} . For the steady state flow model, an average value of PET was applied. It was observed that, the seasonal PET variability was large but repetitive throughout subsequent 6 years, (Figure 40). In contrast, the spatial PET variability was rather low as notified by (Obakeng, 2007).

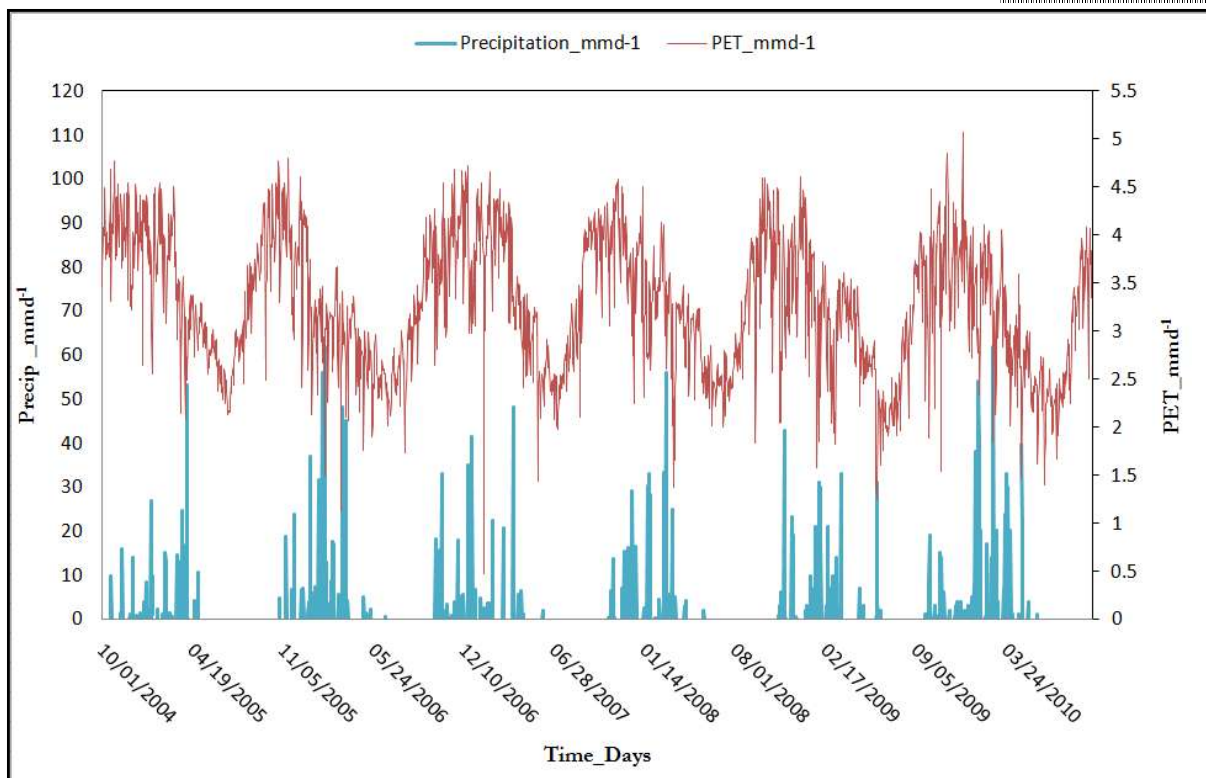


Figure 40: Relationship between Precipitation, PET and mean temperature in LNKB area.

3.4.2. Model hydrostratigraphy

From the cross section (O-P) in (Figure 6), five model layers are envisaged. They are Kalahari Sand, Stormberg Basalt, Ntane sandstone, M-K Mudstones & Siltstone and Ecca Sandstone. Everything below Ecca Sandstone was considered impermeable basement aquiclude. The Kalahari Sand, Ntane Sandstone and Ecca Sandstone were simulated as aquifers while the Stormberg Basalt and M-K Mudstones & Siltstone were aquitards. The western edge of the model begins at BH 2334, where the Ecca aquifer is shallow being also the recharge zone for the Ecca aquifer. The M-K Mudstone & Siltstone wedges out between BH 16123 and W 3, making the Ecca aquifer unconfined in the western side. The Stormberg Basalt in the model is presented by a very thin layer observed between BH 9237 and BH 9241. At around this area, the Ntane Sandstone aquifer is confined. Moreover, the Ntane Sandstone and Ecca Sandstone are hydraulically in contact at the BH 9237 where the M-K Mudstone & Siltstone wedges out. Generally, the Ntane Sandstone aquifer is observed dominant in the eastern part of the LNKB model, where as the Ecca Sandstone aquifer dominates the western side of the model boundary.

3.4.3. Calibration parameters

Model calibration involved number of parameters which include horizontal and vertical hydraulic conductivities (HK and HV) for both confined and unconfined aquifers and the vertical conductivities of the confining bed, (VKCB). After the calibrated model, the HK values ranged from 0.9 m day⁻¹ to 8.5 m day⁻¹ for the saturated part of Kalahari Sand layer, 0.4 m day⁻¹ to 2.0 m day⁻¹ for Ntane and Ecca aquifer, Figure 43 through 46, present the parameter values after calibration, from layer 1 to 5, (without layer 2). After calibration, the VKCB of the 2nd aquitard layer was 2 E-7 m d⁻¹, while the 4th layer ranged from 1.5 E -7 m day⁻¹ to 2 E-3 m day⁻¹. The head distribution after model calibration for Ecca Sandstone aquifer were presented in Figure 45 which show the groundwater flow direction in LNKB eastwards, where a GHB was applied.

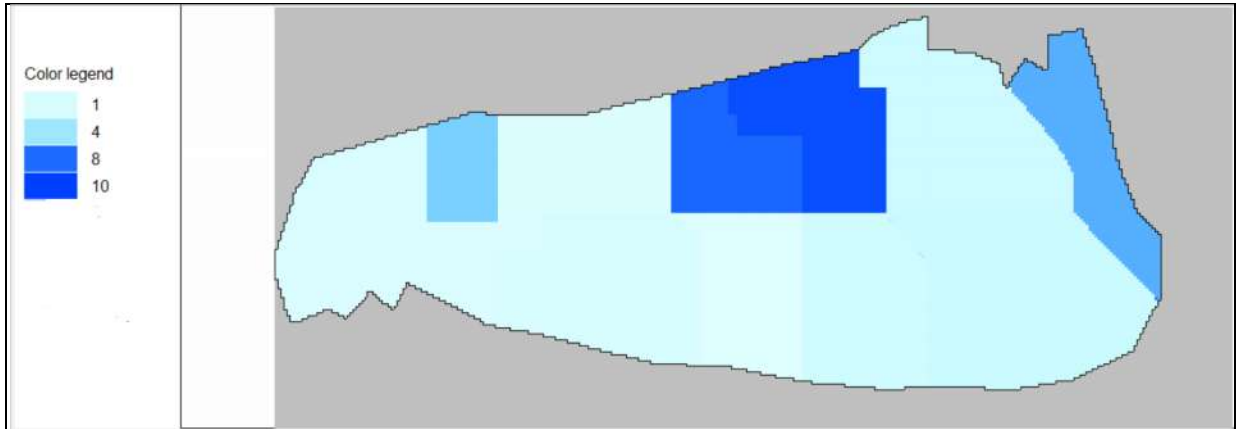


Figure 41: Horizontal hydraulic conductivity (m day⁻¹) of the Kalahari Sand aquifer

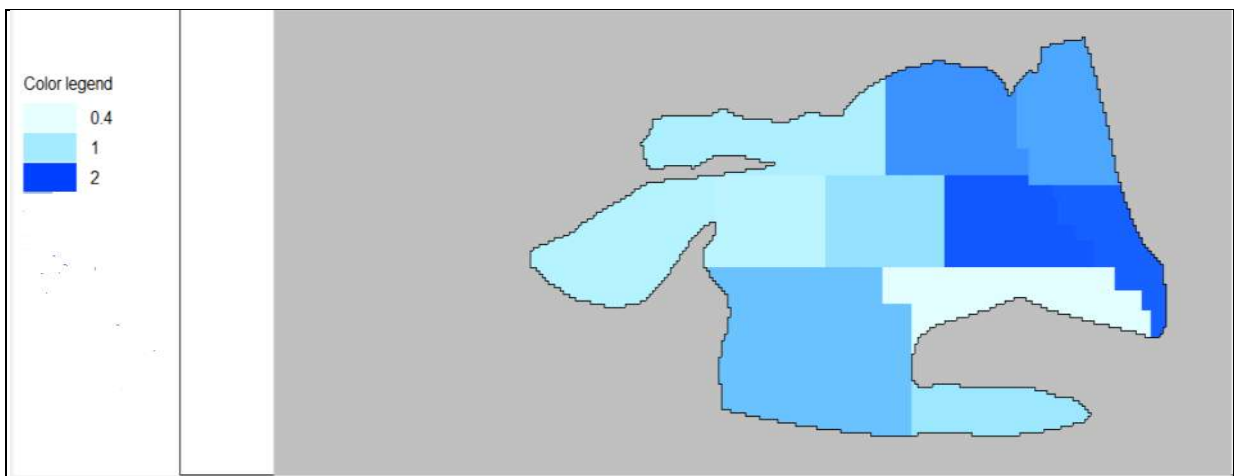


Figure 42: Horizontal hydraulic conductivity (m day⁻¹) of the Ntane Sandstone aquifer

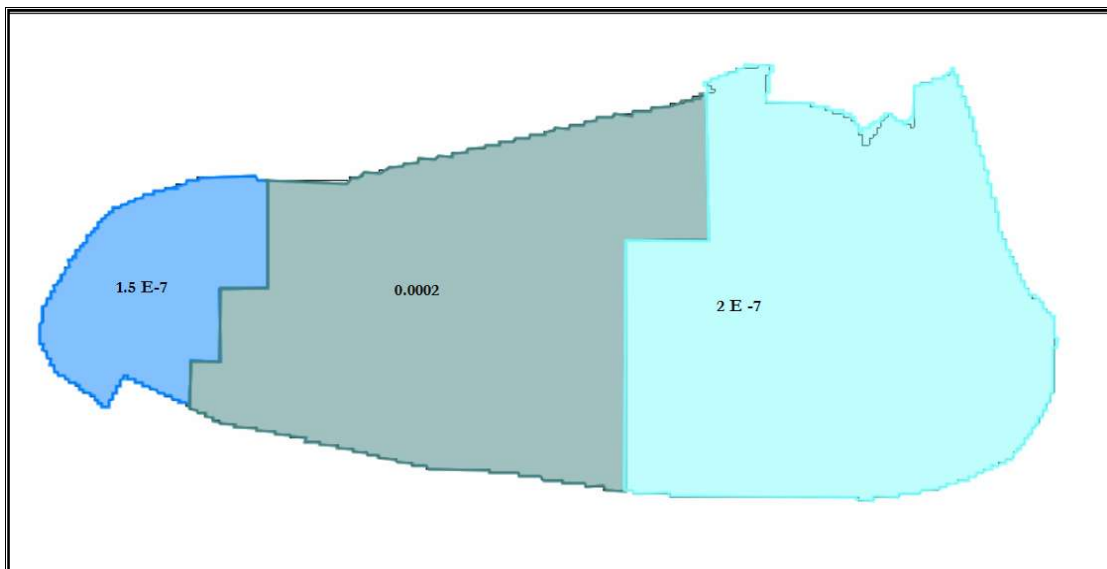


Figure 43: Vertical hydraulic conductivity (VKCB) in (m day⁻¹) for M-K Mudstone aquitard.

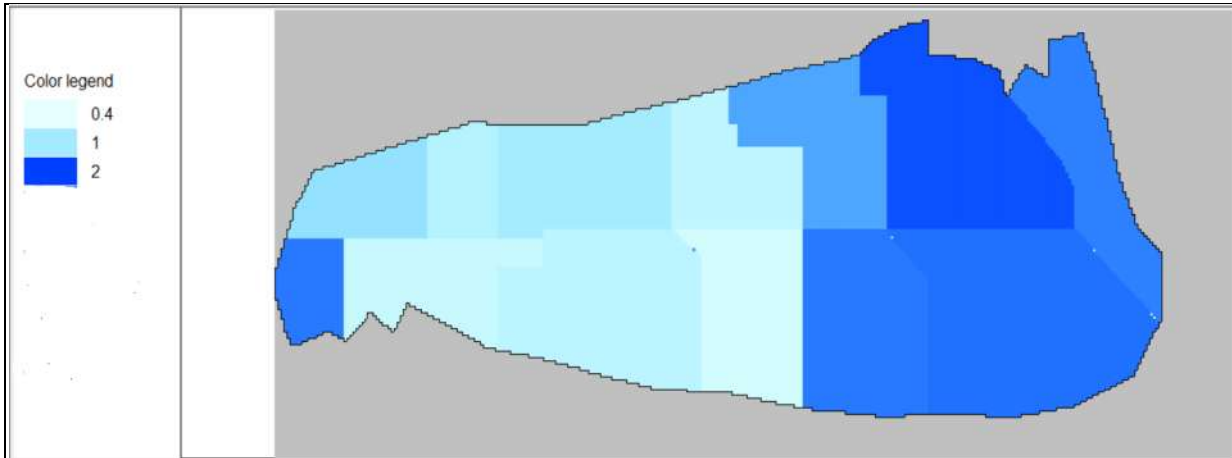


Figure 44: Horizontal hydraulic conductivity (m day^{-1}) of the Ecca Sandstone aquifer

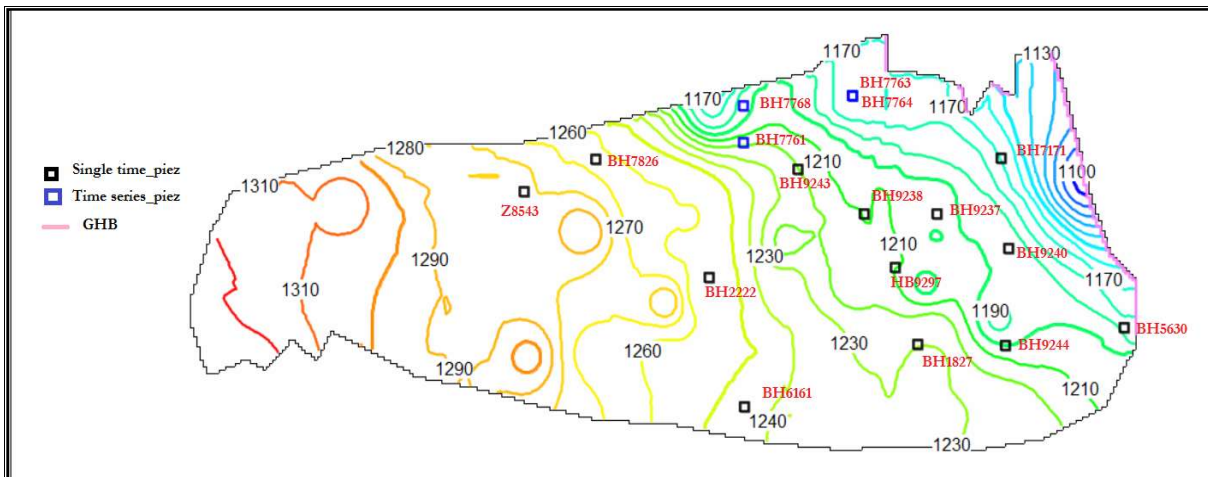


Figure 45: Head distribution in Ecca Sandstone aquifer after steady-state model calibration.

3.4.4. Error assessment

The mean error (ME), mean absolute error (MAE) and root mean square error (RMSE) were calculated following Equations 11, 12 and 13. The values obtained are 0.29, 0.29 and 0.56 for ME, MAE and RMSE respectively, (Table 4). The simulated head variations in the area ranges from 1162.17 m to 1265.87 m. This results in head difference in the study area in order of 103.70 m. The ratio of the calculated RMSE to the total head loss was 0.54 % which was acceptable when compared to the maximum acceptable percentage error, which is 10%, according to (Anderson & Woessner, 1992).

Table 4: Error assessment of heads after steady-state model calibration

	AQUIFER	X	Y	Obs_ heads (m)	Sim_ heads (m)	Error_(m)	Squared Error (m 2)	Absolute error(m)
BH 1827	Ntane	2232941	-2595322	1195.6	1195.08	0.52	0.27	0.52
BH 9237	Ntane	2239068	-2556210	1201.84	1201.94	-0.1	0.01	0.10
BH 9238	Ecca	2216247	-2556043	1188.52	1188.26	0.26	0.07	0.26
BH 9240	Ntane	2261673	-2566659	1175.24	1174.73	0.51	0.26	0.51
BH 9297	Ntane	2225935	-2572310	1179.68	1179.22	0.46	0.21	0.46
BH 2222	Ntane	2167635	-2575485	1212.81	1212.37	0.44	0.19	0.44
BH 5630	Ntane	2297689	-2590296	1162.98	1162.17	0.81	0.66	0.81
BH 7826	Ntane	2132043	-2539853	1266.37	1265.87	0.5	0.25	0.50
BH 9243	Ntane	2195332	-2542739	1195.38	1195.85	-0.47	0.22	0.47
BH 9244	Ntane	2260636	-2595777	1177.36	1178.27	-0.91	0.83	0.91
BH 9294	Ntane	2168951	-2559403	1226.85	1226.8	0.05	0.00	0.05
Z 8543	Ntane	2109411	-2549506	1194.96	1194.67	0.29	0.08	0.29
6161	Ecca	2178747	-2614138	1196.02	1195.20	0.82	0.67	0.82
3010	Ecca	2122239	-2568040	1224.60	1223.30	1.3	1.69	1.30
7171	Ecca	2259143	-2539511	1117.80	1118.00	-0.2	0.04	0.20
BH 7761	Ecca	2178330	-2534776	1194.96	1194.67	0.29	0.08	0.29
BH 7764	Ecca	2212642	-2520706	1171.3	1171.28	0.02	0.00	0.02
BH 7763	Ecca	2212557	-2520614	1171.64	1171.00	0.64	0.41	0.64
BH 7768	Ecca	2178244	-2523705	1183.76	1183.52	0.24	0.06	0.24
						0.29	0.56	0.29

The scatter plot of the observed versus simulated heads is presented in Figure 46, showing a random distribution of points with a good correlation between the observed and simulated heads. This reflects the good model performance which leads to the good match between the simulated and measured heads reflected by regression coefficient (R^2) of 99%.

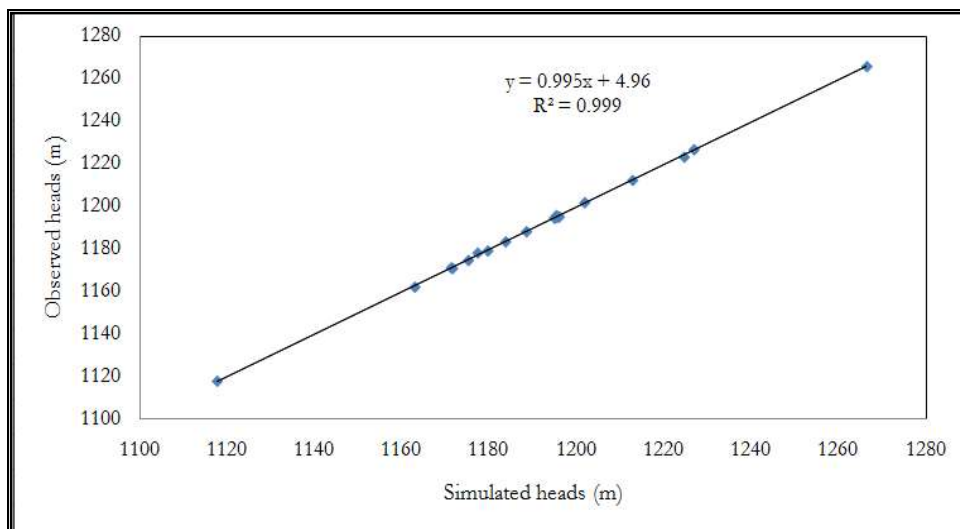


Figure 46: Scatter plot of observed and simulated heads after steady-state calibration.

3.4.5. Sensitivity analysis of the parameters

Sensitivity of the model was judged with respect to its response to changes of RMSE of hydraulic heads and was measured after varying the calibration parameters, (Figure 47) and UZF parameters and GHB conductances (Figure 48). The model shows a sensitivity response as the result of increase and decrease of HK values. However, when comparing the two variations, the model is more sensitive upon decreasing the HK values than increasing. The VKCB and VK parameters show a very low response upon increase or decrease of the values.

In contrast, the model is non responsive to any of the UZF package parameter, while showing quite a large sensitivity to changes made in the GHB conductances. With these results, the UZF parameters were kept constant while the GHB conductances were varied the minimum error was obtained as described in 2.5.8. A great care has to be taken during model calibration, while adjusting sensitive parameters, because small changes in these parameters usually result in large changes in model solution so also in residual error (Bear & Cheng, 2010). In contrast, any changes of non-sensitive VKCB, VK and UZF parameter did not result in any substantial model change, although a very small response was observed upon varying the VK and VKCB parameter, while the UZF parameters were totally insensitive.

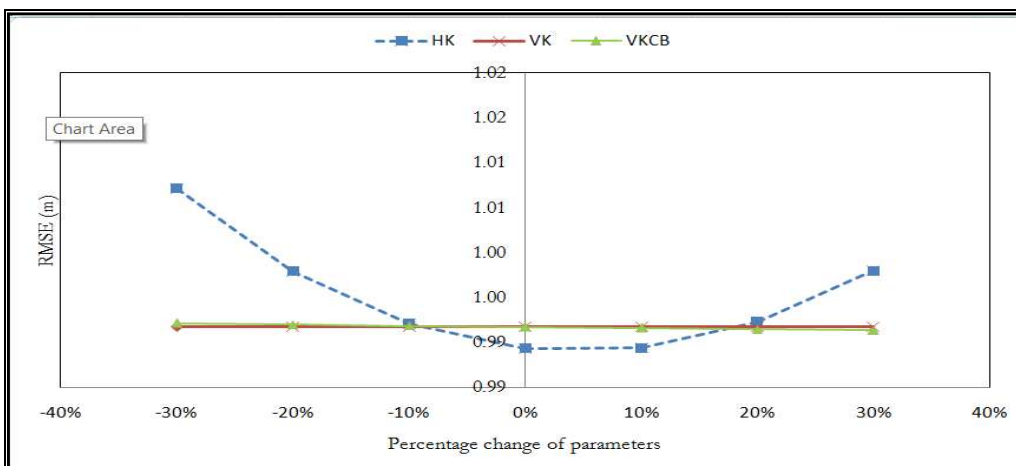


Figure 47: Sensitivity of model parameters under steady-state calibration.

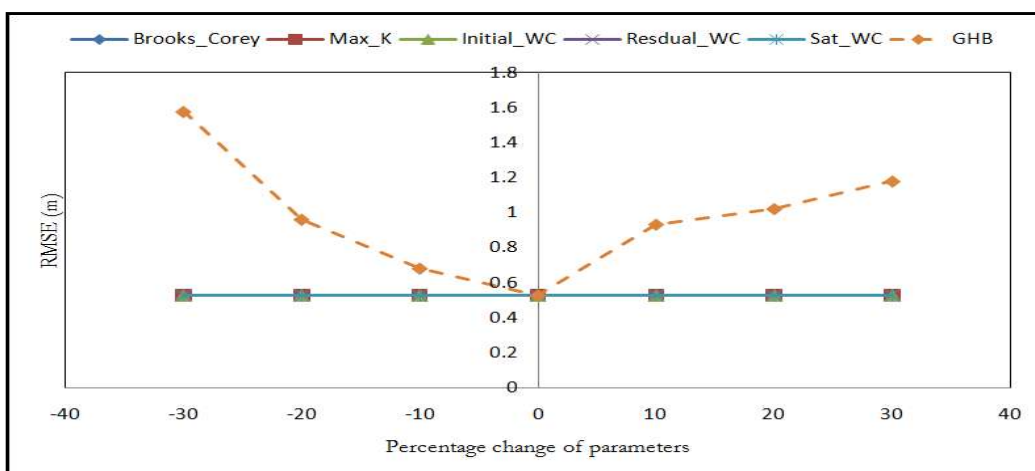


Figure 48: Sensitivity of the UZF parameters and GHB conductances under steady-state calibration.

3.4.6. Water budget

The water budget (WB) for individual saturated layers was obtained and presented separately, i.e. 1st layer (Kalahari Sand), 3rd layer (Ntane Sandstone) and the 5th layer (Ecca Sandstone). Volumetric flow WB is tabulated in Table 5 and appendix 1, with a graphical presentation on Figure 49. The budgets were calculated in the Zone Budget, post processor. The calculation follows Equation 20 which for each of the saturated layer has the following forms;

The water budget of Kalahari Sand unconfined layer was estimated according;

$$Q_{Lin} + Q_{Vin} + R_g = ET_g + Q_{Lout} + Q_{Vout} \quad (22)$$

The water budget of the Ntane Sandstone aquifer;

$$Q_{Vin} = Q_{Lout} + Q_{Vout} \quad (23)$$

The water budget of the Ecca Sandstone aquifer

$$Q_{Lin} + Q_{Vin} = +Q_{Lout} + Q_{Vout} \quad (24)$$

Table 5: Volumetric water budget (m³ day⁻¹) of the individual aquifers after steady state calibration.

FLOW BUDGET COMPONENT	KALAHARI (m ³ d ⁻¹)		NTANE (m ³ d ⁻¹)		ECCA (m ³ d ⁻¹)	
	IN	OUT	IN	OUT	IN	OUT
Q _{Lin} /Q _{Lout}	0.00	0.00	6.57	8184.51	4994.37	1219.66
UZF ET _g	0.00	25355544	0.00	0.00	0.00	0.00
UZF R _g	25359978.00	0.00	0.00	0.00	0.00	0.00
Exf _{gw}	0.00	0.00	0.00	0.00	0.00	0.00
Q _{Vin} /Q _{Vout}	343.88	9762.93	13888.90	5689.46	5345.64	4125.97
Total	25365316.25	25365306.93	13895.46	13873.97	5345.64	5345.64
IN-OUT	9.32		21.50		0.00	
Percent Discrepancy	0.00		0.00		0.00	

The volumetric water budget components were converted to fluxes in mm yr⁻¹ based on the surface area of each aquifer layer. After the conversion, the total inflow components to the model were 194.10 mm yr⁻¹, out of which, 194.06 mm yr⁻¹ was contributed by the UZF recharge component (Precipitation-Interception), which basically means the infiltrating water after interception. This means, about 99.9% of the inflow to the model was contributed by the UZF recharge, with 0.1% of the inflow coming from lateral flows.

Likewise, 194.03 mm yr⁻¹ which is about 99.9% of the outflows leave the Basin as ET with only 0.1% discharged to the KKB eastern side of the LNKB model boundary as lateral flow. This ET refers to the total ET contributed by both ET_u and ET_g components, with a large percent coming from the ET_u component. The UZF package combines the ET_u and ET_g under steady state conditions, and gives out a total ET value, which becomes a challenge on the use of this package under steady state conditions in the LNKB. Likewise, it should be taken with great care that, the UZF recharge component should not be mixed with the net groundwater recharge in the LNKB, which is explained below on 3:7:6.

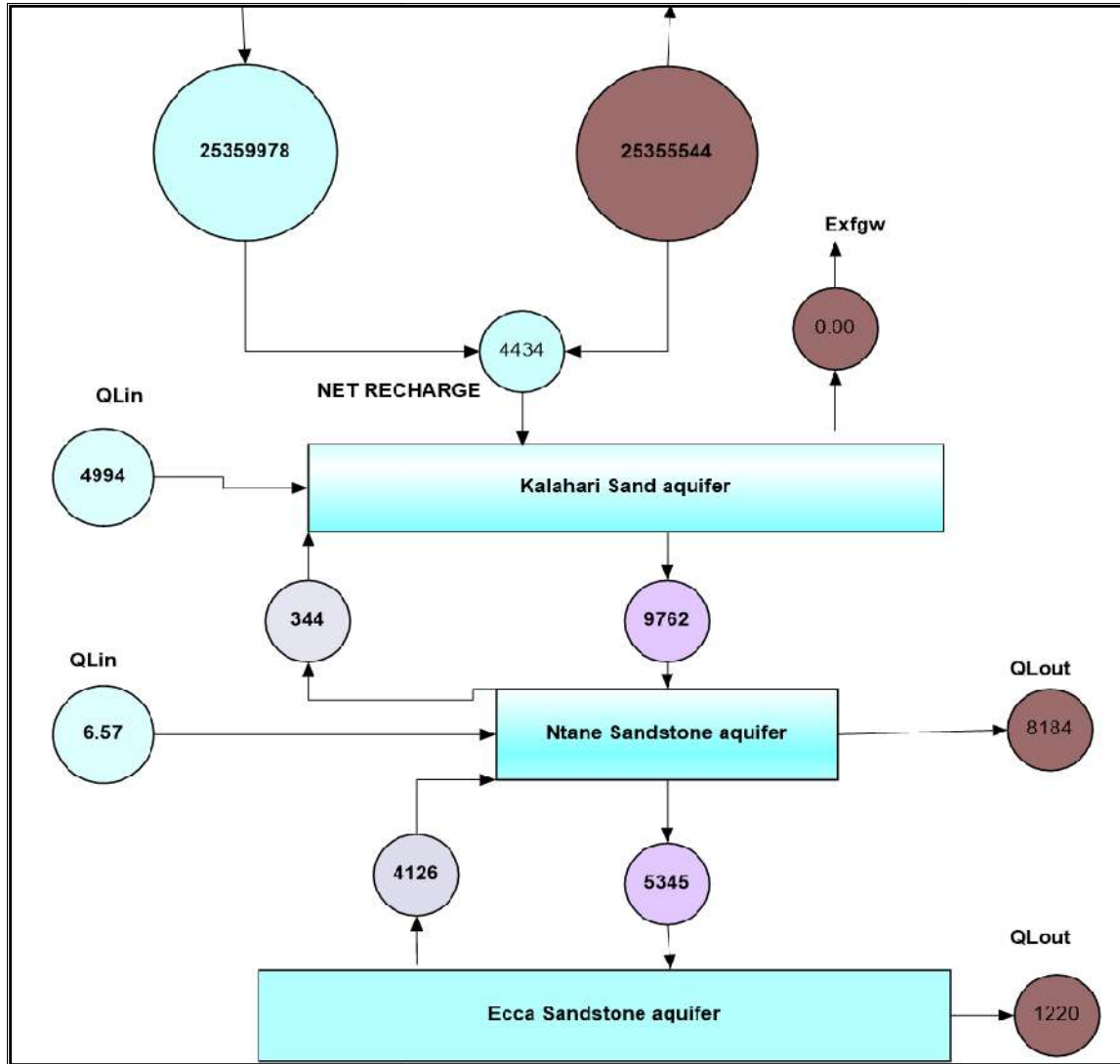


Figure 49: Schematized water budget ($m^3 d^{-1}$) per each saturated layer obtained in steady state calibration.

Moreover, the composite water budget was also calculated at the same time (Table 6). The total inflows and outflows to the model are summed up to obtain the water budget. The UZF gross recharge and ET differ by a very small magnitude, which leads to a small net recharge in the area which comply with (de Vries et al., 2000) suggestions

Table 6 : Volumetric water budget ($m^3 day^{-1}$) for composite model after steady state calibration.

FLOW BUDGET COMPONENT	FLOW ($m^3 d^{-1}$)	
	IN	OUT
QLin/QLout	5000.93	9404.17
UZF ET _g	0.00	25355544
UZF R _g	25359978.00	0.00
Ex _{fgw}	0.00	0.00
Q _{Vin} /Q _{Vout}	19578.42	19578.36
Total	25384557.35	25384526.53
IN-OUT		30.82
Percent Discrepancy		0.00

The schematic representation of the composite water budget is presented in Figure 50 below. The inflow and outflow fluxes balances, giving a proper closure of the water budget, with 0% discrepancy.

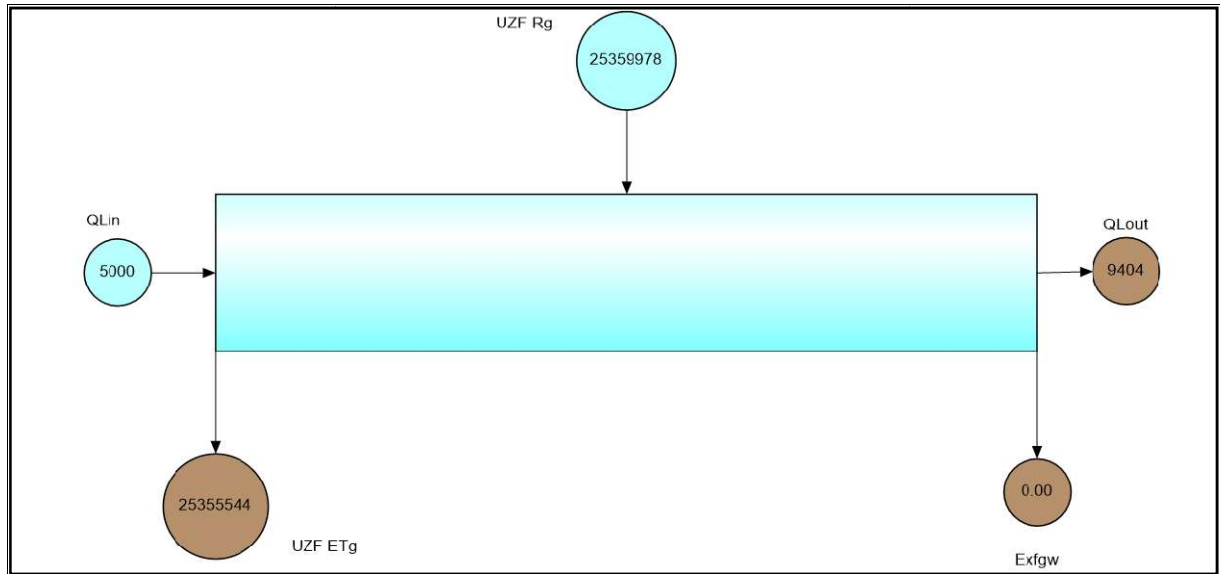


Figure 50: Schematized water budget ($\text{m}^3 \text{d}^{-1}$) for entire LNKB aquifer system after steady-state calibration.

3.4.7. Annual recharge estimation

The net recharge was calculated from Equation 25 below;

$$Rn = R_g - Exfgw - ET_g \quad (25)$$

$$R_g = 194.06 \text{ mm yr}^{-1}$$

$$ET_g = 194.03 \text{ mm yr}^{-1}$$

$$Exfgw = 0 \text{ mm yr}^{-1}$$

Therefore, net recharge for the entire model area of the Ncojane Lokalane Karoo Basin from the calibrated steady state model was **0.03 mm yr⁻¹**.

3.4.8. Spatial variability of the groundwater fluxes in the LNKB

MODFLOW-NWT under ModelMuse calculates the water budgets in volumetric units ($\text{L}^3 \text{T}^{-1}$). Fluxes such as groundwater recharge (GW RECHARGE) and groundwater evapotranspiration (ET) are not calculated in the units of length per time (LT^{-1}). Conversion into these units was done, in which the $\text{m}^3 \text{day}^{-1}$ was converted into mm day^{-1} . The function *Grid or Mesh | Block Area Top*, which gives the cell area, was used. The data sets with calculated GW RECHARGE and ET values were divided by the cell area to give the spatial distribution of fluxes in millimetres per day.

The spatial distribution of total GW RECHARGE for the averaged six years from 1st Oct 2004 to 30th September 2010 is shown in Figure 51. It can be deduced from the figure that the Basin has low spatial variability of GW RECHARGE fluxes. Also, the recharge covers almost the entire area of the Basin with the exception of cells on the northern boundary of the study area, where a no flow boundary was assigned based on the geological boundary. The northern part outside the boundary is the Dwyka and Ghanzi rocks, which are not part of this GW-flow model. Moreover, the low spatial variability of recharge might be caused by a low variable rainfall rates as indicated in Figure 7, which lead to low variable infiltration

rates (Figure 38), as the interception was considered constant for the entire LNKB. The depth to water table, vertical hydraulic conductivity and terrain slope, look more or less uniform in the LNKB. The total recharge fluxes varied to about 1.36 mm d^{-1} in which, the cells with total recharge of 0.91 and 1.06 mm d^{-1} cover a large part in the model.

The averaged spatial distribution of ET for the model period 1st Oct 2004 to 30th Sept 2010 is shown in Figure 52 which shows a variation in the ET from 0 mm d^{-1} to 1.61 mm d^{-1} . The ET does not vary much and most of the cells in the Basin have the ET range from 0.89 mm d^{-1} to 1.61 mm d^{-1} , with most of the cells having the value of 0.89 mm d^{-1} and 1.07 mm d^{-1} . Generally, the ET and GW recharge values have a very small difference which attributes to a small net recharge in the area.

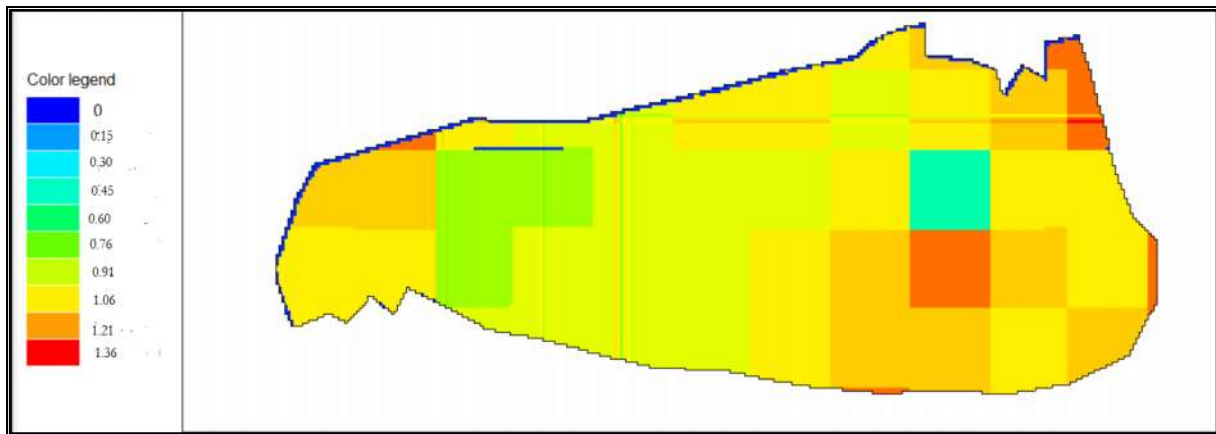


Figure 51: Averaged UZF gross recharge in mm d^{-1} for the period 1st Oct 2004 to 30th Sept 2010.

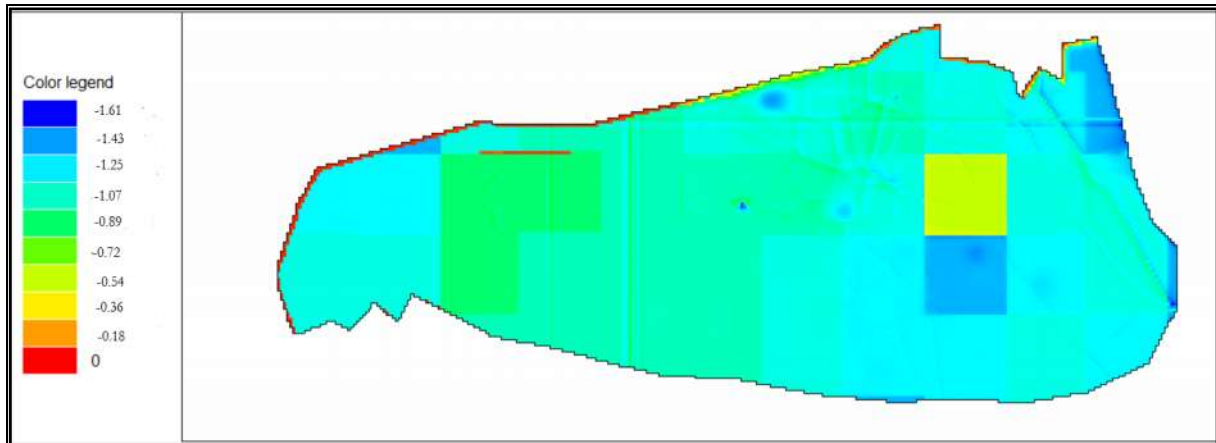


Figure 52: Averaged UZF- ET_g in mm d^{-1} for the period 1st Oct 2004 to 30th Sept 2010.

3.5. Water resources evaluation

The volume of the entire Ntane Sandstone aquifer in the LNKB was calculated in Rockworks which was $1.35 \times 10^{12} \text{ m}^3$, with a total area of $9.99 \times 10^9 \text{ m}^2$. The total volume of the Ecca aquifer in the Basin was $1.52 \times 10^{14} \text{ m}^3$, with an area of $1.55 \times 10^{12} \text{ m}^2$. From these values, the Ntane Sandstone aquifer occupies a smaller area than Ecca Sandstone aquifer. Even though, the Ntane Sandstone is thicker than Ecca Sandstone aquifer. Transmissivity of the Ntane Sandstone aquifer in the area range from 8 to $50 \text{ m}^2 \text{ d}^{-1}$ as suggested by (WCS, 2001), while (Rahube, 2003) presented the value range of 2.5 to $113.8 \text{ m}^2 \text{ d}^{-1}$ for Ntane Sandstone aquifer and 2 - $97 \text{ m}^2 \text{ d}^{-1}$ for the Ecca Sandstone aquifer. The range of hydraulic

conductivities for all the previous studies, including this study follows under the same range for both Ntane Sandstone and Ecca Sandstone aquifers.

This means, comparing the two aquifer systems in the LNKB, the Ntane Sandstone aquifer is more resourceful as compared to Ecca aquifer, though, it has a limitation of the area coverage.

3.6. Comparison with other studies.

3.6.1. Horizontal hydraulic conductivity

The hydraulic conductivity values of this study were slightly different than those by Rahube, (2003). Who came up with the horizontal hydraulic conductivities ranging from 0.08 - 1.8 m day⁻¹ for the Ntane aquifer and 0.01-0.13 m day⁻¹ for the Ecca aquifer, whereas, in this study, the hydraulic conductivity for Ntane aquifer ranged from 0.4 to 1.65 m day⁻¹ (Figure 42) and for the Ecca aquifer from 0.4 to 1.7 m day⁻¹ (Figure 44). According to WCS (2001), the Ntane Sandstone aquifer hydraulic conductivities ranged from 0.14 to 0.47 m day⁻¹.

The Kalahari Sand was never been considered in the previous studies, because only standalone models were used so far in the LNKB area, while that layer is not an aquifer, being partially and not only locally saturated while the majority of its thickness represents unsaturated zone. Use of UZF package allowed to assign Kalahari Sand layer as the first saturate/unsaturated with the horizontal hydraulic conductivities for the saturated layer ranging from 0.4 to 8.5 m day⁻¹ (Figure 41). For the vertical hydraulic conductivities (VK), Rahube, (2003), assumed VK to be one tenth of the HK. For this study, the vertical conductivity as defined for each zone with the range of 0.1 to 0.8 m day⁻¹ for Kalahari Sand, 0.01 to 0.08 m day⁻¹ for Ntane Sandstone aquifer and 0.01 to 0.05 m day⁻¹ for the Ecca Sandstone aquifer. The Stormberg Basalt was not included in Rahube's model, while in this study it is the confining layer, with the VKCB value of 2 E-7 m day⁻¹. Likewise, the Mosolotsane - Kwetla layer VKCB values ranged from 1.5 E-7 to 2 E-4 m day⁻¹ (Figure 43) in this study, while the previous study by Rahube (2003), it was assumed to have no vertical conductance through this layer. Even though, the sensitivity analysis has shown a very low response of the model to the changes of VK and VKCB parameters.

3.6.2. Net recharge

This study has resulted into an overall recharge of 0.03 mm yr⁻¹. This is less than isotope estimate made by Rahube (2003), who defined minimum recharge was 1.46 mm yr⁻¹ and the maximum being 2.5 mm yr⁻¹. Such low recharge is due to the very thick Kalahari Sand (>60 m) unsaturated zone representing large unsaturated zone capacity.

This is in agreement with de Vries et al., (2000), who stated that, groundwater recharge in Kalahari decreases from eastern side where the Kalahari net recharge is the highest, in order of 5 mm yr⁻¹, towards the western side of Kalahari Botswana, where the net recharge decreases to <1 mm yr⁻¹. Lokalane-Ncojane Karoo Basin (LNKB), net recharge of 0.03 mm yr⁻¹, being on western margin of KKB complies well with the statement.

3.6.3. Water balance

The water balance (WB) components were compared against the obtained values from Rahube, (2003). The volumetric aerial recharge into the Ntane Sandstone aquifer was 9762 m³ d⁻¹ (Table 5), which gives the average recharge of 0.08 mm yr⁻¹ over the entire modelled Ntane layer. The previous recharge suggested a higher average recharge to the Ntane Sandstone equal to 0.18 mm yr⁻¹. The aerial recharge to Ecca aquifer for this study was over estimated as compared to the previous study. The overall aerial

recharge was $5345 \text{ m}^3 \text{ d}^{-1}$ (Table 5), which lead into a net recharge of 0.07 mm yr^{-1} , while the previous study suggested only $4.2 \times 10^{-6} \text{ mm yr}^{-1}$ of net recharge to Ecqa aquifer.

A volumetric rate of $1878 \text{ m}^3 \text{ d}^{-1}$ was suggested in (Rahube, 2003) as a lateral flow into the Ecqa aquifer through a general head applied on the western boundary of LNKB, this study used a no-flow boundary over the western side, where Ecqa Sandstone is exposed on surface. The value of $4994.37 \text{ m}^3 \text{ d}^{-1}$ resulted as the lateral flow to the first layer which needs an investigation to assess if this volumetric recharge is coming from the Ecqa Sandstone which is the higher possibility. However, a value of $6.57 \text{ m}^3 \text{ d}^{-1}$ inflows to the Ntane aquifer was noted for this study. This was not anticipated and might have been an error within the model. The outflow on eastern boundary from the Ntane and Ecqa aquifers for this study were $8184 \text{ m}^3 \text{ d}^{-1}$ and $1220 \text{ m}^3 \text{ d}^{-1}$ respectively, while lateral outflows suggested in the previous study were $4270 \text{ m}^3 \text{ d}^{-1}$ and $1336 \text{ m}^3 \text{ m d}^{-1}$ for Ntane and Ecqa aquifers respectively.

The previous study showed the vertical groundwater exchange between the two aquifers is both upwards and downwards, with the volumetric net leakance of $543.9 \text{ m}^3 \text{ d}^{-1}$ towards Ntane aquifer for the previous study. This study, the net vertical groundwater exchange between the two aquifers is towards the Ecqa aquifer. The vertical leakance from Ntane to Ecqa aquifer was $5345 \text{ m}^3 \text{ d}^{-1}$, while Ecqa to Ntane was $4126 \text{ m}^3 \text{ d}^{-1}$, which resulted to a net vertical leakance of $1219 \text{ m}^3 \text{ d}^{-1}$ towards the Ecqa aquifer.

The Kalahari Sand aquifer was not evaluated in the previous studies; therefore not discussed under this context.

3.7. Limitations of the study

The time has been the major limiting factor for this research. The initial plan was to move to a transient calibrated model, which could not be met due to time shortage. Moreover, groundwater data was another limiting factor, especially on the Namibian side. Likewise, the groundwater level data available in the Botswana side had steady state data, with only 4 piezometers with transient data. These piezometers were all situated in the northern side of the LNKB (Figure 8), which are not representative for the transient model calibration.

There was also a technical limitation. Under the steady state conditions, the UZF package does not separate the ET_g from ET_u , providing all the infiltrating water as gross recharge compensated by UZF ET_g . The lack of separate calculation of ET_u , increases gross recharge and UZF ET_g , although fortunately the net recharge estimate remains realistic. The mentioned technical limitations are not present in transient solution but as mentioned, the lack of time did not allow for transient simulation.

4. CONCLUSION AND RECOMMENDATIONS

4.1. Conclusion

The main objective of this study was to evaluate the groundwater recharge and groundwater resources in the LNKB using numerical, distributed model. Such a task requires a conceptual model, which in turn requires understanding of the geometry and lithology of the hydrologic system. For that purpose first 3D stratigraphic model of the large KKB area was done and further converted to 3D hydrostratigraphic model. With the 3D hydrostratigraphic model, all thicknesses and volumes of hydro-stratigraphic layers could be determined. In total, five hydrostratigraphic layers were defined on top of the impermeable basement. These included; Kalahari Sand Saturated/unsaturated aquifer, Stormberg Basalt aquitard, Ntane Sandstone aquifer, Mosolotsane-Kwetla Mudstone aquitard and Ecca Sandstone aquifer.

The use of professional Rockworks software allowed building understanding of the spatial extent of the hydrostratigraphy of the Kalahari Karoo Basin through the dense network of cross-section well depicting horizontal and vertical heterogeneity of the layers. These cross-sections allowed also selecting external boundaries of groundwater prospecting LNKB area and defining geometry of the 5-layer flow system applied in the numerical distributed LNKB model.

LNKB integrated hydrological model was set up using (MODFLOW-NWT) with UZF1 to simulate interaction of groundwater with the surface. The model used data covering a period from 1st Oct 2004 to 30th Sept 2010. The model was calibrated under steady state condition by a trial and error method, assessing ME, MAE and RMSE calculated between the observed and measured groundwater heads. The values of ME, MAE and RMSE after a steady state model calibration were 0.29 m, 0.29 m and 0.56 m respectively.

The sensitivity analysis of the steady state model indicated that i) the model was sensitive to changes of horizontal conductivities (HK) being more sensitive to decreasing than increasing, ii) the model was less sensitive to changes of the vertical hydraulic conductivities for both VK and VKCB iii) the model showed a large sensitivity to changes made in the GHB conductances for both increasing and decreasing the values and iv) the model was non responsive to any changes of the UZF parameters.

The overall water budget for the model after a steady state calibration was calculated by considering the inflow and outflow components. The UZF gross groundwater recharge obtained was 194.06 mm yr⁻¹, the UZF groundwater ET was 194.03 mm yr⁻¹, hence resulting to 0.03 mm yr⁻¹ net recharge. The lateral in flow to the model contributed 0.04 mm yr⁻¹ and the losses by lateral flow, which occurs at the discharge point on the Ntane and Ecca aquifer was 0.038 mm yr⁻¹. This means, there is no lateral outflow of groundwater in the first layer, which is a saturated/unsaturated zone and only vertical flow to the second layer occurs, which is favoured by the high infiltration rate of the Kalahari beds, which does not favour the lateral flow. These fluxes were calculated based on the total surface area of independent aquifer.

4.2. Recommendations.

This study has suffered scarcity of the monitoring point data especially for groundwater levels. It is therefore recommended to set the monitoring stations, mainly in the Namibian side and increase number of groundwater level monitoring points, because only 4 piezometers had transient groundwater level data and they all are located in one corner of the area so are not representative for such a big area.

A transient model set up has to be implemented for proper understanding of the interactions between surface and groundwater systems, (Calderón Palma & Bentley, 2007). With a transient model, not only technical steady state model solution problems (see 3.7) will be avoided but also aquifers' storage the specific storage and specific yields of each aquifer be defined and understood so that one can conclude which aquifer system is more productive not only on the base of geometry and transmissivity but also on the base of aquifer storage property. Moreover, since the area has abstraction boreholes, it is important to include this aspect in future, in order to have a proper water budget closure and understanding of the resource in the area, which will lead to a proper suggested abstraction rates for sustainability of the resource.

LIST OF REFERENCES

- Ambayo, D. (2005). Spatial and temporal groundwater recharge assessment using GIS and 1D Reservoir modelling Lokalan case study . Msc Thesis, International Institute for GEO-Information Science and Earth observation (ITC), Netherlands, 53pp
- Anderson, M. P., & Woessner, W. W. (1992). *Applied Groundwater Modeling: Simulation of Flow and Advective Transport, Volume 4* (Vol. 2). Gulf Professional Publishing. Retrieved from <https://books.google.com/books?hl=en&lr=&id=IMs97HvH2TcC&pgis=1>
- Bear, J. (2012). *Hydraulics of Groundwater*. Retrieved from [http://ezproxy.utwente.nl:2181/\(S\(0zfa5wrgknyjpsy4s13fadju\)\)/Reader.aspx?p=1894683&oc=1200&u=2zh5%2fSxewAd34wnxMEwY2Q%3d%3d&t=1432547294&h=EE5CA83EFC4DAE3BA810B79F82897142B80612A8&s=36493586&ut=3997&pg=1&r=img&c=-1&pat=n&cms=-1&sd=2](http://ezproxy.utwente.nl:2181/(S(0zfa5wrgknyjpsy4s13fadju))/Reader.aspx?p=1894683&oc=1200&u=2zh5%2fSxewAd34wnxMEwY2Q%3d%3d&t=1432547294&h=EE5CA83EFC4DAE3BA810B79F82897142B80612A8&s=36493586&ut=3997&pg=1&r=img&c=-1&pat=n&cms=-1&sd=2)
- Bear, J., & Cheng, A. H.-D. (2010). *Modeling Groundwater Flow and Contaminant Transport*. Springer Science & Business Media. Retrieved from <https://books.google.com/books?hl=en&lr=&id=cbFCAAAAQBAJ&pgis=1>
- Bordy, E. M., Segwabe, T., & Makuke, B. (2010). Sedimentology of the Upper Triassic-Lower Jurassic (?) Mosolotsane Formation (Karoo Supergroup), Kalahari Karoo Basin, Botswana. *Journal of African Earth Sciences*, 58(1), 127–140. doi:10.1016/j.jafrearsci.2010.02.006
- Calcagno, P., Chilès, J. P., Courrioux, G., & Guillen, a. (2008). Geological modelling from field data and geological knowledge. Part I. Modelling method coupling 3D potential-field interpolation and geological rules. *Physics of the Earth and Planetary Interiors*, 171(1-4), 147–157. doi:10.1016/j.pepi.2008.06.013
- Calderón Palma, H., & Bentley, L. R. (2007). A regional-scale groundwater flow model for the Leon-Chinandega aquifer, Nicaragua. *Hydrogeology Journal*, 15(8), 1457–1472. doi:10.1007/s10040-007-0197-6
- Corbett, E. S., & Crouse, R. P. (1968). Rainfall Interception By Annual Grass and Chaparral. *USDA Forest Service Research Paper, PSW-48*. doi:10.1080/00382167.1962.9629728
- De Vries, J. J., Selaolo, E. T., & Beekman, H. E. (2000). Groundwater recharge in the Kalahari, with reference to paleo-hydrologic conditions. *Journal of Hydrology*, 238(1-2), 110–123. doi:10.1016/S0022-1694(00)00325-5
- Ely, D. M., & Kahle, S. C. (2012). Simulation of groundwater and surface-water resources and evaluation of water-management alternatives for the Chamokane Creek basin, Stevens County, Washington. *Scientific Investigations Report*. Retrieved from <http://pubs.er.usgs.gov/publication/sir20125224>
- Hassan, S. M. T., Lubczynski, M. W., Niswonger, R. G., & Su, Z. (2014). Surface-groundwater interactions in hard rocks in Sardon Catchment of western Spain: An integrated modeling approach. *Journal of Hydrology*, 517, 390–410. doi:10.1016/j.jhydrol.2014.05.026

- Kaufmann, O., & Martin, T. (2009). Reprint of “3D geological modelling from boreholes, cross-sections and geological maps, application over former natural gas storages in coal mines” [Comput. Geosci. 34 (2008) 278-290]. *Computers and Geosciences*, 35(1), 70–82. doi:10.1016/S0098-3004(08)00227-6
- Lewandowski, C. M. (2015). *RockWorks Manual. The effects of brief mindfulness intervention on acute pain experience: An examination of individual difference* (Vol. 1). doi:10.1017/CBO9781107415324.004
- Lubczynski, M. W. (2009). The hydrogeological role of trees in water-limited environments. *Hydrogeology Journal*, 17(1), 247–259. doi:10.1007/s10040-008-0357-3
- Ministry of Minerals, E. and W. R. (1991). *Botswana National Water Master Plan. Unpublished.* Gaborone.
- Ministry of Minerals, E. and W. R. (2006). *Botswana National Water Mater Plan Review* (Vol. 4). Gaborone, Botswana.
- Niswonger, R.G., Panday, S., Ibaraki, M. (2011). MODFLOW-NWT, A Newton Formulation for MODFLOW-2005. Retrieved June 1, 2015, from file:///D:/Msc_Botswana/modflow_NWT Version.pdf
- Nossent, J., Bauwens, W., Pereira, F., Verwaest, T., & Mostaert, F. (2014). Are the driving forces of hydrological models really driving the model output? *Proceedings of the 7th International Congress on Environmental Modelling and Software, June 15-19, San Diego, California, USA.*
- Nxumalo, V. (2011). Stratigraphy and Basin Modelling of the Gemsbok Sub-Basin (Karoo Supergroup) of Botswana and Namibia. Msc. Thesis, Faculty of Science, University of Witwatersrand, Johannesburg-South Africa, pp 1-181
- Obakeng, O. T. Soil moisture dynamics and evapotranspiration at the fringe of the Botswana Kalahari, with emphasis on deep rooting vegetation (2007). Retrieved from <http://www.loc.gov/catdir/toc/fy0713/2007385396.html>
- Rahube, T. B. (2003). Recharge and groundwater resources evaluation of the Lokalane-Ncojane Basin (Botswana) using numerical modelling. Msc Thesis, International Institute for GEO-Information Science and Earth observation (ITC), Netherlands, pp 1–119.
- Richard G. Allen, Luis S. Pereira, Dirk Raes, M. S. (1998). *Crop evapotranspiration - Guidelines for computing crop water requirements - FAO Irrigation and drainage paper 56.* Retrieved from <http://www.fao.org/docrep/x0490e/x0490e00.htm>
- Schmoll, O., & Organization, W. H. (2006). *Protecting Groundwater for Health: Managing the Quality of Drinking-water Sources.* World Health Organization. Retrieved from <https://books.google.com/books?id=ArlDvUKbzJwC&pgis=1>
- Science, A. (2004). Canopy structure in savannas along a moisture gradient on Kalahari sands. *Global Change Biology*, 292–302. doi:10.1046/j.1529-8817.2003.00703.x
- Smith, R. M. H. (1984). *The Lithostratigraphy of the Karoo Supergroup in Botswana, Volume 26, Issue 1.* Geological Survey Department with the authority of Ministry of Mineral Resources and

- Water Affairs, Republic of Botswana. Retrieved from <https://books.google.com/books?id=xCQZmwEACAAJ&pgis=1>
- USGS. (2015). Shuttle Radar Topography Mission (SRTM) 1 Arc-Second Global | The Long Term Archive. Retrieved February 11, 2016, from <https://lta.cr.usgs.gov/SRTM1Arc>
- Wang, D., Wang, G., & Anagnostou, E. N. (2007). Evaluation of canopy interception schemes in land surface models. *Journal of Hydrology*, 347(3-4), 308–318. doi:10.1016/j.jhydrol.2007.09.041
- Water Resources of Arid Areas: Proceedings of the International Conference on Water Resources of Arid and Semi-Arid Regions of Africa, Gaborone, Botswana, 3-6 August 2004. (2004) (p. 588). Taylor & Francis. Retrieved from <https://books.google.com/books?hl=en&lr=&id=PC96AgAAQBAJ&pgis=1>
- Wellfield Consulting Services. (2001). *Hunhukwe/Lokalane Groundwater survey Project* (Vol. 1), Main Report . Unpublished Report ,Department of Geological Survey, Gaborone,Botswana.
- Wellfields Consulting Services. (2012). *Botlhapatlou Groundwater Exploration and wellfield Development Project*. Unpublished report. Department of Geological Survey, Gaborone,Botswana.
- Wellfields Consulting Services. (2014). *POST – Auditing of the Serowe Groundwater Model (WELLFIELDS 1 AND 2)*. Unpublished report (Vol. Tender No.). Department of Geological Survey, Gaborone,Botswana.
- Winston, R. B. (2009). ModelMuse: A Graphical User Interface for MODFLOW-2005 and PHAST: U.S. Geological Survey Techniques and Methods 6–A29, 52. Retrieved from <http://pubs.usgs.gov/tm/tm6A29/tm6A29.pdf>
- Wu, J., & Zeng, X. (2013). Review of the uncertainty analysis of groundwater numerical simulation. *Chinese Science Bulletin*, 58(25), 3044–3052. doi:10.1007/s11434-013-5950-8
- Wu, Q., Xu, H., & Zou, X. (2005). An effective method for 3D geological modeling with multi-source data integration. *Computers & Geosciences*, 31(1), 35–43. doi:10.1016/j.cageo.2004.09.005

APPENDICES

APPENDIX 1: SUMMARIZED WATER BUDGET FOR INDIVIDUAL AQUIFERS.

FLOW BUDGET COMPONENT	KALAHARI (m ³ d ⁻¹)		NTANE (m ³ d ⁻¹)		ECCA (m ³ d ⁻¹)	
	IN	OUT	IN	OUT	IN	OUT
QLin/Q _{Lout}	4994.37	0.00	6.57	8184.51	0.00	1219.66
ET _{uzf} / ET _g	0.00	25355544	0.00	0.00	0.00	0.00
UZF R _g	25359978.00	0.00	0.00	0.00	0.00	0.00
Exf _{gw}	0.00	0.00	0.00	0.00	0.00	0.00
Q _{Vin} /Q _{Vout}	343.88	9762.93	13888.90	5689.46	5345.64	4125.97
Total	25365316.25	25365306.93	13895.46	13873.97	5345.64	5345.64
IN-OUT	9.32		21.50		0.00	
Percent Discrepancy	0.00		0.00		0.00	
FROM ZONE 0	0.06		0.00		0.00	
FROM ZONE 1	0.00		9762.93		0.00	
FROM ZONE 2	343.82		0.00		5345.64	
FROM ZONE 3	0.00		4125.97		0.00	
Total IN	25365316.25		13888.90		5345.64	
	OUT		OUT		OUT	
CONSTANT HEAD	0.00		0.00		0.00	
HEAD DEP BOUNDS	0.00		8184.51		1219.66	
GW ET	25355544.00		0.00		0.00	
UZF RECHARGE	0.00		0.00		0.00	
SURFACE LEAKAGE	0.00		0.00		0.00	
TO ZONE 0	0.50		0.00		0.00	
TO ZONE 1	0.00		343.82		0.00	
TO ZONE 2	9762.93		0.00		4125.97	
TO ZONE 3	0.00		5345.64		0.00	
Total OUT	25365306.93		13873.97		5345.64	
IN-OUT	9.32		14.93		0.00	
Percent Error	0.00		0.00		0.00	